flexRISK – Flexible Tools for Assessment of Nuclear Risk in Europe

Final Report. PRELIMINARY VERSION MAY 2013

Petra Seibert[1], Dèlia Arnold[1], Nikolaus Arnold[2], Klaus Gufler[2], Helga Kromp-Kolb[1], Gabriele Mraz[3], Steven Sholly[2], Antonia Wenisch[3]

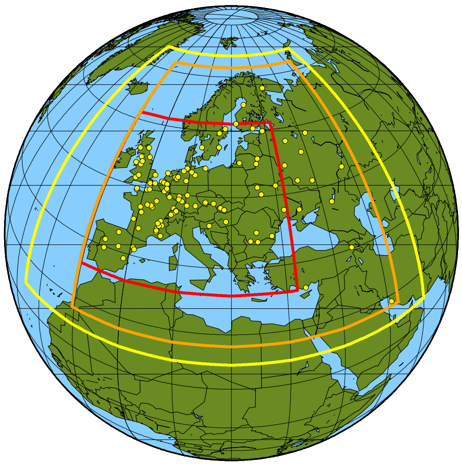

[1] Institut of Meteorology, University of Natural Resources and Life Sciences, Vienna (BOKU-Met)

[2] Institute of Safety and Risk Sciences, University of Natural Resources and Life Sciences, Vienna (ISR)

[3] Austrian Institute of Ecology (ÖÖI)

Project financed by the programme "New Energies 2020" of the Austrian Climate and Energy Fund (KLI.EN)

powered by klima+ energie fonds

Institut für Meteorologie (BOKU-Met)
Department Wasser – Atmosphäre – Umwelt
Universität für Bodenkultur Wien

May 2013

ISSN 1994-4179
ISSN 1994-4187 (on-line)

BOKU-Met Report 23

flexRISK – Flexible Tools for Assessment of Nuclear Risk in Europe

Final Report
PRELIMINARY VERSION MAY 2013, v2 (July 2015)

Petra Seibert, Dèlia Arnold, Nikolaus Arnold,
Klaus Gufler, Helga Kromp-Kolb, Gabriele Mraz,
Steven Sholly, Antonia Wenisch

BOKU-Met Report 23
May 2013

Diese Publikation sollte folgendermaßen zitiert werden:
This publication should be quoted as follows:

Petra Seibert, Dèlia Arnold, Nikolaus Arnold, Klaus Gufler, Helga Kromp-Kolb, Gabriele Mraz, Steven Sholly, Antonia Wenisch (2013): Flexrisk – Flexible tools for assessment of nuclear risk in Europe. Final Report. PRELIMINARY VERSION MAY 2013, v2 (July 2015)
BOKU-Met Report **23**, 116 pp. ISSN 1994-4179, ISSN 1994-4187 (on-line). Available at `http://www.boku.ac.at/met/report/BOKU-Met_Report_23_PRELIMv2_online.pdf`.

Our colleague Antonia Wenisch unexpectedly passed away in July 2012. A large part of her professional life was dedicated to making visible and to minimize nuclear risks. She had an essential part in flexRISK. We therefore dedicate this report to her.

Please see page 93 for the acknowledgements!

Version 2 (July 2015) apart from the correction of some typos, implements the following corrigenda:
1. Nuclides used in dose calculation corrected from 15 to 20 (Section 4.3.1)
2. Equation 4.6 in Section 4.4, r.h.s. to be inverted.

Medieninhaber und Herausgeber:

Universität für Bodenkultur Wien
Department für Wasser-Atmosphäre-Umwelt
Institut für Meteorologie
Peter-Jordan-Str. 82
1190 Wien, Österreich

URL `http://met.boku.ac.at/`

Contents

List of Tables

List of Figures

Abstract

Risks and hazards associated with potential severe accidents in nuclear power plants in Europe and adjacent regions (Turkey, Iran) were assessed in an interdisciplinary approach.

For all the 183 nuclear power plants (NPPs) in the project domain, existing, under construction, or in an advanced planning stage, key data were collected from the open literature, including published probabilistic safety analyses (PSAs). This includes geographical coordinates, nuclear inventories, expected lifetimes etc. For each NPP, a severe accident with large release and not too low expected frequency was identified.

Using FLEXPART, a state-of-the-art Lagrangian particle transport and dispersion model, the contamination of the surface and the concentrations in air near ground over Europe were calculated. This was done, assuming a certain type of accident at each site (and if reactors on a site had accident sequences with different release shapes, for each release shape), for 2,788 different, climatologically representative weather situations during the years 1995 and 2000–2009. A noble gas and an aerosol species were simulated. Using inventories and release fractions, deposition and concentration fields were calculated for all relevant nuclides, considering radioactive decay including some decay chains in postprocessing.

Radiation doses were derived from these concentration and deposition values with appropriate dose models. The risk of exceeding intervention levels was assessed, the likelihood for exceedance of thresholds of ground contamination and the likelihood of achieving a lifetime dose above radiation protection limits were calculated. All this was done for each single NPP, and for all the NPPs of each of the nuclear countries together, and finally for the overall reactor park. Three different scenarios for the reactor park were considered, pre- and post-Fukushima and a scenario where all reactors in operation before 1980 were considered to be shut down. Among the factors for uncertainties, the release frequencies assigned to different plants are considered to have the strongest influence on the results.

Results are mostly presented in the form of maps. While some samples are contained in this report, their total number is too large for a printed document. A comprehensive set of resulting figures is accessible through the project web site, `http://flexrisk.boku.ac.at/`.

The geographical pattern of the risk depends on the severity of the threshold applied. Low threshold can be exceeded at distances on the order of 1000 km off source sites and thus the risk distribution is smooth. It has a maximum over Eastern Europe due to source distribution and prevailing westerly winds. For high thresholds, the risk is concentrated around plants and thus regions with high density of NPPs, especially of NPPs assigned a high accident frequency. Among the high-risk areas are the Rhône Valley in France, an arc from Czech Republic through Slovakia to Hungary, and regions near Kozloduy (Bulgaria), Rovno (Ukraine), Sosnovy Bor / St. Petersburg. On the other hand, Ireland, the west and south of the Iberian Peninsula, southern Italy and Greece and most of Norway as well as northern Sweden enjoy the lowest risk. By shutting down the relevant plants in a region, the risk for events with severe consequences can be strongly reduced in that region.

An important finding was that regions where intervention measures could become necessary are larger than anticipated in current emergency planning of many European countries. Administration of stable iodine could become advisable anywhere in Europe, and pre-distribution especially for children as in Austria would be desirable.

1 Introduction

1.1 Motivation for the project and existing work

The attempted renaissance of nuclear power, some 15 or 20 years after the shock of the Chernobyl accident, has been a controversial issue in media and political debate. It has been kept alive by the climate change issue and the need for mitigation, as well as by the approaching end of “cheap oil”. The accident at Fukushima added to the debate. It enhanced awareness of risks on the one hand, with subsequent decisions to phase out nuclear, e. g. in Germany, but has, on the other hand, triggered defiance reactions leading to a forceful drive for a stronger commitment to nuclear energy, as for example in the Czech Republic.

In Europe, large radioactive releases following severe accidents in nuclear power plants threaten public health, ecological systems and economies across national boundaries. Due to geography and population density, accidents at most Western and Central European sites would have far worse consequences than Chernobyl (most of the heavily contaminated areas were very sparsely populated) and Fukushima, where only 20% of the caesium released into the atmosphere was deposited over land, the majority being taken up by the Pacific Ocean (Stohl et al., 2012). National and international efforts have continuously been made to reduce severe accident risks, and legal instruments were created to share the burden of mitigating the adverse effects of such accidents (e. g. through the Vienna and the Paris Convention). Comparatively little attention has been given to the analysis of consequences of potential accidents. Integrated assessments of the risk emanating from the operation of nuclear facilities across Europe do not exist. This is partly due to the complexity of the problem: The risk posed by accidents in nuclear power plants at any specific place is a function of the likelihood of a large-scale release of radionuclides from nuclear facilities, the amount and composition of the radionuclides released (source term), the atmospheric transport and deposition of the released radioactivity, the vulnerability of the people and economic assets (involving dose-effects relationship), the persons and properties at risk (for example, the number of persons, hectares of agricultural land exposed) and policies that may affect the afore mentioned. Another constraining fact is that most of these factors can only be determined with a high level of uncertainty. Thus, the existing risk and consequence estimates are typically limited to one facility (usually a power plant), and often focus on a relatively small area. Accidents involving simultaneously more than one reactor or additional facilities such as nuclear fuel storage would have been scoffed as totally irrelevant before the Fukushima accident.

flexRISK was an interdisciplinary project aiming to assess risks and hazards associated with potential severe accidents in nuclear power plants in Europe and adjacent regions (Turkey, Iran). It aims to

- demonstrate the geographical distribution of the risk caused by severe accidents in nuclear power plants in Europe;
- make risks of the nuclear option visible;
- compare the contribution of different nuclear power plants according to type and geographical location;
- study the effects of phase-out scenarios;
- support Austrian decision makers in their efforts for enhanced nuclear safety in Europe.

To achieve this, nuclear inventories, expected lifetimes as well as possible release fractions and release frequencies for severe accidents have been researched in accessible literature. Using a state-of-the-art transport and dispersion model, the contamination of the surface and the near-ground concentrations of air were calculated all over Europe for 2,788 different, climatologically representative weather situations and all relevant sites, considering all relevant radionuclides. Radiation doses were derived from these dispersion calculations with the use of dose models. The risk of exceeding intervention levels was assessed, the likelihood for exceedance of thresholds of ground contamination and the likelihood of achieving a lifetime dose above radiation protection limits were calculated.

flexRISK is not the first project of its type: Several integrated nuclear risk assessments in the form of risk maps of Europe (Andreev et al., 1998; Lembrechts et al., 2000; Sinyak, 1995, 1996; Slaper et al., 1994), or recently, of the world (Lelieveld et al., 2012), depicting specific aspects of nuclear risks, have been produced. flexRISK is, however, in many ways considerably more sophisticated than these assessments.

The first map of risk in Europe due to severe accidents for all European NPP (Slaper and Blaauboer, 1995) mapped the probability of excess cancer deaths after severe accidents in European NPP units. Since detailed safety analyses were not available for many of the more than 200 European NPPs, a generalisation was made to estimate accident probabilities and probabilistic releases by relating each reactor type to a specific probability and release category. Dispersion of the radioactive plume was evaluated by the OPS Gaussian puff model. Acute health effects in the vicinity of the NPP and countermeasures to reduce radiation doses were excluded.

Sinyak (1995) used empirical factors to describe the influences of geography resulting in normalised damage factors for the main cities of Europe. Rigina and Baklanov (2001) evaluated transboundary impacts of nuclear accidents focusing mainly on the environmental and health consequences of severe accidents of NPP units on the Balkan region. An alternative statistical description for estimating the risk associated with a large accidental release of hazardous material at long range was developed by Smith (1998).

The project RISKMAP (Andreev et al., 1998, 1999; Hofer et al., 2000), which can be considered a predecessor project of flexRISK, simulated dispersion and deposition with a Lagrangian particle model and calculated the frequency of exceedance of certain thresholds for the long-lived radionuclide Cs-137, regarded as risk indicator. Sensitivity analysis demonstrated that the results strongly depend on the release frequencies assumed for different reactor types. Additionally, GIS-based export/import matrices of risk were calculated for the European countries.

Baklanov et al. (1998, 2002) used an isentropic trajectory model and cluster analysis technique to assess possible impacts of a hypothetical nuclear accident in northern regions of Europe. Long-term health consequences were estimated on the basis of the Chernobyl accident exposures in Scandinavia. Mapping of the regional nuclear risk and vulnerability was realised for Scandinavia by two different approaches based on integration of mathematical modelling and GIS-analysis (Rigina and Baklanov, 2001).

CEC (1995) evaluated in detail the costs and benefits of various energy options, including the impact of NPP accidents. Economic damage as a part of nuclear risk mapping was studied by Lembrechts et al. (2000). Based on the approach of Lembrechts et al. (2000), costs for severe accidents in NPPs were estimated for different scenarios. The costs and benefits of a so-called technology-driven scenario assuming that there is a gradual reduction in the number of high- and medium-risk-category reactors by 2010 were evaluated and compared with other scenarios. The study also incorporates information on policy options and measures.

All of the above listed risk map approaches have their individual shortcomings (uncertainties) and advantages. Typically, more or less uniform source terms are assumed for all nuclear power plants. flexRISK differentiates types of reactors: for each unit, a severe accident scenario with substantial release of radioactivity was identified and a release probability attributed. Inventories, release fractions and probabilities were either taken from publicly available sources or estimated on the basis of data available for similar facilities. 82 sites in Europe with a total of about 220 reactor units under operation or construction were studied in detail. The selection of meteorological conditions for which dispersion is calculated is more extensive in flexRISK than in all other studies. Numerical dispersion calculations were carried out for over 2700 meteorological conditions taken from 10 consecutive years using the particle dispersion model FLEXPART. For the sake of comparison with the RISKMAP study (Andreev et al., 1998, 1999; Hofer et al., 2000), 88 cases of the year 1995 were analysed as well.

The most recent assessment, the study by Lelieveld et al. (2012)[1], made calculations for one full year using a Eulerian dispersion model. However, this study used a single (relative) source term and one accident frequency for all the NPPs in the world, and the analysis of results was based on annual average deposition, and thus does not permit to determine the frequency of exceedance of intervention or other limits.

[1] Concerning shortcomings of this study, see Seibert et al. (2012).

The output of the dispersion calculations in flexRISK consists of air concentrations and ground contaminations on a geographical grid. The distributions show high spatial variability, influenced by climatological features such as wind distribution and precipitation patterns.

The modular approach adopted by flexRISK is based in part on recent developments in catastrophe modelling. A catastrophe model integrates assessments of the probability of a specified hazard in a particular geographic region. In order to provide an output of the probability of losses exceeding a certain level, catastrophe modellers use two different approaches, one mainly deterministic, and the other probabilistic. The technique in probabilistic modelling is to run many hypothetical events covering a range of possible outcomes. This allows the modeller to assess the probabilities and severity of loss (i.e. loss likelihood) and to create a distribution of exceedence probability, the chance that a loss will exceed a certain level. This has become possible by advances in computing power that now allow to combine and visually display the results from numerous simulations. This probabilisitic approach makes it possible to identify the contribution of every single reactor and every weather situation to the overall risk in flexRISK. This opens a wide range of possibilities: The risk from individual reactors or power plants can be analysed for example, import and export of risk can be determined country-wise or the effect of different shut-down scenarios on risk can be assessed. Only selected analyses have been made so far, the data set produced in within the framework of this project offers many more possibilities.

However, there are a number of, to a certain extent, arbitrary, though not unfounded, decisions as well as substantial uncertainties that should not be overlooked when interpreting the flexRISK results:

Source terms and severe accident frequencies

An inherent problem regarding source terms is that potential beyond-design-base accidents can only be foreseen to a certain extent. All severe nuclear accidents so far were due to unforeseen sequences. However, the ultimate release of radionuclides into the environment can only occur by a limited number of paths, e. g., containment bypass or containment failure. Thus, assessments of source terms are feasible, based on nuclear inventory and design-specific accident sequences.Unfortunately, transparency is not one of the strengths of the nuclear industry, and data regarding the inventory, potential accident sequences and ensuing source terms for severe accidents are scarce. Therefore, to assess risks on a European (or global) level, much has to be inferred from the few published data, requiring a thorough understanding of the individual reactor and power plant designs. However, upgradings or unresolved issues that are site specific can not be taken account of if not published in the open literature. The European stress tests made some additional information available in this respect, but several country reports are geared to make inferences for individual plants difficult.

The same problems are encountered for severe accident frequencies, but they are aggravated by the fact that uncertainties are very high, even with full access to data. There is a general lack of data for the comparatively young nuclear technology. Even though the likelihood of a severe nuclear accident is small – estimated to be on the order 1 in 10 million operation years for many plants (comparable to winning national lottery) – the damage caused is very large. The frequencies of occurrence of severe accidents assumed in flexRISK are derived from the calculation of the failure rates in all event sequences. The figures provided by the operating companies come from probabilistic safety analyses (PSA), which, however, are not always based on comparable assumptions: Some only consider accidents caused by failure of nuclear power plant components, within which the aging of materials is difficult to include, others take accidents caused by external hazards into consideration (flooding, earthquakes, plane crash, . . .). Human error is especially difficult to quantify. There is a general understanding that the resulting overall probabilities of failure in PSAs are not to be taken at face value. PSAs are tools to identify comparative risks within one system. In analogy, severe accident frequencies published or derived for flexRISK could be considered more as comparative than absolute probabilities. High uncertainties are inherent in the estimated frequencies of severe accidents (factors of 10 and more).

A further unresolved problem concerns the selection of accidents considered in flexRISK. Computational and time constraints severely limit the number of accidents that can be considered. Therefore a “worst case” or “near worst case” was selected for every plant for the present study, based on expert judgement that remains somewhat arbitrary. It would have been desirable to define a set of possible accidents coupled with probability of occurrence and to pick from this two dimensional array according to certain criteria a “representative” severe accident (high release, but not too unlikely) and an extreme case (very high release with lower probability). However, this would require an effort not feasible within this project. This problem is addressed in more detail in Chapter 2.

Dispersion calculations

FLEXPART, the model used in flexRISK, is probably the most frequently used Lagrangian dispersion model and, due to the open source policy of the developers and the active user network, also very well evaluated. Nevertheless, choices regarding, e. g., grid size, time steps, etc. can influence results and certain parameters, e. g. the rain-out and wash-out coefficients for radionuclides are not as well established as might be wished for. Therefore, uncertainties remain, as with every model. The model uncertainties are of less importance than the uncertainties in source terms and especially for accident probabilities.

Other limitations

Due to its methodology, flexRISK does not describe impacts in the immediate vicinity (20 – 30 km). These areas are generally covered by the emergency plans of the nuclear power plants and well-established tools exist for consequence assessment at this range .

flexRISK does not aim at being used in real time as an emergency management tool for an ongoing accident situation. It may, however, help authorities to optimise emergency procedures and contingency plans beyond the immediate plant vicinities. Decision makers can be better informed about possible impacts of accidents and the distribution of adverse effects over the affected populations and areas.

flexRISK at present includes only releases from nuclear power plants, not from adjacent facilities such as spent-fuel storage tanks, and not from other facilities within the nuclear fuel cycle such as reprocessing plants or final nuclear waste storage facilities. This is mainly due to the fact that very little information on these facilities, possible accident sequences and releases is available.

Keeping these issues in mind, the results of flexRISK can be of use to policy makers, and stakeholders in general, in many ways:

- by illustrating which nuclear power plants pose the greatest risk to a given area, flexRISK can provide useful information for the setting of risk-reduction priorities;
- by providing information on risk “exporters” and risk “importers”, flexRISK can be a valuable input to international liability agreements, like the Vienna and Paris Convention, and help to set fair contributions to the nuclear accident risk pool;
- by providing easily accessible information on nuclear accident risks, flexRISK can be valuable to all stakeholders concerned with nuclear accident risks in Europe, e. g., authorities, nuclear and insurance industry, environmental and citizen groups;
- by providing reliable information to policy makers and the public, flexRISK may help to address public concerns and build a bridge of communication between the regulatory authorities and the public at large;
- by publishing severe accident emission scenarios based on expert judgement for lack of real data, flexRISK might trigger more transparency in the nuclear industry regarding severe accidents.

The present report cannot show all results. More material is available on the project website `http://flexrisk.boku.ac.at/`.

1.2 Structure of the project and the report

The project was structured into five work packages, three of which (2 to 4) were technical. Work package 2 dealt with the collection of base data on the nuclear facilities and the identification of accident scenarios with their source terms and frequencies. Work package 3 was devoted to the atmospheric dispersion simulations including pre- and postprocessing. Work package 4 dealt with doses and consequences. Work package 1 was administration and work package 5 publicity and distribution of results.

In this Final Report, the methodological aspects of work packages 2 to 4 are described in Chapters 2 to 4. Results are reported all in Chapter 5. Chapter 6 which contains conclusions and recommendations includes a few high-level results to support and illustrate some of the conclusions.

The main part of the report is followed by a glossary, acknowledgments, references, and three appendices. The first one contains a list of all facilities with some basic information. The second one lists the source terms for all reactor blocks considered, and the third one gives an overview of the accident sequences.

A comprehensive set of figures is provided on the project web site, `http://flexrisk.boku.ac.at`, which is recommended as a source for additional material, links, and interactive browsing of base information on NPPs as well as of results.

2 Nuclear facilities and accident scenarios

Inventories of nuclear power plants, source terms and release frequencies are not among the easily accessible data of nuclear power plants. Although the available data contain some uncertainties, a data set of sufficient quality has been created on the basis of information collected for European facilities (operating and planned). Data were collected from plant-specific probabilistic safety analyses (PSA), reports of the IAEA and OECD/NEA, the EU as well as publications in journals, etc.

Within Work package 2, nuclear power plants, nuclear fuel cycle facilities and large research reactors were identified and appropriate characteristics researched and collected.

2.1 Selection of nuclear facilities

To create a working basis for the project it was basically decided to include nuclear facilities, if one of the following criteria was met on the 1st of January 2010:

- reactor in operation;
- reactor currently not in operation, but not in permanent shutdown conditions;
- nuclear facility under construction;
- facility where the construction phase has not yet started, but the siting process is finished;
- significant research reactors;
- significant nuclear fuel cycle facilities.

The status of operating nuclear power plants can easily be determined from various sources, e.g., the IAEA "Database on Nuclear Power Reactors" (IAEA, 2011b) or the "WNA Reactor Database" (WNA, 2011).

As for facilities of the nuclear fuel cycle, several of them are operating within the project area, in Belgium, France, Germany, the Netherlands, the United Kingdom, Romania, Russia, Spain, Sweden and Switzerland. They were included in the list of nuclear facilities alongside with three "large" research reactors (40 MWth or more). Due to lack of information on source terms and accident scenarios, it was decided to exclude the research reactors and fuel cycle facilities from the final dispersion calculations, although they were included in the evaluation of facilities.

Finally, an evaluation of planned capacities had to be done. There is no unique list of forecast nuclear power plant capacity within the project area for a time horizon such as 2030. To illustrate this: an AREVA presentation in 2007 showed seven different forecasts for the world, which estimated worldwide nuclear power plant capacity between 414 and 740 GWe (Teller, 2007). The situation was no different in 2010 when this work was completed. There are a number of projections of nuclear power plant capacity extant, for example the following:

- The *International Atomic Energy Agency (IAEA), Energy, Electricity and Nuclear Power Estimates* for the period up to 2030 (IAEA, 2009) , which forecasts a world nuclear power plant capacity in 2030 between 511 and 807 GWe.
- The *World Nuclear Association (WNA) Nuclear Century Outlook* (WNA, 2010), which is periodically revised, forecasts a world nuclear power plant capacity in 2030 between 602 and 1350 GWe.
- The *OECD Nuclear Energy Agency (NEA) / International Energy Agency (IEA) Nuclear Energy Technology Roadmap* (IEA/NEA, 2010) targets a nuclear capacity of 1200 GWe by 2050; a graph indicates a 2030 world nuclear power plant capacity between about 650 and 950 GWe.

To summarize, four nuclear power capacity projections for 2030 give capacity estimates ranging from 414 to 1350 GWe. Obviously, such a wide range of projections implies very different numbers and distributions of nuclear power plants regionally, including the region reflected in the flexRISK project area.

Certain NPP construction projects were included in flexRISK. The decision which projects were included considered the status of planning, or, respectively, the construction in 2010. More specifically, it was demanded that the site selection process had been concluded and the decision on the reactor type had been made.

In trying to keep pace with changing circumstances and to fulfill the project aim of creating flexible tools, nuclear power plants (and other nuclear facilities) could be added or deleted from the calculations (although adding at the stage after major calculations comes at the expense of the respective computational efforts). This came in handy especially after the Fukushima events and the following impact on the European nuclear landscape.

2.2 Collection of base data for nuclear facilities

As base data, the following information was collected for each of the nuclear facilities:

– facility name and alternative name
– country
– geographic coordinates
– unit numbers or names (numeric or alphanumeric, as used by operator) for multi-unit sites
– facility type (power reactor, research reactor, etc.)
– reactor type, thermal power, electrical power, vendor and up to four additional system specifications for NPPs, e.g., information on containment type and layout
– recent core-damage frequency (CDF) and large release frequency (LRF) as far as available
– start-up and expected shutdown years

This information was entered into a spreadsheet workbook, and encoded in a way that the information could be read out automatically. Further calculations were based on these spreadsheets, containing all the relevant information of the nuclear facility in the flexRISK domain. The information was collected from different sources like IAEA PRIS (IAEA, 2011b), technical reports, and plant specific reports. The geographic coordinates were identified and quality-controlled in a two/step process. A first value for the geographical coordinates of the location was obtained from public WorldWideWeb resources. Then, the coordinates were verified with on-line map services such as Google Maps, Bing Maps, or WikiMapia, where the reactors can be identified well in available satellite or aerial imagery. On the flexRISK web site, links to Google Maps were constructed automatically from the coordinates as recorded in the spreadsheet, and again verified that they would point to the right location by visiting all of them. Experience in RISKMAP had shown that existing tabulated coordinates were not free from errors.

Figure 1 shows the locations of the nuclear facilities in Europe. As some of them are very close to each other, Fig. 2 provides a zoomed map for Western Europe.[1]

2.3 Accident scenarios

One of the project plan characteristics of flexRISK was to make efforts for identifying plant-specific accident scenarios and use them wherever possible. For the calculations of consequences and associated risks, basically two kinds of information are needed for each accident sequence to be considered:

1. source term (see below for details), and
2. its associated frequency.

The source term comprises:

1. Number of release phases (up to 2 were considered).
2. Time since stop of chain reaction at beginning of phase 1.

[1]Note that the version of the map provided on the flexRISK web site shows the site names as tooltips upon pointing on the symbol with the mouse. Clicking it will open a page with detailed site information.

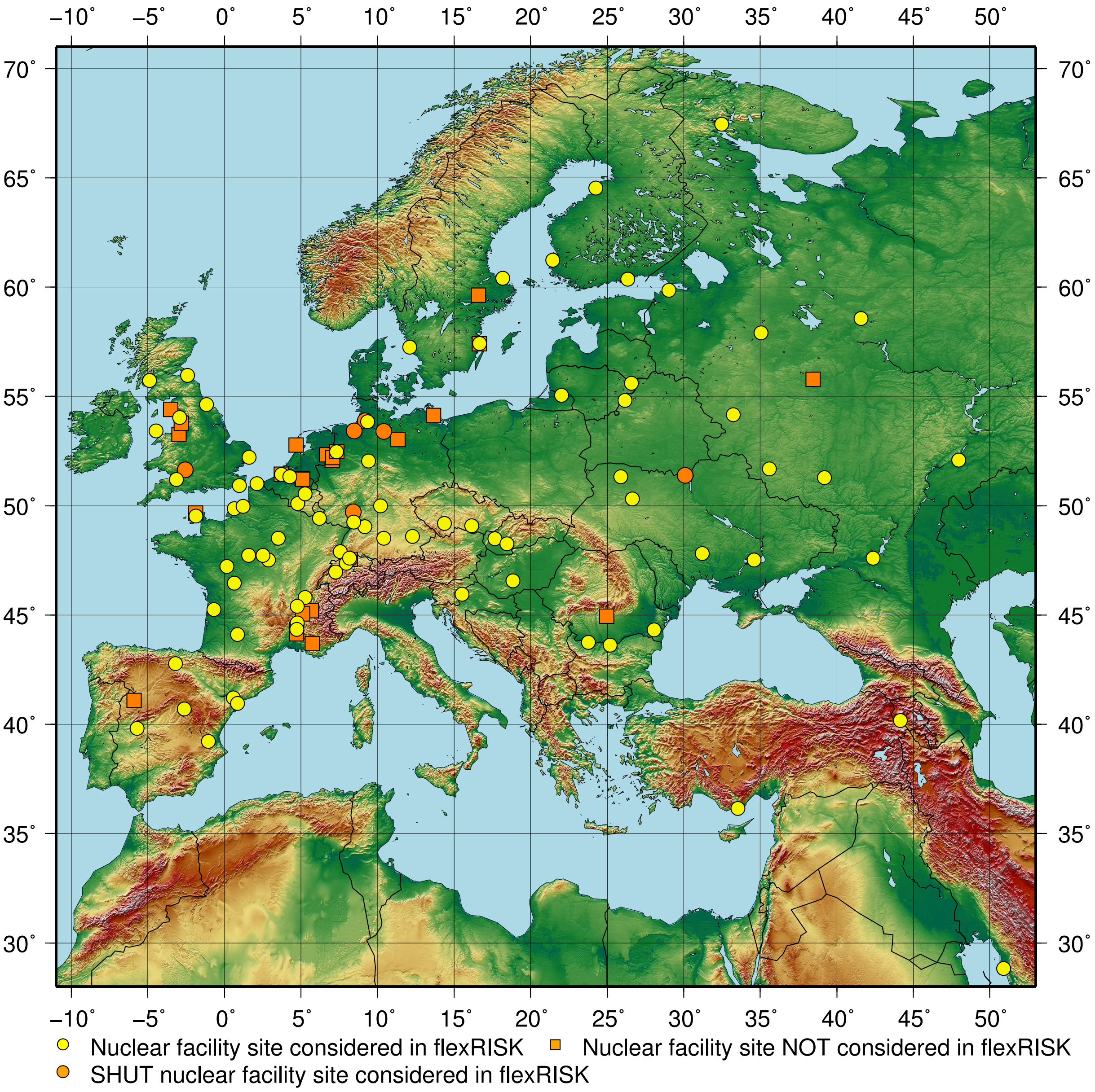

Figure 1: Map of the coarse output domain with sites of nuclear facilities as identified in flexRISK marked. Note that, while NPPs which have been shut down are indicated, active and planned plants are not distinguished.

3. For each phase,
   i. duration of the phase
   ii. an effective release height interval
   iii. the fraction of the core inventory being released into the ambient atmosphere for each nuclide group (cf. Table 1)
4. the core inventory of each nuclide considered (see also Table 1)

We refer to the number of phases, their duration and height collectively as the *release shape*. The release shape is important for dispersion calculations, as each different release shape requires its own set of dispersion calculations, whereas in the case of one or more units / accidents at a site having the same release shape, a single set of dispersion calculations is sufficient for them, with appropriate scaling done in the postprocessing.

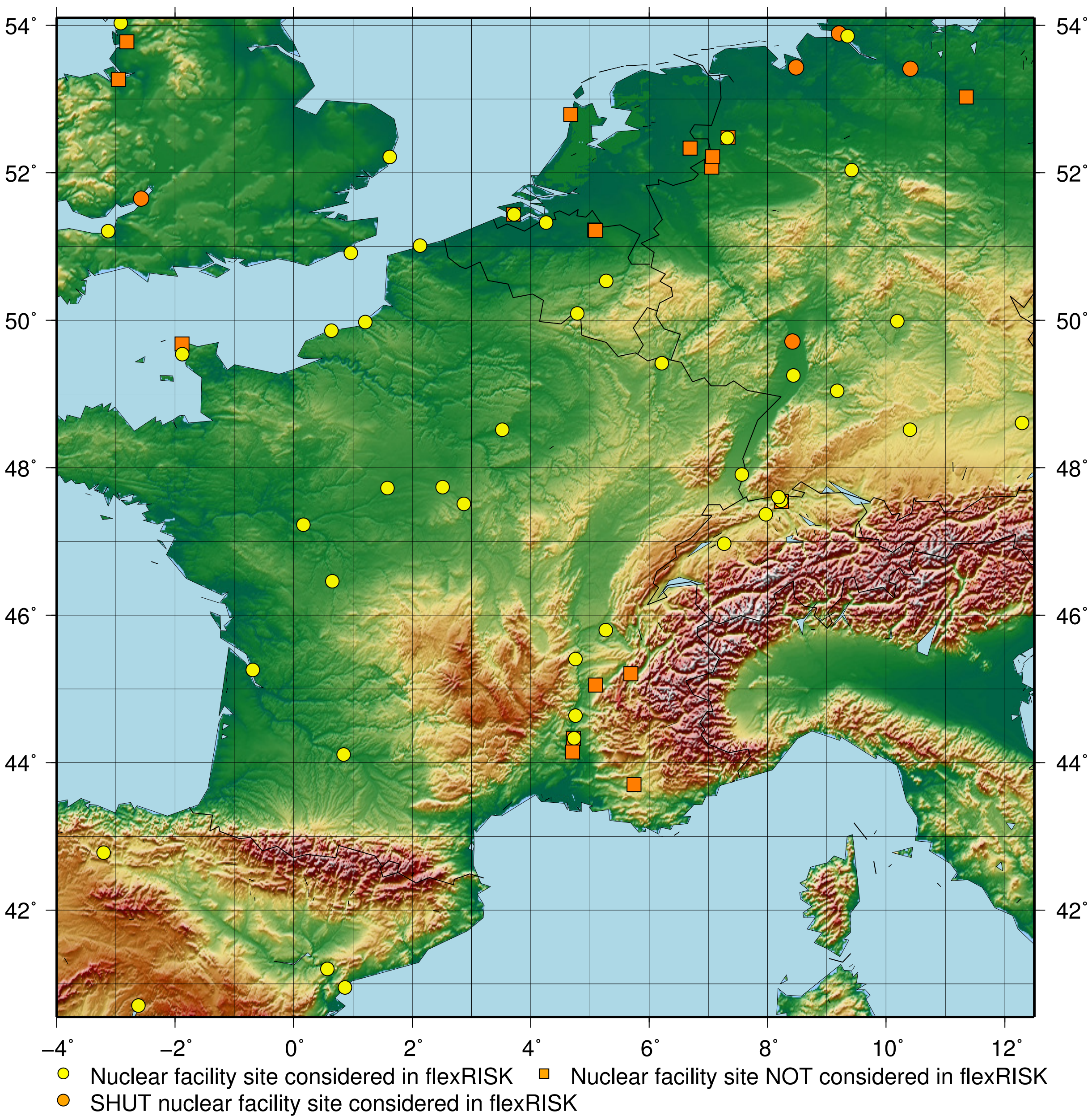

Figure 2: Like Figure 1, but zoomed into Western Europe.

Reactor specifications and the additional system specifications play a crucial role for the source terms and accident frequencies. Furthermore, an approximate equilibrium core radionuclide inventory is needed for the different reactor types.

At the beginning of the project it was decided to identify two potential severe accident sequences. One accident scenario with a relatively high frequency and relatively low radioactive release – usually a late release – and a second one with a lower frequency, but a greater radiological impact – a large early release – were identified for the different reactor types. The first accident type mostly comprises steam generator tube rupture accidents (SGTR) in PWRs and bypass accidents in BWRs. The second, more severe accident type includes mainly accidents with containment failure and interfacing systems loss-of-coolant accidents (ISLOCA). The originally intended limitation of two accident sequences, necessary for practical reasons, would have meant that the whole spectrum of possible accidents would be represented by only two points. This approach had to be modified due to the findings in the first months of the project. It turned out that the assumption that late releases would linked with relatively low releases having a relatively high frequency, whereas early releases would mainly be associated with higher releases at lower frequency was often not fulfilled. The only viable solution to this problem was to reduce the spectrum to a single accident sequence per reactor type. The selected accident for each reactor type would need to meet both of the following criteria:

1. Severe accident sequence which has a “relatively large” radioactive release
2. Severe accident sequence which has a “reasonable” (not too small) probability

The frequency estimates for the occurrence of accidents with severe releases assumed in flexRISK are derived from the calculation of the failure rates in all event sequences. The figures provided by the operating companies come from probabilistic safety analyses (PSA), which, however, are not always based on comparable assumptions: Some only consider accidents caused by failure of nuclear power plant components, within which the aging of materials is difficult to include, others take accidents caused by external triggers into consideration as well (flooding, earthquakes, . . .). Human error is especially difficult to quantify. The estimated frequencies of severe accidents are therefore afflicted with high uncertainties (factor of 10 and more).

The above-mentioned criteria of not too small release and probability led to a range of probabilities for the selected accident sequences between 1E-5 per year down to almost 1E-9 per year.

Due to the lack of publically available information, generic source terms had to be used for some reactor types (e.g., AGR source terms based on Slaper et al. (1994), some Framatome, Siemens and Westinghouse reactors based on Khatib-Rahbar (2001), or VVER-440 based on USNRC (1995)).

2.3.1 Release shapes

For all postulated accidents, starting time of release (relative to the stop of the chain reaction), duration of the release, and the effective release height interval were determined .If necessary, up to two phases of the release were defined, to characterize the shape of the release. The nuclear facilities were grouped into installations with similar characteristics and then the release shapes for each group were adopted. Following the original plan, two release scenarios for each group were created, resulting in a total of 17 release shapes, even though some were not used after the reduction to one scenario per reactor.

2.3.2 Release fractions

In the next step, more details were elaborated for the accidents in different reactors. The reactors were grouped into 24 , and a total of 47 types of accidents were selected, in general two per type, corresponding to the original approach. These two accidents and their frequencies were extracted from the literature where such information was available. If no appropriate, reactor-specific information was found„ generic accident frequencies per reactor type were assigned . The generic accident frequencies were based on data from similar reactors and on expert judgement. Finally, release fractions were assigned for each nuclide groups as defined in Table 1 and each release phase. Radionuclides to be considered in the calculations were selected according to their radiobiological relevance. Details are reported in Chapter 4. These nuclides were assigned to release fraction groups, with each nuclide in a group assumed to have the same release fraction.

2.3.3 Inventories

Core inventories had to be identified and assigned to the different reactor types and cores (LEU, MOX). The core inventories at equilibrium burn-up were taken from publically available sources. Seventeen core inventories were found for different reactor types. In order to obtain the inventories of all the facilities, the inventories were scaled linearly according to the thermal power output of the reactors. As mentioned before, few data on core inventories can be found in publicly accessible documents. Thus, for those reactors where no specific values were found, inventories of similar reactor types were applied. In the case of boiling-water reactors, only a single core inventory was available, which was applied to all of the BWRs. This inventory (from the Spanish NPP Cofrentes) showed slightly different isotope ratios and was rather large in particular for the cesium isotopes.

Table 1: Nuclide groups.

Group	Nuclides
Noble gases group	Kr-87, Kr-88, Xe-133, Xe-135
Iodine group	I-131, I-132, I-133, I-134, I-135
Caesium group	Rb-88, Cs-134, Cs-136, Cs-137
Tellurium group	Te-131m, Te-132
Strontium group	Sr-89, Sr-90, Sr-91
Ruthenium group	Ru-103, Ru-105, Ru-106

2.4 Limitations and uncertainties

2.4.1 General discussion

This work was limited in several ways concerning availability and comparability of data. While there is a lack of publically available PSAs, the few available PSAs are not always directly comparable. Most of the available PSAs take only internal events into account, while only some also consider external events. Due to this lack of data, it was necessary to use the available data as far as possible, and in some cases to use generic accident scenarios and source terms. For certain plant types (i.e. MAGNOX and AGR) no PSA data were available at all.

There are different factors contributing to the accident scenarios and progression. A state of the art approach is to group the core damage sequences to plant damage states (PDS), which reflect the state of the power plant at the moment of core damage. The PDS affect the further accident progression and the macro-consequences, while the sequence of events that lead to this state are less relevant (see (UK-EPR, 2011) for further Information). Within the flexRISK project, it was not possible to identify or to analyse all the accident scenarios or plant damage states in order to have one comparable accident for every different reactor type. This leads to limitations when trying to compare the results, as in some cases rather generic accident scenarios and in other cases specific accident scenarios were used.

In order to perform the analysis in a detailed manner and to reduce the above discussed limitations, what would be required would be on the order of the following:

- A consistent methodological approach for a full-scope probabilistic safety assessment (PSA) for each nuclear power plant, spent nuclear fuel reprocessing plant, and large research reactor within the scope of the study. Such an approach would have to consider the full gamut of internal events[2], events arising from all relevant external man-made hazards[3] and natural phenomena hazards[4], as well as full consideration of all of these events at both power operation and shutdown conditions (including refuelling, repair, modification, and maintenance evolutions)[5].
- Deterministic consideration of possible accident sources not susceptible to probabilistic analysis, such as acts of sabotage and terrorism[6].

[2] Such internal events could include: (a) loss of coolant accidents; (b) various types of transients; and (c) events resulting from inadvertent human actions (mistakes during operation, surveillance tests, or plant maintenance).

[3] Such man-made hazards could include: (a) fires; (b) flooding resulting from process line and fluid storage tank leaks and failures internal to the facility; (c) on-site and near off-site ground and water-based transportation accidents (motor vehicles, rail, and ship/barge traffic); (d) turbine failures resulting in generation of missiles that penetrate the turbine casing and can impact on the structures and components outside the turbine (in facilities with turbines, such as nuclear power plants); (e) aircraft crash; and (f) electromagnetic interference.

[4] Such natural phenomena hazards could include: (a) flooding from sources external to the facility (streams, rivers, impoundments, lakes, seas, and oceans); (b) wildfires spreading onto the plant site; (c) lightning; (d) high winds (including those resulting from tornadoes and hurricanes); (e) earthquakes and earthquake-related phenomena; (f) tsunamis; and (g) volcanic phenomena.

[5] The scope and methods of the PSAs should be consistent with international guidance (IAEA, 2010b,a).

[6] Such accident sources are not susceptible to probabilistic analysis because there is no technically justifiable way to estimate their likelihood of occurrence. Use of historical data is inherently unreliable because it is limited as regards nuclear facilities, and because there is no discernible linkage between past sabotage and terrorism motivations and capabilities and those that might exist in the future. It should be noted that consideration in PSAs of hazards arising from malicious actions is not considered to be within the scope of the relevant IAEA Safety Guides; see Specific Safety Guides 3 and 4, fully referenced in the preceding footnote.

– Unfettered access to plant documentation and data, and necessary access to plant experts for consultation for the purpose of carrying out the PSAs and deterministic accident assessments[7].
– Appropriate computer codes and models (including state-of-the-art models of accident progression, containment/confinement response, fire and flood propagation, and structural response) for use in the PSAs and the deterministic accident assessments.
– State-of-the-art consideration of uncertainties (considering incompleteness, modelling, and parameter uncertainties) in the PSAs and the deterministic accident assessments.
– And (not the least) the requisite budget and manpower to carry out the analyses. Essentially what we are talking about here are teams of experts (a dozen or more experts) for each facility and a budget of the order of EUR 10-15 million per facility. The numerous teams would have to carry out the analyses simultaneously so that a current "view" of risk at each facility would be achieved by approximately the same date.
– And then each analysis would have to be periodically updated (typically, for nuclear power plants, following each refuelling outage where plant modifications are undertaken) to take account of changes in design, operation, and the influence of external man-made and natural phenomena hazards on the facilities. That is to say, we would need so-called "living PSAs" and current deterministic accident assessments.

Even then, were this mammoth technical work carried out, the uncertainties would still be significant. In addition, there would still be judgment involved in selecting the two accident scenarios for which source terms and frequencies are estimated, and for which accident consequence analyses are performed. Even then, the project will still not have estimates of risks because there are (far) more than two possible source terms per nuclear power plant and other nuclear facilities.

It almost goes without saying that the enormous level of effort discussed above has not been attempted here. What was done is to accumulate published PSA results and results of other related studies, and drawn inferences and made judgments about the plausible risk-dominant accident scenarios and their likelihoods. The uncertainties in such an approach are clearly very large, and therefore no claim that the work is closer than an order-of-magnitude to the truth. Still it was endeavoured to be as thorough as possible within the limits of available resources, data, and analysis. In many cases, due to lack of available data, the represented accident scenarios, core inventories, source terms, and accident likelihoods represent little more than "placeholder" values pending the receipt of better information.

2.4.2 Description of uncertainties using the example of Temelín nuclear power plant

To take an example, the 2003-era PSA results for the Temelín nuclear power plant in the Czech Republic are used here in the absence of more recent results. It is clear that there have been changes in plant design (new turbines and considerable secondary system rework are not the least of which) and procedures that would very likely affect the results should a current PSA be performed or made available. In addition, there would be seven more years of plant-specific hardware reliability data available for quantification were a current PSA available. Even if a current, full-scope PSA quantification (Level 1 and 2) for Temelín was available, there would still be the practical limit within this project of representing risk-dominant sequences with only two source terms – what can be characterized as a large, early release, and what can be characterized as a longer-running or later release. For Temelín, these two source terms represent those accident sequences ending in early containment failure or containment bypass due to an interfacing systems LOCA (the large, early release source term), and containment bypass sequences resulting from steam generator tube ruptures (the longer-running sequence). In contrast, in the 2003 version of the Temelín PSA, there were twenty source term categories – not the two source terms used here. (Of course, it is true that at least some of the source terms in the Temelín PSA are probably not important contributors to risk, such as those in which the containment does not fail, or in which the containment leaks when containment sprays are running.)

[7] The extent of access to data and documentation is alluded to in §4.1 and §5.83 of IAEA (2010a).

A survey of VVER Level 2 PSAs conducted for OECD/NEA in 2007 found the number of source terms for the various studies ranging from five to twenty, and only one of the six studies in question had fewer than nine source term categories. A range of 10-20 source term categories is broadly typical for nuclear power plants of all types (OECD/NEA, 2007a).

* * *

In view of the underlying uncertainties and the fact that only one source term was considered in the calculations for every reactor, the results can, strictly speaking, not be characterised as a representation of nuclear risk. However, lack of information on source terms and release frequencies cannot justify not analysing possible effects of severe nuclear accidents. In flexRISK, contamination and dose levels and, to a certain extent, likelihoods of contamination and dose were calculated based on published severe accident source terms and plausible assumptions where such source terms are lacking. Combined with real-world meteorological conditions, flexRISK results therefore show individually for every plant as well as aggregated for countries and for all of Europe what specific selected severe nuclear accidents could mean for consequences in terms of contamination and doses for Europe.

2.5 Reactor-park scenarios

Three different reactor-park (operation) scenarios were considered for all the evaluations where consequences from a set of plants were aggregated:

- **S1**: Plants in operation 1/2011;
- **S2**: Plants in operation 1/2012;
- **S3**: Plants in operation 1/2012, but assuming that old plants, connected to the grid before 1980, have been shut down.

S1 is the baseline scenario. S2 was introduced to take into account, and to assess the effect of, the shut-downs which were implemented during the year 2011 in Germany as a consequence of the debate on the Fukushima disaster. In addition, in the UK, the two MAGNOX reactors at the Oldbury site (started up in the 1960ies) were taken out of service. Annex A lists for each unit the scenarios to which it belongs (is considered).

The main rationale for the phase-out scenario S3 was to keep it simple. Of course, one could consider many types of phase-out scenarios, based, for example, on political decisions or declarations of intent for phasing out nuclear power in a country or for specific plants, or the time when current operating licenses would expire, or by removing plants that were assigned the most unfavourable accident parameters. But none of these is very clear and political decisions might easily be reversed, as experience has shown. However, due to the step-wise and flexible methodology of flexRISK, it is not much work to produce results for any desired scenario. One should also note that plants which are still under construction or just planned are not included in any of the scenarios. The results associated with them are available in the context of single-plant results (contaminations and doses).

2.6 Technical aspects

As mentioned, the data were collected in a spreadsheet workbook, containing several sheets with information on sites, units, release shapes, release fractions, nuclide groups, and inventories. The *site list* sheet contains information such as site name, alternative site name, country, coordinates, and the URLs for links to the NNI website of the Austria Institute of Ecology.

The *unit list* contains information , grouped by site, on the different units at the site: the release shapes used, the basic reactor information, the thermal and the electrical power, the unit type, the reactor type, the confinement and containment information, the CDF, the LRF, the start-up data, the expected shutdown year, the accidents assigned, the relevant reference inventory, and several other pieces of information.

The *release shapes list* includes the information on the release shapes: release time, release duration, and release height, for each phase.

The *release fractions list* contains information on the probabilities, the reactor type and the accident description of the selected accidents. Furthermore, it includes the release fractions of the nuclide groups for the selected accidents according to the phases of these accidents. The *nuclide group list* lists the nuclides associated with each nuclide group. The *inventory list* lists the inventories of all the required nuclides for a set of reference reactors.

Definitions and abbreviations were collected in further sheets.

The information from these sheets was read by `python` scripts to generate the input to dispersion and dose calculations and, in combination with the `genshi` templating engine[8], to populate the project web site `http://flexrisk.boku.ac.at/`.

[8] `python` and `genshi` are free software.

3 Atmospheric dispersion modelling

3.1 Background

Radionuclides released into the atmosphere in a nuclear accident are transported with the mean wind, dispersed by turbulence, and, with the exception of noble gases, deposited on the ground, either through precipitation (wet deposition), or/and just sticking to the surface (dry deposition). These processes are simulated by atmospheric dispersion models (also called atmospheric transport models). A wide range of such models exists. In the context of assessing consequences of nuclear accidents, models based on the Gaussian approach have been widely used. Gaussian plume models which calculated dispersion for a single set of meteorological parameters, assumed to be constant in time and space, are suitable only for the close environment, up to at most 10 or 20 km, and this only if additional conditions such as homogeneous terrain are met. Segmented plume models such as PC-COSYMA (European Commmission, 1995) consider temporal variability and thus extend the possible range of use to some tens of kilometres. For longer distances and universal applicability, fully numerical dispersion models are required. These can be either Eulerian models, working on a grid fixed in space, or Lagrangian particle dispersion models (LPDMs) which represent the substance transported by computational particles. Only when particle positions and masses are evaluated for concentrations, a grid is applied. The transport itself is Lagrangian and thus does not suffer from effects of finite grid resolution, namely the inability to represent structures smaller than the grid cell size, and artificial diffusion as a consequence of the numerical schemes. The former is important especially initially, as releases are point releases, and plumes can stay narrow for long distances. For nuclear accident applications at the scale of flexRISK, covering hundreds or thousands of kilometres, LPDMs are thus the method of choice.

For the consequence assessment, two model output parameters are needed,

- the near-surface concentration of airborne nuclides, which determines inhalation and cloudshine doses, and
- the surface contamination, which determines the groundshine doses and the contamination of agricultural products, and thus the ingestion doses.

For both parameters, their time integrals finally determine the dose. However, while air is contaminated only while the plume is passing, surface contamination remains even after the plume is gone. Some resuspension from deposited nuclides may occur, but this is considered a second-order effect and it was not taken into account in flexRISK. Thus, long-term consequences are related to the ground contamination. The ground contamination (integrated deposition flux, or in short, deposition) is strongly influenced by precipitation, because wet deposition is much more effective than dry deposition. Dry deposition rates are proportional to near-ground concentration, while wet deposition is able to scavenge a whole (tropospheric) column of air. Wet deposition rates depend strongly on precipitation intensity. Therefore, the distribution of precipitation, or more exactly, the co-location of airborne radioactivity with the occurrence of rain or snowfall is crucial for the deposition patterns.

If contaminated air passes through a sufficiently large and intense precipitation area, concentrations can easily be reduced by a factor of 10. Therefore, in most places where the integrated concentration is high, the surface contamination is only moderate, and vice versa. This makes the influence of the weather on the consequences and their distribution quite complex.

It is also important to understand that atmospheric structures constantly change and move and straight-line patterns of contamination are thus rare on scales beyond some tens of kilometres. Contamination patterns will often be quite complex.

3.2 Principles of the approach

The basic approach with respect to atmospheric dispersion for an assessment of environmental risks from severe nuclear accidents depends on the risk parameters one wants to consider. If only average values of contamination or dose are of interest, these could be obtained at moderate computational cost by simulating a continuous release over a prolonged period (the approach of Lelieveld, see Lelieveld et al., 2012; Seibert et al., 2012; Seibert, 2012).

The basic methodological approach is to generate simulations for a large number of possible meteorological situations, so that statistical evaluations of the results will reflect the climatological dispersion properties of the atmosphere in the respective regions. Ensuing criteria are:

1. The number of simulations should be large enough so that results are not unduly influenced by sampling statistics.
2. Simulations should be evenly distributed over the calendar year.
3. Simulation starts (release times) should be evenly distributed over the hours of the day, without seasonal or geographical biases.

Criterion 1 is difficult to fulfil. If one is interested in so-called ‘worst-case scenarios’, which is an important and legitimate approach in the context of nuclear accident assessment, one is per definition interested in the very tail of the frequency distributions of consequences, which is inherently affected by the effects of a finite sample. Therefore, the only practical consideration was to find the maximum number of simulations which would be compatible with available CPU resources for the calculations and hard disk storage space as well as post-processing CPU resources with respect to the output produced. Then, this number determines where the limits to the usefulness and statistic stability of the output are. This is discussed in more detail in the Results chapter.

As many of the internal model parameters of the dispersion model have a direct impact on the two main resource requirements (CPU and storage), a trade-off which in the end is a subjective decision is necessary. This decision was made after several test runs with different set-ups, and the parameters selected are documented below.

3.3 Dispersion model

The dispersion calculations have been carried out with the Lagrangian particle dispersion model FLEXPART (Stohl et al., 1998, 2005). This model was developed at BOKU-Met by Andreas Stohl, and through Petra Seibert as a co-developer, good knowledge of the model was available within the flexRISK team. In RISKMAP (Andreev et al., 1998, 1999; Hofer et al., 2000), FLEXPART was used in version 2.0 whereas for flexRISK, version 8.1 was available initially and version 8.2 later (Stohl et al., 2010). LPDMshave distinct advantages for the simulation of dispersion from point sources, as they avoid the artificial smoothing and broadening of the plume or puff due to the grid resolution, as happens in Eulerian models (Arnold et al., 2013). Furthermore, compared to other LPDMs, FLEXPART is fast and produces comparably small output, both critical features for the application in flexRISK.

It can be run in a pure random-walk mode or, more slowly but also more accurately, solving a Langevin equation considering turbulent time scales. Turbulence is assumed to be Gaussian and turbulent velocity components are derived from surface heat and momentum flux in the input data and a boundary-layer height diagnosed within FLEXPART. In addition, a parameterisation of mesoscale meandering is applied.

FLEXPART has a detailed representation of dry deposition considering surface properties. FLEXPART can optionally consider moist convection (Forster et al., 2007).

The wet deposition of versions prior to V8 were based on a scavenging rate S proportional to the precipitation rate I or some power B of it, in the form $S = AI^B$. With V8, a scheme differentiating between in-cloud and sub-cloud scavenging was introduced (Stohl et al., 2010).

3.3.1 Modifications to the official FLEXPART versions

In the first year of flexRISK, the latest version of FLEXPART was V8. As it was announced as having several improvements, especially in considering in-cloud and below-cloud scavenging separately and by making sure that particles located above the top of the precipitating clouds would not undergo washout, it was seen as desirable to use this version. For making use of most recent fixes, the latest, unofficial version of FLEXPART 8.1 was obtained from NILU. This version is close to 8.2 for which documentation is available (Stohl et al., 2010). Modifications were made to this version in order to enhance calculation speed and to minimise output size:

– termination of a run if the total airborne mass of all species falls below 0.5% of their initial values (see discussion below in Section 3.5.2);
– writing out only the sum of dry and wet deposition instead of both components separately (saves space and time for writing);
– writing out incremental deposition instead of accumulated deposition fields (saves space and time for writing).

Some test runs were inspected and appeared to be reasonable. Then, in autumn 2010, the production runs were carried out. Unfortunately, when a larger number of contamination plots were produced and looked at after all the dispersion calculations had been performed, it turned out that a significant number of them contained checkerboard-like or other rectangular patterns which were obviously a kind of artefacts. In some cases, these patterns would be visible even in averages over many runs.

It took time and efforts to identify causes. The implementation of the below-cloud/in-cloud wet scavenging scheme was found to be inconsistent and oversimplified. It was also discovered that this new scheme did not properly consider convective precipitation. In the meantime, version 8.2.3 of FLEXPART had been released, but with the same wet deposition scheme. While some efforts were made towards fixing these deficiencies, finally, the above-mentioned modifications were implemented in version 8.2.3 and the old wet deposition scheme which does not differentiate between in-cloud and sub-cloud scavenging was re-introduced. Calculations were then redone early 2012 with this model version which is the base for reported results.

3.4 Model input data

Apart from input data packaged with the code, such as land surface information for dry deposition, two kinds of input are required. Firstly, the meteorological data, and secondly, the release data.

3.4.1 Meteorological input data

For the application in flexRISK, the ERA-Interim reanalysis data set from ECMWF (Dee et al., 2011) has been selected and extracted on a geographical grid with 0.75° grid spacing for all model levels. The domain can be seen on the title graphics and in Fig. 4; the exact size is given in Table 3. It includes all of Europe, Northern Africa, the Near and parts of the Middle East. It was deliberately chosen larger than the output domain (see Section 3.5.1). If a plume moves near the domain boundary, first leaving and then re-entering, the particles having left the domain are lost and the re-entry would be missed. This enlargement of the meteorological domain with respect to the output domain will thus reduce, and hopefully mostly eliminate, such effects.

The ERA-Interim data set gives the best available description of the state of the atmosphere over Europe during the time period under consideration, and it was produced with a single version of the ECMWF model, so that the temporal homogeneity is better than those from operational analyses.

The precipitation climatology was a major criterion for the selection of the meteorological input, as wet deposition climatology depends on it. In RISKMAP, it was found necessary to improve the operational data of the year 1995 (at 1°) based on observed precipitation. However, ERA-Interim is much better and as shown in Fig. 3, the characteristic climatological features of precipitation in the flexRISK-domain are well reproduced:

– Mountain regions have more precipitation and therefore also a higher risk for ground contamination.
– Most parts of the Mediterranean, especially the southern areas, have very low precipitation.
– Western Europe and especially the northwestern coasts have more precipitation than Eastern Europe.

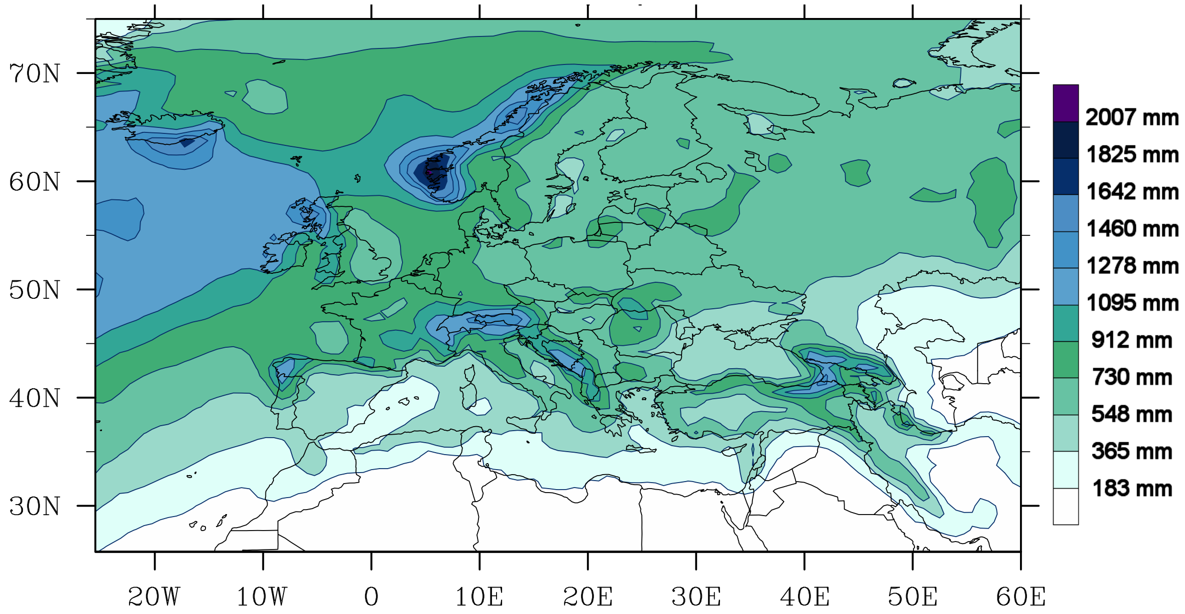

Figure 3: Mean annual precipitation (rain, snowfall, etc.) in the ERA-Interim data, years 1990–2002.

Maxima and gradients appear to be satisfactory on the given resolution. Even if one would try to improve these data with observations, it would be very difficult to do this in a consistent manner due to the lack of observations over the oceans and the thin coverage in sparsely populated areas of eastern and northern Europe as well as at high elevation. Results (see Figures 33, 35, 36) nicely reflect the expected influence of both the flow around mountains and (Fig. 21) the increased deposition on the windward side where the flow goes over mountains.

3.4.2 Release data

For each release shape (see Section 2.3.1), one dispersion calculation is done which simulates two species (see Section 3.5.1). The release is always started at time zero, thus the start of the calculation is the start of the release. FLEXPART allows to specify a release as a vertical column. This is used to implement an effective release height, as FLEXPART has no mechanism for calculating an effective release height from heat flux and ambient meteorological conditions. The effective release height is not assumed as a single height but as a height interval. This takes care of the uncertainty and variability of the effective release height, building wake effects, plume dispersion during plume rise, etc.

The release is given a unit strength as only source-receptor calculations are to be performed, and ambient concentration and deposition is determined for each nuclide by post-processing. If there are two release phases, each phase is given a unit release strength, and the number of particles is partitioned equally between both phases, as there is no general rule as to which release would be more important. The two release phases are considered separate sources in FLEXPART and tracked separately, thus in the post-processing they can be scaled separately and then their contributions added up.

3.5 Model set-up

3.5.1 Internal model parameters

Table 2 lists the key internal FLEXPART parameters and the values used, most of which are set in the COMMAND file. These settings are a trade-off between maximising accuracy and computational resources (CPU and disk space). The output frequency of 3 h means that we can determine first

Table 2: Values of key internal FLEXPART parameters.

Parameter	Value
Output frequency	10,800 s (3 h)
Output integration time	10,800 s (3 h)
Output sampling interval	300 s (5 min)
Particle splitting	no
Synchronisation time step	300 s (5 min)
Time step	Lagrangian time scale / 3.0
Vertical time step	time step / 4
Subgrid terrain effect parameterisation	on
Convection	off
Units	mass units for source and receptor
Number of output layers	1
Output layer height	150 m
Minimum mixing height	100 m
Number of particles per run	250,000

Table 3: Specification of FLEXPART domains for flexRISK (domain borders, grid cell sizes, grid cell numbers). "outgrid" stands for output grid, x values refer to geographical longitude, y values to latitude. The border coordinates refer to the outermost grid points in the case of the meteorological fields, whereas for the output domains, they indicate the edges of the outermost grid cell.

Domain	x_{min}	x_{max}	y_{min}	y_{max}	Δx	Δy	n_x	n_y	$n_x n_y$
meteo fields	−25.50	60.00	24.75	75.00	0.75	0.75	114	67	7,638
coarse outgrid	−11.00	53.00	28.00	72.00	1.00	1.00	64	44	2,816
fine outgrid	−10.00	31.91	36.00	61.20	0.127	0.090	330	280	92,400

arrivals within an interval of 3 h, and that for the purpose of decay correction (see Section 4.4), it has to be assumed that radionuclide concentration was constant during intervals of 3 h. Obviously, this is a good approximation at larger distances and less good at shorter distances. We are using the full Langevin equation and not the fast random walk mode as this is not sufficiently accurate for surface concentrations (in previous tests, deviations up to 30% were found). The convection parameterisation would have been desirable, but unfortunately it was too costly in terms of CPU time. However, for the climate region under consideration it is not as crucial as in tropical areas. The output layer height needs to be not too small, firstly, because small values would require more particles to ensure good particle sampling statistics, and secondly, because of cloudshine calculation based on a single layer, it should be roughly representative of the penetration depth of gamma rays in air. Adding a second layer was considered, but found too costly in terms of storage. The particle number (250,000) is fine, traces of single particles are found in contamination plots only with very low concentration or deposition values.

The output is generated on two nested grids whose specifications are provided in Table 3 and which are visualised both on the title graphics and in Figure 4. Grids are latitude-longitude, thus the East-West cell size varies with latitude. Grid cell sizes in kilometres are thus (N–S, E–W, approximately at 45°N) for the meteorological fields 83 km ×58 km, for the coarse output grid 111 km × 75 km, and for the fine output grid 10 km × 10 km. These specifications are a compromise. The fine-grid resolution of 10 km is what is appropriate to resolve a plume at source distance of 50 to 100 km and larger. However, resolving the large domain to this detail would have caused the output to become too big to store on the available disk space and would have been a heavy burden for post-processing. It was therefore necessary to limit the fine output domain to an area where the bulk of the European NPPs are located. It extends from Spain in the southwest to St. Petersburg in the northeast, and includes all the Swedish NPP sites, the existing Finnish sites and the Russian Sosnovy Bor / Leningrad site with its RBMK reactors. It includes all the European Union with the major exception of middle and northern Scandinavia, Cyprus (too far east) and some islands. On the other hand, the coarse output domain (a map of it with nuclear sites marked is provided as Fig. 1, which is not so costly, was made large enough to include all the North African coast (which receives a part of the risk from European NPPs,

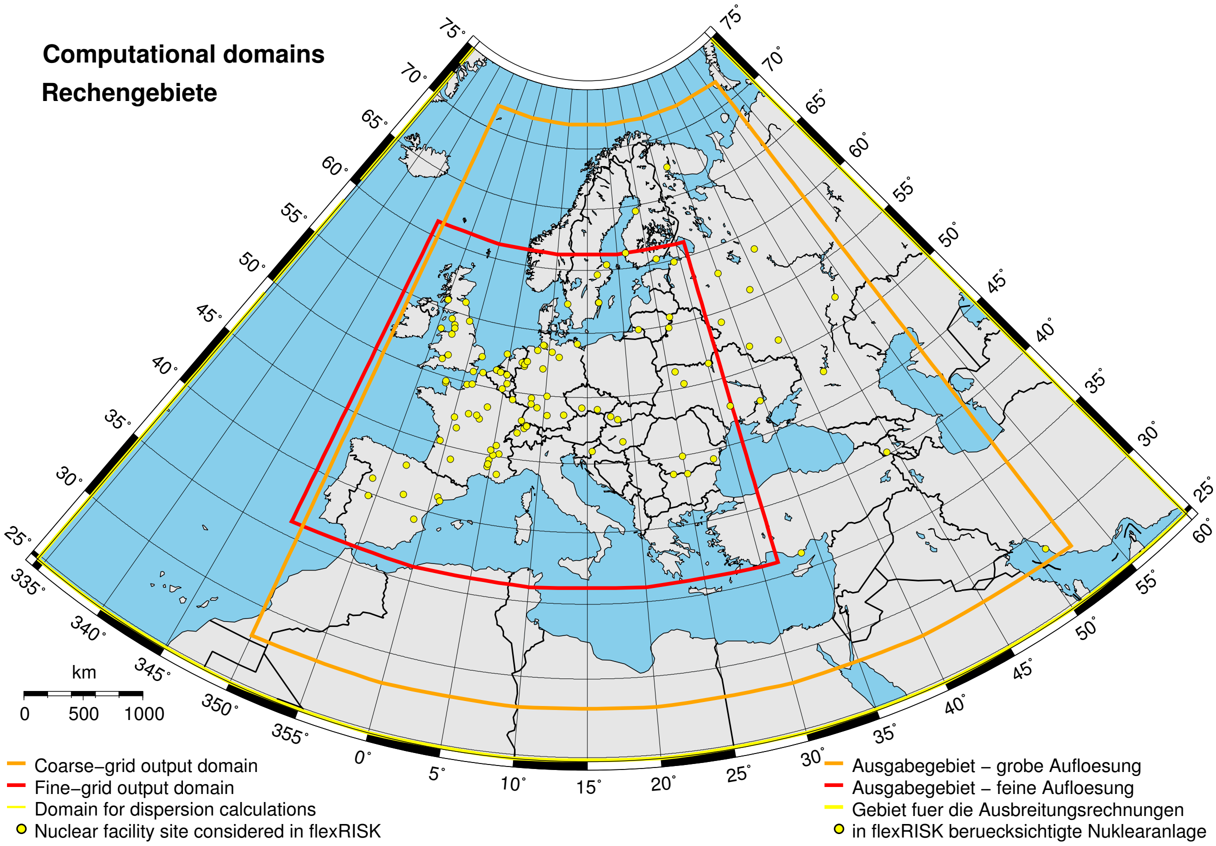

Figure 4: Domains used in the FLEXPART calculations for flexRISK.

Table 4: Parameters governing the deposition of the aerosol species.

Parameter	Value
Half-life	infinite (no on-line decay)
Wet deposition parameter A	1.E-4
Wet deposition parameter B	0.62
Density	2500 kg/m^3
Mean diameter	0.6 µm
Log variation of diametre	0.3

and where discussions to build nuclear power plants have started in some countries). It was also decided to include Busher, where Iran has recently started up an power reactor, and thus all the near and most of the middle east is included as well. The Ural mountains and nuclear installations there are not included; they are of little relevance for Austria or other central European countries.

Two computational species were used, noble gas, which is assumed to have no dry or wet deposition, and an aerosol species, which is given typical characteristics of accumulation-mode aerosol. Most radionuclides, the exceptions being noble gases and to some extent iodine, attach themselves to ambient aerosol particles and thus share their fate. The deposition parameters for the aerosol species are listed in Table 4. Usually, simulations of radionuclide dispersion apply at least a third species, for gaseous elemental iodine (I_2). We could not easily afford this computationally. If we had considered it, we would have to implement reductions elsewhere. Considering the very large uncertainty for the fraction of iodine that is occurring as gaseous iodine compared to aerosol-bound iodine, and the fact that differences in their behaviour are moderate, we subsumed all iodine under the aerosol species.

FLEXPART has the option to include radioactive decay by reducing the mass of a species during each time step by the factor $\exp(-\Delta t/\beta)$, where the decay constant $\beta = T_{1/2}/\ln 2$ is determined from the half life $T_{1/2}$ of the species. Not only does this calculation consume CPU time, if decay would be done on-line, for each nuclide with significantly different decay a separate computational species were needed, and this would increase the amount of output far beyond what is feasible. Decay chains may lead to alteration of the physical form of radionuclides. For example, the gaseous or iodine-bound ^{133}I decays to the noble gas ^{133}Xe. Therefore it would be desirable to calculate this on-line. However, such decay chains are not yet implemented in FLEXPART, and as explained, for an application like flexRISK, it would be too costly in terms of storage. Thus, the decay and decay chains are taken care of in post-processing (see Section 4.4).

3.5.2 Date, time, number and length of simulations

Based on the experience of RISKMAP, the duration of each simulation was set to 15 days maximum. If practically all (99.5%) radioactivity had left the air in the simulation domain before, runs would be terminated prematurely. As in flexRISK, a noble gas species is considered which does not undergo deposition, the criterion for early termination can be reached only if the contaminated air leaves through the domain boundaries, not by washout.

Two different periods form the base for the simulations, the year 1995, and the years 2000–2009.

The reason for selecting 1995 was that this period was used in RISKMAP. By repeating the simulations for the same release dates and times as used in RISKMAP, we are able to do comparisons. That is not the main purpose of flexRISK, however, such comparisons were used as plausibility tests, and the data are available for further investigation. There are 88 release start times in 1995; the interval between them was 4 d 1 h 32 min. From the results of RISKMAP, it was known that 88 cases are by far insufficient to obtain the climatological distribution of high-contamination events. For flexRISK, these dates and times were kept, only the starting times were rounded to the nearest full hour.

Even considering that the year 1995 had been selected on the base of a flow pattern statistics for the Alpine area to find a year that is as close as possible to the average with respect to wind direction frequencies, a single year is also short for climatological representativeness. In climatology, the normal period is 30 years. However, 10 years can give already a good sample of the climatological variability.

Quite some effort was invested in finding an algorithm that would generate a set of simulation start times (equal to release start times) that would fulfill the following conditions:

1. to equally sample the different seasons or months of the year,
2. to equally sample the different times of the day, and
3. not to have too much variability in the time intervals between subsequent releases.

(The first two conditions were already mentioned in Section 3.2, p. 26.)

Condition 1 is needed because dominant synoptic patterns (preferred large-scale flow directions), precipitation amounts and probabilities, and atmospheric stability have characteristic annual variations.

Condition 2 is needed because convective precipitation and atmospheric stability have characteristic diurnal variations. Obviously, it is also desirable that this condition is not only fulfilled on the average over a year or the whole 10 years, but it has to be fulfilled in each season or month as much as possible.

Finally, also condition 3 should be fulfilled, because meteorological variables are autocorrelated. This autocorrelation is significant on the 1- to 2-day time shift implied by the number of simulations done in flexRISK. If two calculations would start within a few hours, they would by far not be statistically independent samples. Such sample pairs would be contrary to making best use of the available number of calculations in the sense of statistical information.

While mathematical sampling theory provides a method (Latin squares) which would fulfill conditions 1 and 2, this method fails with condition 3. A simpler, ad-hoc scheme was thus used. A base interval of 1 d 8 h is used. Every third time, an additional hour is added. This ensures almost constant intervals, and we alternate sampling, at first, midnight, morning, afternoon, but through the leap hour, after 12 days (4 leap hours added) the sampling pattern has shifted to early morning, noon, evening, and so on. Figure 5 shows the properties resulting with the total period of 10 years minus 15 days (because of meteorological input data limits, there are no runs started after 2009-12-15). Note that not only

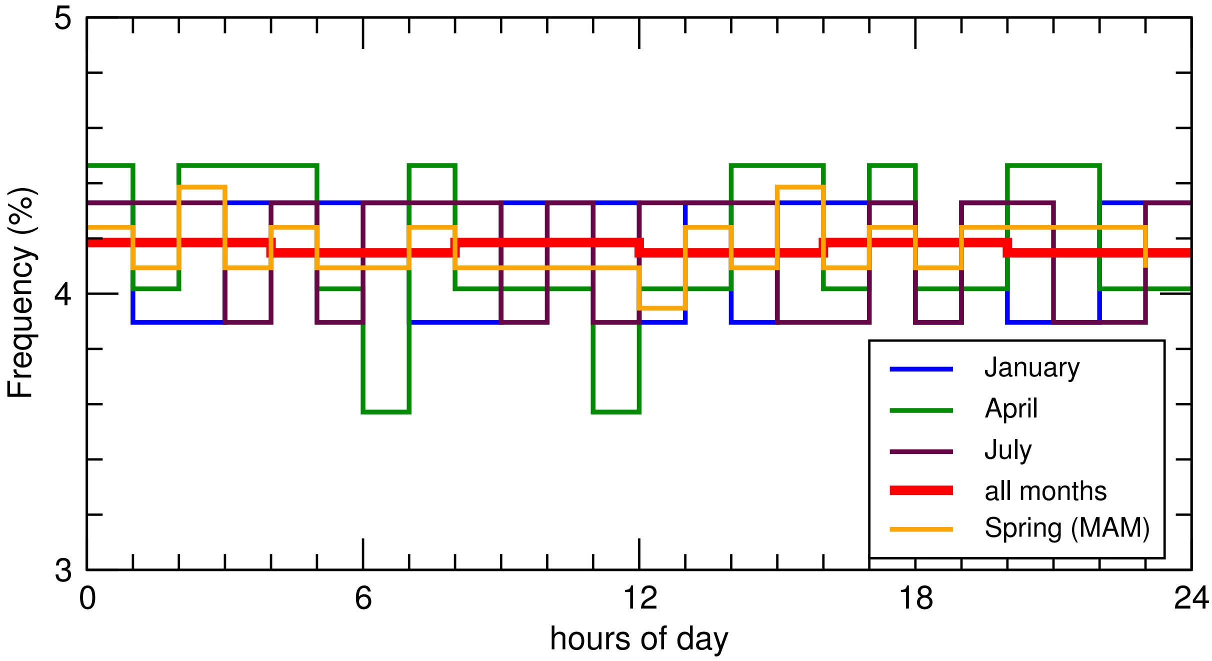

Figure 5: Frequency of occurrence of the hours of the day for the starting times of runs.

deviations from a homogeneous distribution are small even for single calendar months, and as their sign keeps changing, they cancel out over parts of the day. This satisfactory result could, however, only be reached with a relatively short interval and thus high number of runs. Increasing the density of runs much more would not make much sense because of the already mentioned autocorrelation. If more samples were desired, one should add more years.

This algorithm uses 2700 starting dates in the years 2000–2009 (270 to 272 in each year, 259 in 2009 so that runs end before the end of the year), or a total, including the year 1995, of 2788 dates.

Some sites host reactor blocks with designs different enough to yield different release shapes. For those sites, more than one run had to performed. In the 2010 runs, with two accident scenarios per reactor, even more release runs were needed. The total number of runs (2012) was 278,800, indicating that there were on the average 100 runs per date; with 88 sites, on average there are thus about 1.14 of release shapes per site.

3.6 Technical aspects

3.6.1 Preparation of the runs

It is not trivial to manage hundreds of thousands of FLEXPART runs. The first step was setting up a hierarchical directory structure (Fig. 6). The structure is organised by site, year, date, release shape. Then there is an `Options` directory which holds all the input data. Those input data which are the same for all runs are just symlinks. Output was collected in a separate directory (it consists of many files which were compressed into a `tgz` file by the production run script). Then there is the executable of FLEXPART (also a symlink) and the `pathnames` file which tells FLEXPART where options, output and meteorological input data are found or to be stored. The standard output during the production run is redirected to a file `stdout`.

To create and populate this tree, a `python` script (`mk_tree+input.py`) has been written. It reads the `specifications.xls` file provided by Work package 2 (see Section 2.6), and a list of dates. For creating the `RELEASES` and `COMMAND` files, it makes use of the `Genshi` templating engine which is also used to populate the web site (it can be used to create `xhtml` as well as simple text files like the FLEXPART input files). Input which is not obtained from any of the input files is hardcoded in a specific section of the script.

```
|-- Sites
|   |-- akku
|   |   |-- 1995
|   |   |   |-- 1995010121
|   |   |   |   |-- R1
|   |   |   |   |   |-- Options

|   |   |   |   |   |   |-- SPECIES -> ../../../../../../Static_input/SPECIES
|   |   |   |   |   |   |-- AGECLASSES -> ../../../../../../Static_input/AGECLASSES
|   |   |   |   |   |   |-- COMMAND
|   |   |   |   |   |   |-- IGBP_int1.dat -> ../../../../../../Static_input/IGBP_int1.dat
|   |   |   |   |   |   |-- OUTGRID -> ../../../../../../Static_input/OUTGRID
|   |   |   |   |   |   |-- OUTGRID_NEST -> ../../../../../../Static_input/OUTGRID_NEST
|   |   |   |   |   |   |-- RECEPTORS -> ../../../../../../Static_input/RECEPTORS
|   |   |   |   |   |   |-- RELEASES
|   |   |   |   |   |   |-- surfdata.t -> ../../../../../../Static_input/surfdata.t
|   |   |   |   |   |   `-- surfdepo.t -> ../../../../../../Static_input/surfdepo.t
|   |   |   |   |   |-- Output
|   |   |   |   |   |   `-- output.tgz
|   |   |   |   |   |-- flexpart.out -> ../../../../../Flexpart/flexpart.out
|   |   |   |   |   |-- pathnames
|   |   |   |   |   `-- stdout
```

Figure 6: Directory tree structure of FLEXPART runs. akku stands for the site Akkuyu (a standard 4-letter abbreviation was used for site names). R1 denotes release shape 1. The structure continues with the other sites and dates.

FLEXPART uses a base time step (`LSYNCTIME`) and release durations must be a multiple of it. Thus, the `mk_tree+input.py` script rounds these durations as required.

3.6.2 Production runs on the supercomputer

On a typical present-day Linux server (e.g., a Sun Fire with Xeon 3.0 GHz QuadCore CPU) a single run of the set-up described above takes on the order of 0.5 hours. Thus, a total of 300k runs will take 150k hours, or (1 year has 8760 hours) almost 20 years. A supercomputing facility with the possibility to run, say, 200 jobs in parallel is thus necessary to complete the task in a reasonable period of time (the example would give 0.1 years or about a month). flexRISK production runs were thus carried out on the "Vienna Scientific Cluster", a joint infrastructure of several universities in Vienna[1]. The 2010 runs were done on the VSC-1 machine, and most of the 2012 runs on the VSC-2 machine. VSC is mainly dedicated to standard parallel computing. flexRISK, however, falls into the category of "trivial parallelisation", i.e., to run a large number of serial jobs at the same time. As each run is rather short, block reservation of nodes was done by the VSC staff. Then jobs are mass submitted to the queue by a script. This script runs in `crontab` and resubmits new jobs whenever the number of waiting jobs goes below a defined number, to avoid flooding the queuing system with hundreds of thousands of jobs which would then hardly be manageable. Both for this submission script, and for interactively monitoring the progress of the work, a python script was written which looks for specific tag files created by each production job upon submission, run start and run completion. Figure 7 shows a sample output of the monitoring script. All these scripts were kindly written by VSC staff and proved extremely valuable. The 2012 production runs on VSC-2 (each node equipped with 2×8 cores and 32 GB of memory) could be completed in about two weeks.

Data transfer to and from the VSC was done with `rsync`. If changes have occurred, `rsync` will only transfer the changed files. Also, `rsync` is able to transfer the data without encryption, unlike `scp`, which is quite relevant for 2.6 TB of data. A transfer of the full data set takes a few days.

3.6.3 Postprocessing

Various postprocessing task needed to be done. This included conducting checks on the results, producing graphical output in the form of maps and bar plots, and various aggregation of output. All

[1] Details see `http://vsc.ac.at`.

```
[pesfle@l03 ~/Run_flexpart]$ ./status.py
1995010121 [new: ~][sub: 82-87][run: ~][suc: 1-67,69-72,74,75][cra: 68,73,76-81][err: ~]
1995010523 [new: ~][sub: 1-87][run: ~][suc: ~][cra: ~][err: ~]
1995011000 [new: ~][sub: 1-87][run: ~][suc: ~][cra: ~][err: ~]
1995011402 [new: 1-87][sub: ~][run: ~][suc: ~][cra: ~][err: ~]
1995011803 [new: 1-87][sub: ~][run: ~][suc: ~][cra: ~][err: ~]
1995012205 [new: 1-87][sub: ~][run: ~][suc: ~][cra: ~][err: ~]
1995012606 [new: 1-87][sub: ~][run: ~][suc: ~][cra: ~][err: ~]
1995013008 [new: 1-87][sub: ~][run: ~][suc: ~][cra: ~][err: ~]
1995020309 [new: 1-87][sub: ~][run: ~][suc: ~][cra: ~][err: ~]
1995020711 [new: 1-87][sub: ~][run: ~][suc: ~][cra: ~][err: ~]
1995021112 [new: ~][sub: 1-87][run: ~][suc: ~][cra: ~][err: ~]
1995021514 [new: 1-87][sub: ~][run: ~][suc: ~][cra: ~][err: ~]
1995021915 [new: 1-87][sub: ~][run: ~][suc: ~][cra: ~][err: ~]
1995022317 [new: 1-87][sub: ~][run: ~][suc: ~][cra: ~][err: ~]
1995022718 [new: 1-87][sub: ~][run: ~][suc: ~][cra: ~][err: ~]
1995030320 [new: 1-87][sub: ~][run: ~][suc: ~][cra: ~][err: ~]
1995030722 [new: 1-87][sub: ~][run: ~][suc: ~][cra: ~][err: ~]
1995031123 [new: 1-87][sub: ~][run: ~][suc: ~][cra: ~][err: ~]
1995031601 [new: 1-87][sub: ~][run: ~][suc: ~][cra: ~][err: ~]
1995032002 [new: 1-87][sub: ~][run: ~][suc: ~][cra: ~][err: ~]
1995032404 [new: ~][sub: 1-87][run: ~][suc: ~][cra: ~][err: ~]
1995032805 [new: 1-87][sub: ~][run: ~][suc: ~][cra: ~][err: ~]

.
.
.

1995120504 [new: 1-87][sub: ~][run: ~][suc: ~][cra: ~][err: ~]
1995120906 [new: 1-87][sub: ~][run: ~][suc: ~][cra: ~][err: ~]
1995121307 [new: 1-87][sub: ~][run: ~][suc: ~][cra: ~][err: ~]
1995121709 [new: 1-87][sub: ~][run: ~][suc: ~][cra: ~][err: ~]
1995122110 [new: 1-87][sub: ~][run: ~][suc: ~][cra: ~][err: ~]
2000010100 [new: ~][sub: 71][run: ~][suc: 1-70,72-87][cra: ~][err: ~]
#
#     7221  (new)        (not submitted yet)
#      355  (sub)mitted  (job queued via ./submit.sh)
#        0  (run)ning    (job started)
#      159  (suc)cessful ('CONGRATULATIONS' message found)
#        8  (cra)shed    (status 'running' but not visible in qstat)
#        0  (err)or      (no 'CONGRATULATIONS' message)
#     7743  total
```

Figure 7: Sample output of script to monitor runs' status in VSC. The numbers occurring in brackets refer to sites, which are numbered through softlinking the site directories to consecutive numbers.

the tasks that involved major data handling were done by `Fortran` programmes. Maps were plotted with `Fortran` programmes and the NCAR Graphics plotting library[2]. Bar plots were created with `python` and its `matplotlib`. Several auxiliary `python` and `bash` scripts were written and used for purposes such as preparing input files and launching postprocessing runs.

3.6.4 Web site

The flexRISK web site (`http://flexrisk.boku.ac.at/`) contains basic information about the nuclear facilities in flexRISK as well as a large number of results in graphical form. There are a total of about 700,000 files occupying about 124 GB (this includes all endpoints). Most of the web site was therefore generated and updated automatically. The basic structure was created with a `python` script using the `Genshi` templating engine. Graphical results generated by the above-mentioned (Section 3.6.3) `Fortran` and `python` runs were copied to the web server automatically. A php-based navigation gives access to all the results.

[2]NCAR Graphics is a free scientific visualisation package developed at the U.S. National Center for Atmospheric Research. For download and more information see `http://ngwww.ucar.edu/`. The so-called "Low-level utilities" consisting of Fortran subroutines were used.

4 Consequence assessment and dose calculation

In this section, definitions of doses and models underlying the flexRISK dose calculation are described briefly, and aims and methods of the flexRISK dose calculation are documented.

In flexRISK, we used the dose model of the International Commission on Radiological Protection (ICRP) because it is accepted in a substantial part of the international radiological community and widely used, despite its possible drawbacks. However, it should be noted that different aspects of the ICRP assumptions have been criticised, stating that recent scientific developments including DNA models, solubility factors and other information that would affect the dose model are not considered. These objections are mainly raised from groups or people not associated with the "nuclear establishment" (see, e.g., "Strahlentelex"[1], or Busby et al. (2010)). The decision to use mostly data from ICRP in flexRISK was made because they are complete, comprehensive, widely used and were also recommended by the project advisory group.

An interesting future option could be to compare results using different sets of dose coefficients and factors. Due to the flexible structure and modular programming of flexRISK, this would not be difficult.

4.1 General background on radiation doses

When radiation or radioactive particles are incorporated into human bodies, they may result in health effects even at low doses. To assess such effects, the impact of the activity has to be translated to dose and further on to health risks.

The first step is to calculate the *absorbed dose* D, that is the energy of the ionising radiation absorbed by mass (body tissue) :

$$D = \frac{\bar{E}}{m} \tag{4.1}$$

where $\bar{E}$ is the mean energy and m the mass absorbing the radiation. Its unit is Gray (Gy), 1 Gy = 1 $\mathrm{J\,kg^{-1}}$.

To include the effects of different types of radiation, D has to be multiplied with a radiation weighting factor. This results in the equivalent dose H. The equivalent dose for a specific tissue is calculated as

$$H_T = \sum_R w_R D_{T,R} \tag{4.2}$$

where the index T refers to the tissue type, w_R is the radiation weighting factor, and $D_{T,R}$ is the averaged absorbed dose for tissue T and type of radiation R. Its unit is Sievert (Sv). As Sievert is large unit (1 Sv whole-body dose already leads to acute radiation sickness), in practice milli-Sievert (mSv) is mostly used. Radiation weighting factors recommended by the ICRP are listed in Table 5.

By multiplying the equivalent dose with tissue weighting factors, the effective dose E is obtained as

$$E = \sum_T w_T H_T \tag{4.3}$$

where w_T with $\sum_T w_T = 1$ are the tissue weighting factors (Table 6). The effective dose is the most widely used dose measure. The tissue weighting factors given by the ICRP depend on the radiation type, like the equivalent dose, but also on the different detrimental effects for different body tissues. It is thus a sum of the equivalent doses for the single organs and tissues of the body, weighted by their sensitivity. The weighting factors are of crucial importance and have often been discussed and updated. Initially, in ICRP 26/30, these factors considered only the risk of fatal cancer and of serious hereditary effects. These factors were, however, revisited with a somewhat wider concept of what is considered as "detriment". In the latest ICRP recommendations, the weighting factors for organ radiosensitivity include additional health effects such as morbidity, radiation-induced cancer, and years-of-life lost. In order to properly assess radiation effects on the thyroid, which is very sensitive

[1] `http://www.strahlentelex.de/`

Table 5: Radiation weighting factors (w_R) according to ICRP 103 (ICRP, 2007, p. 64) and ICRP 60 (ICRP, 1991).

Type of radiation	w_R ICRP 60	w_R ICRP 103
Photons	1	1
Electrons and muons	1	1
Protons and charged pions		2
Protons, other than recoil protons, energy > 2 MeV	5	
Alpha particles, fission fragments, heavy ions	20	20
Neutrons < 10 keV	5	*
Neutrons 10-100 keV	10	*
Neutrons >100 keV – 2 MeV	20	*
Neutrons > 2 MeV – 20 MeV	10	*
Neutrons > 20 MeV	5	*

* continuous function of neutron energy

Table 6: Tissue weighting factors (w_T) according to ICRP (2007, p. 65, 69), ICRP 60 (ICRP, 1991) and ICRP 26 (ICRP, 1977).

Tissue	w_T ICRP 26	w_T ICRP 60	w_T ICRP 103
Bladder		0.05	0.04
Bone surface	0.03	0.01	0.01
Bone-marrow (red)	0.12	0.12	0.12
Brain			0.01
Breast	0.15	0.05	0.12
Colon		0.12	0.12
Gonads	0.25	0.20	0.08
Liver		0.05	0.04
Lung	0.12	0.12	0.12
Oesophagus		0.05	0.04
Salivary glands			0.01
Skin		0.01	0.01
Stomach		0.12	0.12
Thyroid	0.03	0.05	0.04
Remainder tissues*	0.30	0.05	0.12
Total	1.00	1.00	1.00

*Remainder tissues according to
ICRP 26: five organs;
ICRP 60: adrenals, brain, upper large intestine, small intestine, kidney, muscle, pancreas, spleen, thymus, uterus;
ICRP 103: adrenals, extrathoraic region, gall bladder, heart, kidneys, lymphatic modes, muscle, oral mucosa, pancreas, prostate (men), small intestine, spleen, thymus, uterus/cervix (women).

to radiation from radioactive iodine accumulating in this organ while thyroid cancers are considered to be relatively well treatable, it is necessary to determine the equivalent dose for the thyroid separately, as it is done also in flexRISK.

For the assessment of the equivalent doses, computational phantoms (male and female) and biokinetic models are used to analyse the distribution of doses to different organs and tissues. From these equivalent doses, the effective dose is calculated. The effective dose of the reference person is averaged over the male and the female phantom. It is planned to develop phantoms for children and for pregnant women and feti.

In an environment exposed to radiation, the rate at which it is absorbed is called the *dose rate* (Sv/s or mSv/h). When the radiation exposure is integrated over a certain time period, one speaks about the *committed* equivalent or effective dose . For exposure from incorporated nuclides, an integration time following the intake of 50 a for adults and 70 a for children is considered (ICRP, 2007, p. 72).

The annual effective dose for members of the public is the sum of the effective dose obtained within one year from external exposure and the committed effective dose from incorporated nuclides within this year (ICRP, 2007, p. 74).

4.2 Endpoints of flexRISK calculations

In the assessment of consequences of nuclear accidents, one refers to parameters resulting from the calculations and used in the assessment as so-called endpoints of the calculations. In flexRISK, there are contamination and dose endpoints. In detail:

1. Ground contamination with ^{137}Cs at the end of the simulation (Bqm^{-2}).
2. Air contamination with ^{131}I, integrated over the duration of the simulation (Bqs/m^3) (for visualisation on the web, also sequences of 3-h mean concentrations of ^{131}I are provided as gif movies to illustrate the time-dependent behaviour of the radioactive cloud.
3. Thyroid dose from inhalation of iodine and tellurium isotopes during 7 d of exposure (mSv) – relevant for administration of stable iodine
4. Effective dose for 7 d of exposure, all nuclides and (considered) pathways (mSv) – relevant for sheltering.
5. Effective dose for 30 d of exposure, all nuclides, only groundshine (mSv) – relevant for temporary relocation of population.
6. Effective dose for 1 a of exposure, all (considered) pathways (mSv) – relevant for comparison with general radiation protection guidelines.

The doses were calculated for children and adults. For children, the age-group achieving the highest dose was chosen (children up to one year).

As primary damage parameter, we considered the frequency of exceedance for certain levels of ground contamination and of doses. For ground contamination, levels that have been used after the nuclear accident of Chernobyl were applied (Table 7). In the case of doses, the primary damage parameters were the probabilities for exceeding dose and intervention levels as defined in:

1. Austrian intervention levels for sheltering, iodine prophylaxis and temporary relocation;
2. Dose limit for members of the public according to the Council Directive 96/29 Euratom, Art. 13 (EURATOM, 1996).

Table 7: Deposition levels in areas contaminated by the Chernobyl accident (Shevchik and Gurachevsky, 2006).

Zone	Effective dose (mSv/a)	Cs-137 (kBqm^{-2})	Sr-90 (kBqm^{-2})	Pu-238, Pu-239, Pu-240 (kBqm^{-2})
Zone of regular radiation control	<1	37-185	5.55-18.5	0.37-0.74
Zone with the right to resettlement	1-5	185-555	18.5-74	0.74-1.85
Zone of subsequent resettlement	>5	555-1,480	74-111	1.85-3.7
Zone of primary resettlement	>5	>1,480	>111	>3.7
Zone of evacuation (exclusion zone)	Territory around Chernobyl NPP, from which population was evacuated in 1986			

4.2.1 Ground contamination levels

After the Chernobyl disaster, levels of ground contamination with ^{137}Cs proved to be of special importance because ^{137}Cs can be easily measured and can be used as a reference nuclide for medium-

Table 8: Intervention levels for starting agricultural measures in Austria and Germany (AG Proben, 2010; SSK, 2008).

Nuclide	Deposition (Bqm^{-2})	Time-integrated concentration in air ($Bqsm^{-3}$)
Cs-137	0.65	6.1E5
I-131	0.70	1.3E6

and long-term consequences. Table 7 shows the deposition levels that were used in the former Soviet Union in the aftermath of the catastrophe of Chernobyl for radiation protection purposes. These levels are useful to categorise ground contamination for constructing damage parameters, and were thus used also in flexRISK. Moreover, a deposition value of 5 kBq ^{137}Cs / m^2 is used to compare contamination to that caused by atomic bomb testing in the second half of the last century. Results for exceedance of the contamination level of 185 kBq ^{137}Cs / m^2 can also be used to compare flexRISK results with those of the predecessor project RISKMAP, where a threshold of 185 kBq ^{137}Cs / m^2 was used.

Agricultural intervention measures

Moreover, results of ground contamination can be used to be compared to the start of certain agricultural intervention measures. These measures include earlier harvesting, closing of greenhouses and covering of plants, putting livestock in stables etc. For these measures, Austria and Germany defined the levels listed in Table 8.

These agricultural measures are quite complex and take some time. This might be especially problematic if there is only very little time between the start of an accident and the arrival of the first radioactive cloud. From the flexRISK results, it is also possible to evaluate arrival times, though this was not done so far.

For very high contaminations above a level of about 7,000 MBq ^{137}Cs / m^2, agricultural area can be no longer used and would probably be afforested (SSK, 2008).

The frequency of exceedance of the following levels was considered:

1. 5 kBq ^{137}Cs / m^2 – relevant for comparison with worldwide fallout of atomic bomb testing
2. 37 kBq ^{137}Cs / m^2 – relevant for lower limit of contamination making radiation controls necessary; defined as “non-contaminated” by the IAEA (IAEA, 2008)
3. 185 kBq ^{137}Cs / m^2 – relevant because of possible exceedance of a yearly dose of 1 mSv, has been highest value in Austria after Chernobyl
4. 555 kBq ^{137}Cs / m^2 – relevant after Chernobyl for subsequent resettlement
5. 1480 kBq ^{137}Cs / m^2 – relevant after Chernobyl for primary resettlement

4.2.2 Intervention measures for population

Some of the most important measures to be taken immediately after a nuclear accident include sheltering and iodine prophylaxis with tablets of stable potassium iodine. Additionally, for flexRISK we calculated intervention levels for temporary relocation – an intervention measure placed in between evacuation and long-term relocation.

It seems sensible to use intervention dose levels that are regulated by law to describe some of the effects on a country or a population group. For Austria, these are primarily dose levels of the Intervention Regulation (Lebensministerium, 2007). Different countries use different intervention levels for these measures. Intervention policy in Austria tends to be more cautious and mostly uses dose levels lower than in Germany or as recommended by the IAEA, as Table 9 shows.

Additionally, a comparison with the former Austrian intervention levels (Rahmenempfehlungen, BMGKS, 1992) is made by assessing the exceedance of effective doses of 2.5, 25 and 250 mSv in the first year.

Table 9: Intervention levels for selected intervention measures, different sources. Austria – Lebensministerium (2007), Germany – SSK (2008), IAEA – IAEA (2011a). Levels for sheltering refer to effective dose in 7 d, for iodine prophylaxis to thyroid dose in 7 d.

Measure	Age group	Austria	Germany	IAEA
Sheltering	Children, pregnant women	1 mSv	10 mSv	100 mSv+
	Adults	10 mSv	10 mSv	100 mSv
Iodine prophylaxis	Children	10 mSv	50 mSv	50 mSv
	Adults up to 40 years, pregnant and nursing women	100 mSv	250 mSv	50 mSv*
	Adults over 40 years	500 mSv	**	

+ fetuses
* before: 100 mSv avertable dose
** Adults over 45 years should not take the iodine tablets at all

These levels were used as lower thresholds for intervention levels II, III and IV. Level II included sheltering for children and pregnant women and administration of iodine tablets to risk groups. In level III, all people should take temporary shelter, evacuations could occur and iodine tablets could be administered also to adults. Level IV included intervention measures such as evacuation and relocation.

4.2.3 Dose limit for members of the public

Effective doses are also compared to the current dose limit for members of the public of 1 mSv per year (from artificial radioactive sources) according to Council Directive 96/29/Euratom. In the case of an intervention, this limit will not be valid in the first time after an accident. For the accident in Fukushima, the ICRP recommended a maximum annual dose of 20 to 100 mSv for the public with the aim of reducing it quickly back to 1 mSv/a (ICRP, 2011). Because Austria often uses limits lower than in countries with a nuclear industry, an intervention dose level between 1 and 20 mSv appears more plausible in the context of Austria.

Because of the missing ingestion pathway (see Section 4.3.2), calculated doses will considerably underestimate real doses in the case of an accident, even if otherwise being conservative.

In flexRISK, the probability of exceedance of the levels and limits listed in Table 10 was calculated.

Table 10: Endpoints of the dose calculation.

Endpoint of dose calculation	Limit/level adults (mSv)	Limit/level children (< 18 a) (mSv)	Type of dose	Nuclides	Pathways	Contamination period†	Integration period for dose calculation
Intervention level for sheltering	10	1	Effective dose	All	Inhalation, ground, cloud	7 d*	Inhalation: lifetime Ground, cloud: 7 d
Intervention level for iodine prophylaxis	100	10	Thyroid dose	Iodines	Inhalation	7 d*	Lifetime
Intervention level for temporary relocation	30	30	Effective dose	All	Ground	30 d	30 d
Dose values considered for members of the public** (average per year)	2.5 / 25 / 250	2.5 / 25 / 250	Effective dose	All	Inhalation, ground, cloud	1 a	Inhalation: lifetime Ground, cloud: 1 a

† Start with first non-zero contamination.
* 7 d and 30 d doses were calculated for the 7 d (30 d) starting from the arrival of the first non-zero value of air or ground contamination, and then for all periods starting subsequently three-hour intervals later until the end of the dispersion calculations. Among these values, the one with the highest dose is presented in the results. This is not always the first one.
** A comparison with the former Austrian intervention levels (Rahmenempfehlungen) (BMGKS, 1992) is made by assessing the exceedance of effective doses of 2.5, 25 and 250 mSv in the first year.

4.3 Methods of dose calculation

4.3.1 Nuclides considered for the dose calculation

Accidental releases from nuclear installations contain many radionuclides but not all of them contribute equally to the dose received by the population. In order to make a first assessment of the radionuclides of interest for flexRISK, some test runs with PC COSYMA (European Commmission, 1995, a code for assessing radiological impacts from accidents based on a segmented Gaussian plume dispersion model) were performed.

The tests were performed with release scenarios from the US EPR final safety report (AREVA, 2009) and reactor inventories described in Germany's Radiation Protection Commission's “Guide for Protection in Radiological Emergencies” (SSK, 2003).

Several runs have been carried out with the most probable early release scenario from AREVA (2009, Release category 304) considering five different stability classes under dry conditions and one test with slight continuous rain to include washout in the evaluation. An additional run using an unlikely early release scenario with maximum activity released (AREVA, 2009, Release category 802) was also undertaken.

The test runs were evaluated with respect to the relative contributions of all major radionuclides to different 7-day organ doses, and in one case also the 1-year doses, at distances of 28 and 155 km from the release point. Of special interest are the effective dose, the thyroid dose and the bone marrow dose (the latter for leukemia risk).

The following radionuclides contribute 98% of the doses (thyroid and bone marrow):

- 20 nuclides if both 28 km and 155 km are considered: Cs-134, Cs-136, Cs-137, I-131, I-132, I-133, I-134, I-135, Kr-87, Kr-88, Rb-88, Ru-103, Ru-105, Ru-106, Sr-89, Sr-91, Te-131m, Te-132, Xe-133, Xe-135
- 19 nuclides if only 155 km is considered: Cs-134, Cs-136, Cs-137, I-131, I-132, I-133, I-135, Kr-87, Kr-88, Rb-88, Ru-103, Ru-105, Ru-106, Sr-89, Sr-91, Te-131m, Te-132, Xe-133, Xe-135 (I-134 falling out of the list)

Fifteen radionuclides contribute 95% of the doses (thyroid and bone marrow) at a distance of 155 km. These nuclides are listed together with their contributions in Table 11.

Comparing the contribution of these nuclides to the effective dose it can be shown that 14 out of these 15 nuclides are also relevant for the short-term effective dose, which is an important indicator according to the Intervention Regulation (Lebensministerium, 2007).

The list of 20 nuclides as given above was used in flexRISK for calculating the doses.

One of the problems that had to be dealt with was the contribution to the dose from the members of the decay chains of the radionuclides selected. Since the decay chains were not explicitly calculated during the transport and deposition processes in the dispersion calculations, a posteriori treatment had to be done to estimate the activity of the progeny. The decay chains implemented were:

$^{131m}\mathrm{Te} \xrightarrow{0.778} {}^{131}\mathrm{Te} \longrightarrow {}^{131}\mathrm{I} \longrightarrow {}^{131m}\mathrm{Xe}$

$^{133}\mathrm{I} \xrightarrow{0.029} {}^{133m}\mathrm{Xe} \longrightarrow {}^{133}\mathrm{Xe}$

$^{133}\mathrm{I} \xrightarrow{0.971} {}^{133}\mathrm{Xe}$

$^{135}\mathrm{I} \xrightarrow{0.154} {}^{135m}\mathrm{Xe} \longrightarrow {}^{135}\mathrm{Xe}$

$^{135}\mathrm{I} \xrightarrow{0.846} {}^{135}\mathrm{Xe}$

$^{91}\mathrm{Sr} \xrightarrow{0.422} {}^{91}\mathrm{Y}$

$^{105}\mathrm{Ru} \xrightarrow{1.0} {}^{105}\mathrm{Rh}$

Note that only radioactive nuclides are included, not the stable end points of the decay. The numbers over the arrows are the branching fractions for the respective decay mode.

Table 11: List of radionuclides that contribute 95% of the doses, together with their contributions.

Nuclide	Contribution to thyroid dose (%)	Contribution to bone-marrow dose (%)
Cs-134	21.2	36.4
Cs-136	6.5	8.0
Cs-137	14.4	9.4
I-131	31.6	5.2
I-132	1.8	6.7
I-133	30.6	3.9
I-135	4.8	4.3
Kr-88	0.0	6.2
Rb-88	0.0	2.9
Ru-103	2.5	6.2
Ru-106	0.0	2.8
Sr-89	0.0	2.8
Sr-91	0.0	1.3
Te-132	9.3	19.4
Xe-135	1.7	2.5

4.3.2 Pathways

Pathways considered in flexRISK dose calculations are ground-shine, cloud-shine and inhalation. For different contamination periods, nuclides and organs only a subset of these are used, however, depending on the endpoints, as prescribed by certain intervention criteria.

Resuspension was not included because the resulting dose is considered to be very small (SSK, 2003). Also the test runs with PC-Cosyma showed that resuspension contributed only a very small fraction to the dose.

The ingestion pathway is not included because the necessary modelling would have been too complex for the scope of this project. Not only are transfer factors dependent on the season (state of vegetation), realistic assessments would need to consider the complex spatial patterns of production and consumption. Realistic consideration of countermeasures would also be very complex and even then, one would not know how close to reality it would be. Moreover, the intervention levels for the countermeasures considered do not depend on the ingestion doses.

However, for the lifetime and one-year doses, ingestion can make a significant contribution to effective and thyroid doses. This has to be kept in mind especially when interpreting these doses.

In Austria, doses resulting from ingestion of ^{131}I, ^{137}Cs and ^{90}Sr after the Chernobyl disaster have been studied (BKA, 1988; Mück et al., 1991).

Thyroid doses for 3-month-old children in Austria resulting from consumption of breast milk contaminated with ^{131}I were 2.1 mSv for the first year after Chernobyl, for consumption of milk or two-third-milk[2] 9.63 mSv. For highly contaminated areas in Austria, up to 13.57 mSv thyroid dose were reached by babies. This is 2 to 5 times more than the inhalation dose that was reached in the same period (BKA, 1988, p. 196).

For adults, thyroid doses resulting from consumption of milk and vegetables contaminated with ^{131}I in the first year were 1.2-1.7 mSv, this is about the same as the inhalation dose.

These thyroid dose assessments are reported to overestimate real thyroid burdens a bit (BKA, 1988, p. 197), especially because food limits and other intervention measures (e.g. ban on green fodder) have been quite rigorous in Austria.

Iodine ingestion doses occurred mainly in the first time after the Chernobyl accident. Food contamination with caesium arises over a much longer period. For babies, the ingestion dose resulting from

[2] Two-third-milk = 2:1 cow's milk : water

Table 12: Effective doses after Chernobyl in Austria, contribution of different pathways. (a) Doses for adults for the first two years (BKA, 1988, p. 226), (b) doses for babies < 1 a fed with milk, first year (BKA, 1988, p. 225).

(a) Adults

Pathway	1st year (mSv)	1st year (%)	2nd year (mSv)	2nd year (%)
External radiation	0.11	19.3	0.045	25.0
Inhalation	0.025	4.4	–	
Ingestion:				
Iodine	0.04	7.0	–	–
Caesium	0.39	68.4	0.13	72.2
Others	0.006	1.1	0.004	2.2
Total	0.57		0.18	

(b) Babies

Pathway	1st year (mSv)	1st year (%)
External radiation	0.12	9.2
Inhalation	0.42	32.8
Ingestion:		
Iodine	0.29	22.6
Caesium	0.46	35.4
Others		
Total	1.29	100.0

intake of ^{137}Cs was assessed as 0.46 mSv in the first and 0.1 mSv in the second year, for adults as 0.39 and 0.13 mSv, respectively (BKA, 1988, p. 204).

The effective strontium ingestion dose for babies was up to 0.9 μSv and for adults 5.9 μSv (BKA, 1988, p. 209).

The contributions of the different pathways in the first two years after the Chernobyl accident are summarised in Table 12. The data show that ingestion is the most important pathway in the first years. The doses also differ with the seasons, the highest first-year doses can be expected for fallout occurring in summer (Mück et al., 1991).

To make an assessment of the underestimation of the total dose by excluding the ingestion dose, one has to distinguish between babies and adults. For babies, especially those who are fed with normal milk, more than half of the total dose is due to ingestion (58%). For adults, this value is 75% for the first year. This may be valid for regions that have similar nutritional habits, contamination patterns (activity, weather, season, . . .) and countermeasures as Austria in 1986/1987.

4.3.3 Inhalation dose

Dose coefficients for inhalation dose calculation used are taken from ICRP (1996). Coefficients for adults and three-month-old children were included for effective and thyroid doses into the spreadsheet continuing the input for the dose calculations (see Section 4.7).

Radioactive substances can be absorbed from the respiratory tract into body fluids in different ways. ICRP publishes for up to four absorption types for each nuclide coefficient. These types are:

- Type F (fast absorption);
- Type M (moderate absorption);
- Type S (slow absorption);
- Type V (very fast absorption).

If the absorption type of the material of interest is not known, ICRP recommends a type. For flexRISK, only these recommended absorption types are used (Jackson, 1996). If no type is recommended, the most restrictive value is used.

Also size, shape and density of the particles carrying the radionuclides have an influence on the resulting dose. For the calculation of exposures of members of the public, the default recommendation (ICRP, 1996) is 1 μm AMAD (Activity Median Aerodynamic Diameter). This was taken into account.

The inhalation dose is influenced by breathing rates. For the ICRP coefficients, the reference subjects are taken to be nose-breathers whose daily time budgets and ventilation parameters are given in ICRP (1995, p. 9ff.). Three-month-old children are assumed to stay indoor all 24 h of the day, be asleep 17 h and do light exercise for 7 h. The reference adult (male) stays indoors 22 hours and outdoor 2 h; he is assumed to sleep 8 h, sit 6 h, do light exercise for 9.75 h and heavy exercise for 0.25 h per day.

4.3.4 External dose from submersion (cloudshine)

The external dose from activity in air was computed assuming a semi-infinite cloud using the Canadian dose coefficients (Health Canada, 1999). These coefficients are taken from the database of Eckerman and Leggett (1996). They were calculated for mono-energetic photons in a semi-infinite cloud source into which a human phantom is placed.

Eckerman and Leggett (1996) give dose coefficients for all nuclides, for the cloud and ground pathways, and with and without including daughter products. Health Canada (1999) additionally published a list of dose coefficients for some of the nuclides considered in flexRISK, including decay products. With the underlying data from Eckerman and Leggett (1996) it was possible to calculate decay products and related doses for all decay chains needed.

4.3.5 External dose from groundshine

Dose coefficients from groundshine were also taken from Health Canada (1999, p. 8 f.), based on the data base of Eckerman and Leggett (1996). These coefficients assume an infinite isotropic source of monoenergetic photons, located at the air-ground interface, with a human adult phantom placed at this interface. This phantom is based on Christy and Eckerman (1987) from the ICRP reference man (mathematical model). The phantom is assumed as hermaphrodite, and Health Canada (1999) does not recommend a gender correction factor. They recommended to consider age dependency by multiplication with a factor of 1.5 for children up to two years. The dose factors are provided with and without the contributions from the decay products of the respective nuclides.

4.3.6 Weighting factors

Because no complete dose coefficient sets were available during the project duration (even the new ICRP weighting factors from 2007 are not complete), dose coefficients with weighting factors from ICRP 60 (ICRP, 1991) were used.

4.3.7 Dose reduction factors

In the sets of external dose coefficients from Eckerman and Leggett (1996), no factors are applied for location, shielding, ground roughness, duration of exposure, non-uniform or finite sources. Especially for long-term doses, such factors are needed to produce more realistic results.

In SSK (2003), a correction factor b for effects of soil roughness and shielding through migration into the soil is introduced, with $b = 1$ for short-term doses and $b = 0.5$ for long-term doses.

In RODOS V06 the following equation is applied:

$$y(t) = 0.6e^{-\lambda t} + 0.4, \tag{4.4}$$

with λ = 1.01E-3 per day, where $y(t)$ is a time-dependent correction factor. This formula does not include effects of soil roughness. For short-term doses, the resulting factor is about 1, and for 1-year doses about 0.8 (Jacob, 1991).

In flexRISK, a factor of 1 is used for 7 d and 30 d doses, and a factor of 0.8 for 1 a doses, and for lifetime doses a factor 0.5, in order to use conservative factors.

A location factor is defined as the ratio of the dose received at a specific location (e.g. in a building) to that received outdoors without shielding. Location factors were applied according to a suggestion of the flexRISK Advisory Group to use the factors from RODOS (Müller et al., 2003), and according to Lebensministerium (2007).

In the Intervention Regulation (Lebensministerium, 2007), a location factor of 1 is assumed for assessing the intervention levels (iodine prophylaxis, sheltering, temporary relocation).

For all other endpoints, the factors from RODOS were applied. Location factors in RODOS are given for

Table 13: Location factors used in RODOS, Päsler-Sauer (2007, p. 17), Müller et al. (2003, p. 54).

Shielding	Inhalation		Cloudshine	Groundshine
	noble gases	aerosols		
Low shielding	1	0.5	0.8	0.5
Medium shielding	1	0.5	0.5	0.1
High shielding	1	0.5	0.2	0.01
Street	1	1	1	1

– streets and three building types (low, medium, high shielding),
– pathways inhalation short-term, inhalation long-term (from resuspension), groundshine short- and long-term, cloudshine, and
– fraction of time spent indoors (default occupancy factor = 0.8).

RODOS uses “shielding grids” for radio-ecological regions (Päsler-Sauer, 2007, p. 17) depending on the population density:

– < 100 people/km^2 (lower limit): low shielding;
– 100-250 people/km^2: medium shielding;
– ≥ 250 people/km^2 (upper limit): high shielding.

The location factor for the 1 a and lifetime doses has to consider shielding for times of staying indoor (80% of the time according to default occupancy factor) and outdoor (20%). For example, the location factor for an individual living in a high density grid cell is calculated as $0.8 \cdot 0.01 + 0.2 \cdot 1 = 0.208$.

Population data on raster of about 1 km^2 (30") cell size from CIESIN (1995) have been used to calculate average dose reduction factors for each model grid cell.

4.4 Calculation of contamination parameters

The FLEXPART calculations (with modifications introduced for flexRISK) deliver

– source-receptor sensitivity (concentration resulting from a unit release) for 3-h mean concentration, $c^*_{j,k,n}$, and
– source-receptor sensitivity (deposition resulting from a unit release) for 3-h accumulated deposition, $d^*_{k,n}$

where j refers to the computational species ($j = 1$ for noble gas and $j = 2$ for aerosol-bound nuclides), k refers to the phases of the release, and n denotes the time interval from the start of the simulation. The duration Δt of each time interval was 3 h.

The actual average concentration $c_{i,n}$ of nuclide i in time interval n from t_1 until t_2, where t is counted from the stop of the chain reaction, is calculated in the postprocessing of the FLEXPART output as

$$c_{i,n} = F_i(t_1, t_2) \sum_k c^*_{j(i),k,n} Q_{i,k}. \tag{4.5}$$

with

$$F_i(t_1, t_2) = \frac{\exp(-\lambda_i t_2) - \exp(-\lambda_i t_1)}{-\lambda_i (t_2 - t_1)} \tag{4.6}$$

where $Q_{i,k}$ is the release of nuclide i in release phase k, and λ_i is the decay constant for nuclide i. $j(i)$ is the index of the computational species of the nuclide i. Note that the average concentration is calculated analytically under the assumption that the source-receptor relationship during the time interval is constant, which is a simplification. Shortly after the release, when gradients are stronger and thus temporal variability of concentrations is higher, the ensuing uncertainty will be larger than after longer transport times. The only option to avoid this is to calculate the decay on-line, which for our problem would be prohibitive in terms of computational and even more storage costs, as explained in Chapter 3. In the code, the factor for the decay had been pre-calculated for each nuclide, release shape and time interval and was read from a look-up table. The time-integrated concentration $C_{i,n}$ (integrated up to the n-th time interval) is calculated as

$$C_{i,n} = \Delta t \sum_{n=1}^{n} c_{i,n}. \tag{4.7}$$

The total deposition D_i at the end of the simulation for a nuclide i with a half-life that is long compared to the duration of the simulation, such as ^{137}Cs, is simply

$$D_i = \sum_{n=1}^{N} \sum_{k} d^*_{j(i),k,n} Q_{i,k} \tag{4.8}$$

with N being the total number of time steps in the simulation. Deposition of nuclides with shorter half-lives was not considered as an endpoint. It is relevant only as an intermediate parameter for dose calculation and is explained in Section 4.5.

4.5 Calculation of doses

4.5.1 General

A dose E (thyroid or effective) incurred due to exposition in the time interval from t_1 until t_2 is calculated as

$$E(t_1, t_2) = \sum_i \left[\sum_{p=1}^{2} \left(f^l_p f^d_{i,p} \sum_{n\in[t_1,t^*]} C_{i,n} \right) + f^r_{p=3} f^l_{p=3} f^d_{i,p=3} \int_{t_1}^{t_2} D_i(t)\mathrm{d}t \right], \tag{4.9}$$

where p refers to the pathway (1 and 2 being inhalation and cloudshine, 3 groundshine), f^l is the location factor (dose reduction due to being indoor), f^d is the dose factor, and f^r the reduction factor for groundshine. Other variables are defined as in the previous section. Note that we are not showing here an index for the type of dose and don't indicate the fact that some factors are different for adults and children in order to make the formula not too complicated. Time t^* is the smaller one of t_2 and the end time of the FLEXPART simulation – after this time we assume that airborne radioactivity is not present anymore. This is the general formula which simplifies according to the pathways considered.

In Eq. 4.9, a time integral over the deposition (ground contamination) appears. In order to calculate this numerically, we calculate the average ground contamination during each FLEXPART output interval as shown in Eq. 4.10. The calculation at each step takes the pre-existing deposition from steps 1 to $n-1$ and adds the deposition arriving during step n. Thus, the time-integrated deposited activity in timestep n, integrated from the beginning of the step at t_1 until the end of the step at t_2, is

$$D^*_{i,n} = D^*_{i,n-1} G_i(\Delta T) F_i(0, 3\mathrm{h}) + F_i(t_1, t_2) \sum_k d^*_{j(i),k,n} Q_{i,k} + P(D^*_{i',n-1}) \tag{4.10}$$

where

$$G_i(\Delta T) = \lambda \Delta T \exp(-\lambda \Delta T) \tag{4.11}$$

serves to convert the average activity from the previous interval to the activity at the end of the previous interval, so that the decay factor F (see Eq. 4.6) can be applied. P stands for progeny in a decay chain (from some nuclide i'). Then this is extended until 30 d after the start of the calculation (the second term does not need to be considered anymore, as no new contributions arrive), so that we can obtain the 30 d doses. For the doses with longer exposition periods (1 a or lifetime, which means 50 a or 70 a), the integral for the period from end of day 30 on is calculated in a single step.

4.5.2 “Seven-day problem”

The Austrian emergency planning guidelines (Lebensministerium, 2007) state exposition periods for which certain doses should be calculated in order to determine the appropriateness of measures to be taken. For instance, administration of stable iodine and sheltering are based on 7-day doses. It is, however, not defined which seven days should be considered. The situation is similar in other countries. Switzerland, for example, uses only a 2-day period of exposure for stable iodine administration which makes the question “which seven (or two) days?” even more relevant. One might think that it is natural to compute the period from the first arrival of radioactivity. However, if the first arrival is not associated with the main peak of concentration, and if significant amounts or radioactivity arrive later than 7 d after the first arrival, this contribution would be excluded. Obviously, the 7 d and even more the 2 d rules have been formulated with a simple event in mind where mainly one cloud of radioactivity moves over the receptor point considered. However, already the Chernobyl disaster has shown that, firstly, releases may be multi-day, and secondly, due to complicated transport patterns, contamination can arrive in multiple batches, separated by days. The Fukushima disaster confirmed this (Stohl et al., 2012).

Now, the question of the statistical relevance of the possible deviation between the first interval and the maximum interval may be posed. Therefore, in flexRISK the 7-d iodine inhalation dose has not only been evaluated for the seven days starting with the first contamination, but for all the following 7-d periods, each starting 3 h later. At the end, the period which gives the highest dose was identified. This is the dose reported in the evaluation. Ratios between the first and the maximum dose were evaluated; corresponding results are reported in Section 5.5.1.

4.6 Aggregated parameters

As explained in Section 4.2, the exceedance of thresholds of contamination and dose was selected as the damage parameter. The risk parameters produced are the frequencies for such exceedance of thresholds. There are different levels of risk aggregation, and their corresponding risk parameters are explained below.

4.6.1 Risk per NPP unit

To map the risk originating from a single nuclear power plant unit l, for each grid cell the empirical probabilities

$$P^l_{i,j,k} = \frac{n_{i,j,k}(D > D_k)}{N} \tag{4.12}$$

were calculated and displayed as maps. Here, i, j refer to the grid cell index (East, North). $n_{i,j,k}(D > D_k)$ is the number of cases where the actual deposition D exceeded the prescribed threshold D_k (the index k denotes different thresholds), and N is the total number of runs. Thus, this parameter includes only the meteorological frequency and does not include frequencies of accidents and releases. It gives the probability, due to the meteorological conditions, that if a release of the defined characteristics (source term) occurs, it will contaminate a certain grid cell above the defined threshold. Risks for exceeding dose thresholds were defined and calculated in completely analogous way.

In addition, also the mean deposition (dose) values were calculated. However, this parameter is of limited value as the frequency distribution of contamination and dose values is L-shaped (roughly lognormal), and thus the mean is very sensitive to the highest values.

These calculations were done for all the NPP units in the domain, regardless of their operational status.

In addition to maps, risk as function of distance was calculated. For this purpose, the distance of the grid cell centres to the NPP sites were calculated and grouped in distance bands of 20 km width (0–20 km, 20–40 km, etc.). Then for each distance band, a frequency distribution of the contamination values occurring within it for all of the N weather situations was constructed, and certain percentiles (50, 75, 90, 95, 98, 99, 99.9, 100) were extracted from it. For example, the contamination or dose value for the 95th percentile is the value that would not be exceeded in 95% of the sample, where the sample includes all the grid points in the respective distance band and all the weather situations. In 5% of the cases, the value would be higher. As the release frequency is not included, this is a conditional probability if a release as defined would happen. Results are shown as graphs with probability versus distance for the various percentiles. As 50% of a distance band is rarely contaminated in one event, the value of the 50th percentile, and still also the 75th percentile, is rather low and not interesting. Most interesting are the high percentiles – they show what the “worst case” would be, where it is open to the reader on which of the high percentiles one wants to settle down. The maximum values (100th percentile) are obviously statistically less well defined, and will also be more affected by details of the dispersion parameterisations. They are therefore not recommended for consideration and will in generally not be shown. To a lesser extent, this applies also to the 99.9th percentile. Sample results are discussed in Section 5.5 (Figures 28, 29).

The latter type of calculation was only done for one site in Belgium which is considered representative for conditions in Central Europe not influenced much by mountains.

4.6.2 Risk originating from countries

In order to determine the total risk from all the nuclear power plants of one country, the probabilities of the NPPs on its territory (selected according to operation scenarios, see Section 2.5) are added up. However, due to different construction and site characteristics, severe accidents are not equally probable for all plants. As a part of Work package 2, the accident sequence selected for each plant was also assigned a best estimate of the frequency of the release, p^l, which has units of per year. The country risk parameter P^m for country m includes these frequencies:

$$P^m_{i,j,k} = \sum_{l \in M} P^l_{i,j,k}\, p^l, \tag{4.13}$$

where M is the set of nuclear power plants in country m. This gives the probability that contamination or dose in a grid cell exceeds the defined threshold, and has units of per year. As the p^l values may vary by up to three orders of magnitude, they are dominant within regions of similar meteorological probabilities.

This parameter was mapped. In addition, it was aggregated spatially over all countries, and the ocean. For each receiving country n, the average of this parameter over this country (only as far as inside the output domain) was calculated as

$$Q^m_{k,n} = \frac{\sum_{i,j \in N} P^m_{i,j,k} A_{i,j}}{\sum_{i,j \in N} A_{i,j}}. \tag{4.14}$$

Here, $i, j \in N$ refers to all grid cells in country n. This parameter gives the average frequency over the territory of country n that nuclear power plants in country m will cause a contamination or dose exceeding the threshold k. As countries have very different sizes, this parameter may not describe well the risks experienced by them. Therefore, we calculated also the frequencies of being over the threshold that are exceeded over certain fractions (percentiles) of the country (0, 5, 25, 50, 75, 95, 100%). Note that this is different from the frequency that, say, 50% of a country is contaminated in a single event! The two extremes give the minimum and maximum value of $P^m_{i,j,k}$ on a country’s territory, and the 50% value is the value of $P^m_{i,j,k}$ which is exceeded over 50% of the territory. Results are displayed as box-and-whisker plots. For each receiving country, there is one box-and-whisker diagram, and all such diagrams referring to one risk-export country are grouped together in a single figure, ordering the receptor countries according to the 5th percentile, so that they are ranked with respect to the risk they receive (see Section 5.6 for results).

The data form (n, m) matrices (n for the risk-importing, m for the risk-exporting country), one for each contamination or dose threshold k.

This parameter indicates which countries (including the originator country, i.e. $n = m$) are most affected by the NPPs of a given country. In addition to single countries as risk originators, also the risk from all NPPs in the domain was calculated. These calculations were done for the three scenarios.

4.6.3 Risk received by countries

The next parameter is the opposite of the previous one, it shows how much each of the NPP countries contributes to the risk received by a given country. This parameter cannot be mapped; only the box-and-whisker plots are produced. It is based on the same data matrix as the previous section, but they are displayed for each risk-receiving country, listing the contributors of the risk again ordered by the rank of the 5th percentile. If one settles down on a given percentile, the total risk to a country can be divided into fractions delivered by the relevant NPP countries.

4.7 Technical aspects

4.7.1 Input data

An spreadsheet workbook with the input data that are to be used in the dose calculations was prepared. It includes

- dose coefficients for the two age groups,
- inhalation rates,
- recommended absorption types,
- shielding, and
- location factors for the relevant pathways and endpoints.

It is read by the Fortran dose programme using CSV representations of its sheets.

4.7.2 Research of source codes of other programs

Two different codes were acquired and checked: TAMOS (Austrian emergency preparedness system, dose code from ZAMG), and an external gamma dose rate calculation code produced at the Institute of Energy Technologies (INTE) of the Technical University of Barcelona. It was also considered to use the Mainframe COSYMA code developed at Karlsruhe (KIT, previous KfK) which is available at BOKU-Met. However, as license / copyright issues could not clarified, this was not further pursued.

TAMOS calculates the doses from air concentrations and ground contamination in a straightforward manner with given dose factors. For the external gamma doses, it relies on the semi-infinite cloud approximation, whereas the INTE code follows a more complex formulation.

Communication with some of the RODOS users provided some insight on the data, limits and parameters used in it. The location factors which are applied in flexRISK are those of RODOS.

4.7.3 flexRISK dose calculations

The dose calculation was implemented in a similar way as the TAMOS code. However, TAMOS was not written with numerical efficiency as a main criterion. Also, it is not written for new FLEXPART v8 output format, and it does not consider decay chains. It expects to receive concentration and deposition data for all nuclides and with decay already considered from FLEXPART. Therefore, the code for dose calculation was written from scratch, in Fortran 90, with TAMOS being used as a guidance.

A challenge in terms of programming is the fact that the ground and air activities are very large arrays with grid location, nuclide and time as indices, and that the order of loops would be different in the part of the programme where these arrays are assigned values from reading the FLEXPART output, and where they are referenced for dose calculation. Thus it is not possible to implement the Fortran rule that the inner loop must be the fastest-varying index, which slows down the computation significantly. As a workaround, in the beginning of the loop over the grid cells in the dose calculation, we assign the subset of the contamination arrays pertaining to the specific grid cell to a work space variable. In this way, the inefficient memory access is done only once, and not for all the different kinds of doses needed. The number of dose values is larger than it would appear at first glance because of the “7-day problem” which requires the calculation of a large number of 7-day doses (see Section 4.5.2).

Also the generation of the graphical output was not a small computational task. One factor was that there are so many dose parameters for each case. Both for dose and contamination, the work flow basically involved the production of the graphics as NCAR graphics metafile by the Fortran dose calculation programme, the conversion of this file to postscript, the generation of a GIF file for the web, and finally the conversion of the postscript to PDF. All these steps take time, last not least because the typical size of a single zoomed-domain PDF file is 1.2 MB, and the Level-1 postscript files produced by NCARG a multiple of that. For this reason (and mass storage limitations), single-case contamination and dose maps were only plotted for the 88 cases of the year 1995.

Thus, even the dose calculations had to be done on the VSC, which was not foreseen before. As the dose calculation needs more RAM than the FLEXPART dispersion calculations with their 250k particles, not all cores in a VSC-2 node could be used. Furthermore, the dose calculation has to be carried out for more reactor units than dispersions calculations needed to be done for. (In theory, some time could have been saved by doing calculations only once for identical units at a site, but implementing this, including graphics where the unit name is in the plot, would have been to much work.) In terms of node-hours used, the dose calculation probably took about 30% of the dispersion calculations.

5 Results

5.1 Nuclear facilities

Within the flexRISK domain, 257 nuclear facilities (228 nuclear power plants, 26 nuclear fuel cycle facilities and 3 large research reactors) falling into the scope of the project were identified and relevant data were collected for them. This group of facilities is made up of operating and planned facilities that were identified as fulfilling of the criteria on January 1st, 2010. The majority of nuclear installations in Europe are Western- and Russian-designed pressurized water reactors of the second generation[1] (Figure 8).

NPPs and nuclear fuel cycle facilities are found in 22 countries. The largest number of facilities are situated in France, the Russian Federation, the United Kingdom, and Germany (Figure 9).

5.1.1 Nuclear power plants considered in flexRISK

Concerning nuclear power plants, there were 193 in operation and 35 units were identified as under construction or in advanced planning phase as of January 1st, 2010. During the project, eight German power plants were shut down following the Fukushima accidents and two British GCRs reached their end of life, leaving 183 NPPs in operation in the domain in March 2012 (see Table 14 and Figure 10).

Nuclear power plants in operation

The 183 NPPs currently (2012) in operation have a total thermal capacity of 496.2 GWth (average 2.7 GWth per unit) installed, corresponding to electrical capacity of 171.6 GWe (average 938 MWe per unit). Three quarters (139 units) of the operating reactors are pressurized light water reactors, either of French, German, Russian or U.S. design. Around 8% each are gas-cooled reactors (16 units) and boiling water reactors (15 units). While the BWRs were designed in Germany, Sweden and the U.S., the concept of gas- cooled nuclear reactors was only implemented in the United Kingdom. Romania is the only country in Europe operating pressurized heavy water reactors. Finally there are still some graphite moderated, water-cooled reactors (RBMK) in operation in Russia and the Ukraine. A detailed picture on reactor types operating in the flexRISK domain is shown in Figure 11.

Figure 12 shows that France is the country with by far the largest number of the nuclear reactors in Europe (58), followed by the Russian Federation (28)[2], the United Kingdom (17) and the Ukraine (15).

[1] See e.g. `http://en.wikipedia.org/wiki/Nuclear_reactor#Classification_by_generation` for differences in reactor generations.

[2] There are five more reactors operating on Russian territory, but they are not within the flexRISK domain.

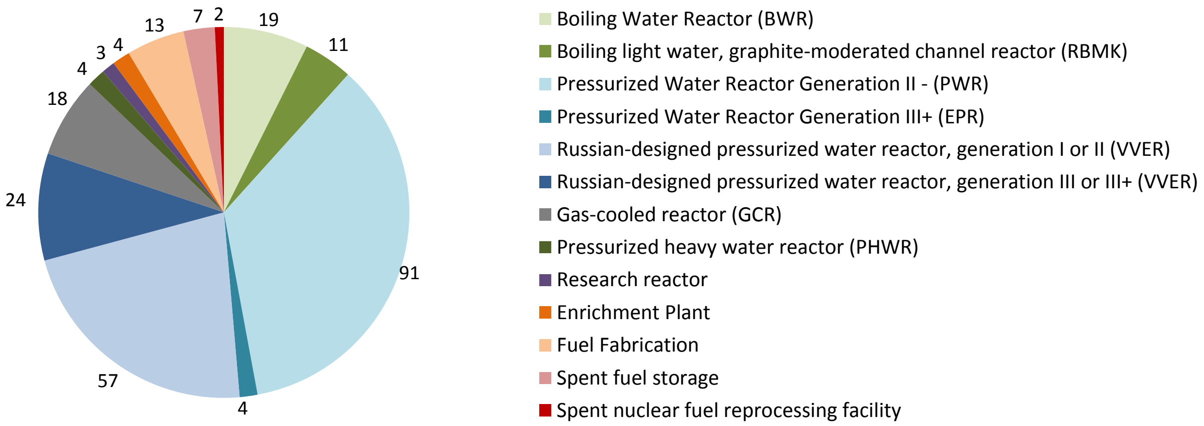

Figure 8: Distribution of nuclear facilities by type.

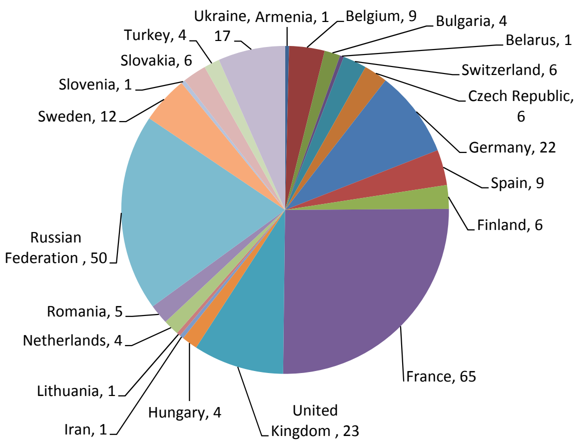

Figure 9: Distribution of nuclear facilities by country.

Table 14: Statistics of NPP types in the flexRISK domain (Status March 2012).

Type	Total	Operating	Under construction or planned	Shut down
Boiling Water Reactor (BWR)	19	15	0	4
Boiling light water, graphite-moderated channel reactor (RBMK)	11	11	0	0
Pressurized Water Reactor Generation II (PWR)	91	87	0	4
Pressurized Water Reactor Generation III+ (EPR)	4	0	4	0
Russian-designed pressurized water reactor, generation I or II (VVER)	57	51	6	0
Russian-designed pressurized water reactor, generation III or III+ (VVER)	24	1	23	0
Gas-cooled reactor (GCR)	18	16	0	2
Pressurized heavy water reactor (PHWR)	4	2	2	0
Total number	228	183	35	10

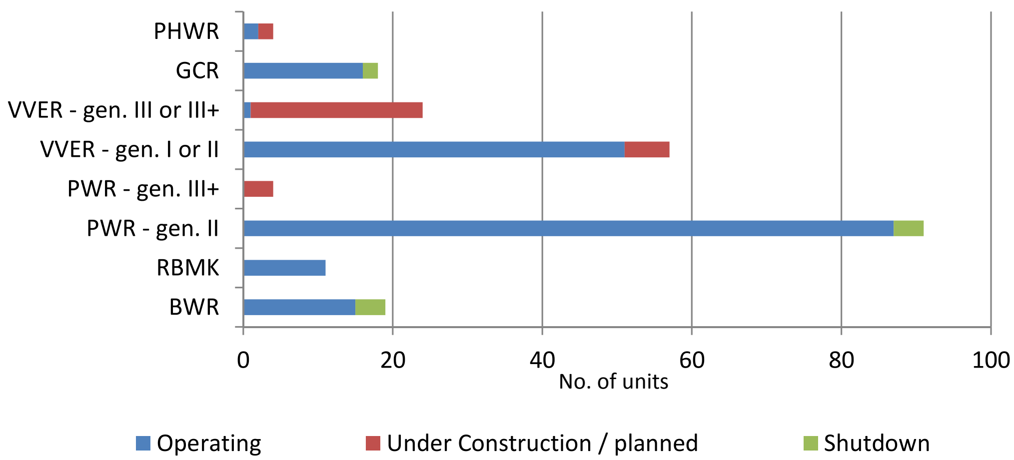

Figure 10: Distribution of NPPs by type and operating status.

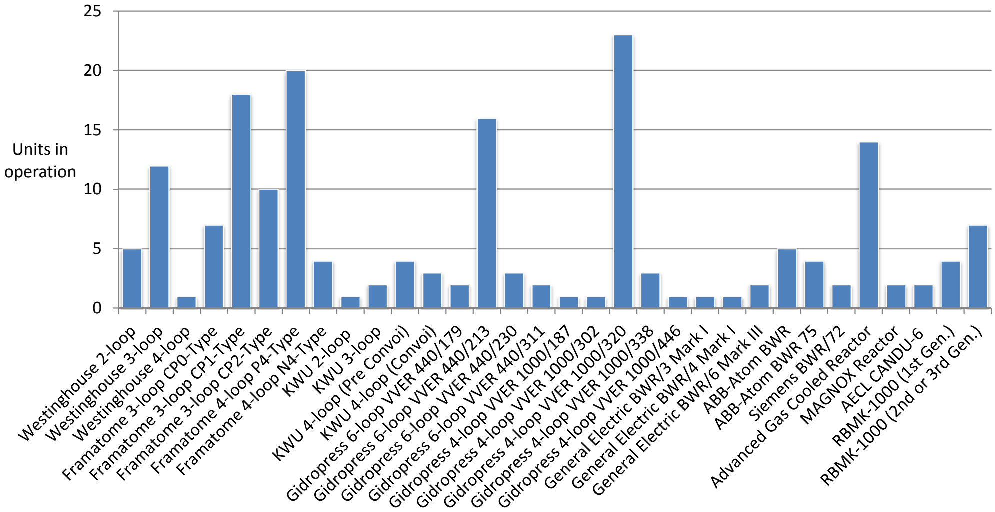

Figure 11: NPPs operating in Europe, types in detail.

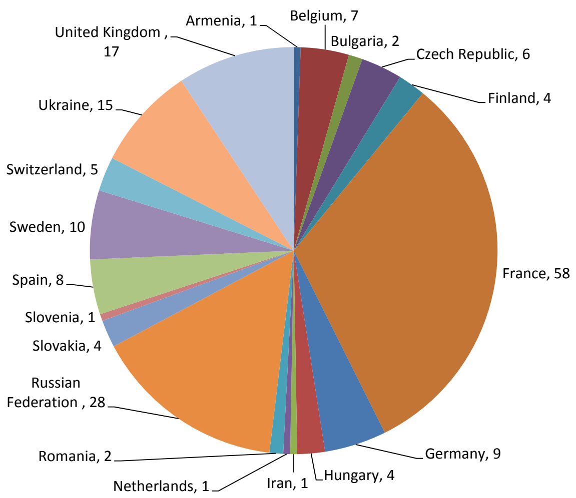

Figure 12: Nuclear reactors in operation by country.

In the past two decades, only a few new reactors have been put into operation in Europe (Figure 13). The reactor fleet is thus quite old, with 77% being 25 years or older, 40% being 30 years or older, and 15% being 35 years or older. This means that many units are reaching the end of their design life, which is characteristically 40 years for generation II reactors. Applications for life time extension or long-term operation licenses have therefore been submitted (and granted), and more can be expected in the coming years.

Although core-damage frequencies (CDFs) were not of primary importance for the project, these frequencies were also collected in the data sheets, if they could be identified. The range of these CDFs is shown in Figure 14 for some European reactor types. The frequencies range from 1E-6 to 7.8E-4 per year. The average for all of the 132 CDF scollected is 4.15E-5 per year. CDFs are highest for the Russian-designed VVERs of the first and second generation, averaging to 8.3E-05 per year.

Development of additional future nuclear capacities

In addition to the 193 NPPs identified as operational in the beginning of 2010, 35 units that were either under construction or in an advanced planning stage in 2010 were added to the NPP data base. They have a total capacity of about 40 GWe. Most of these units (Figure 15) are situated in eastern

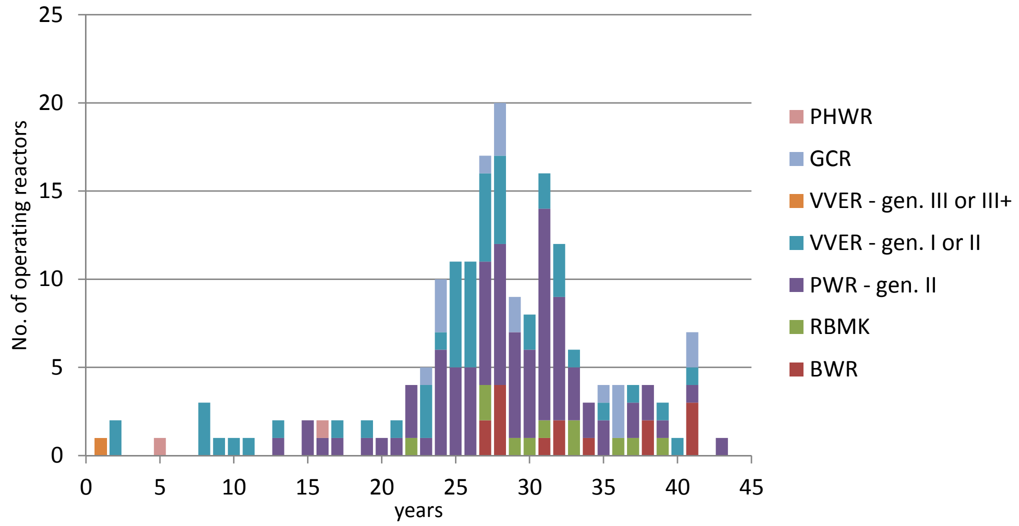

Figure 13: Age distribution of NPPs in operation in Europe (in 2012).

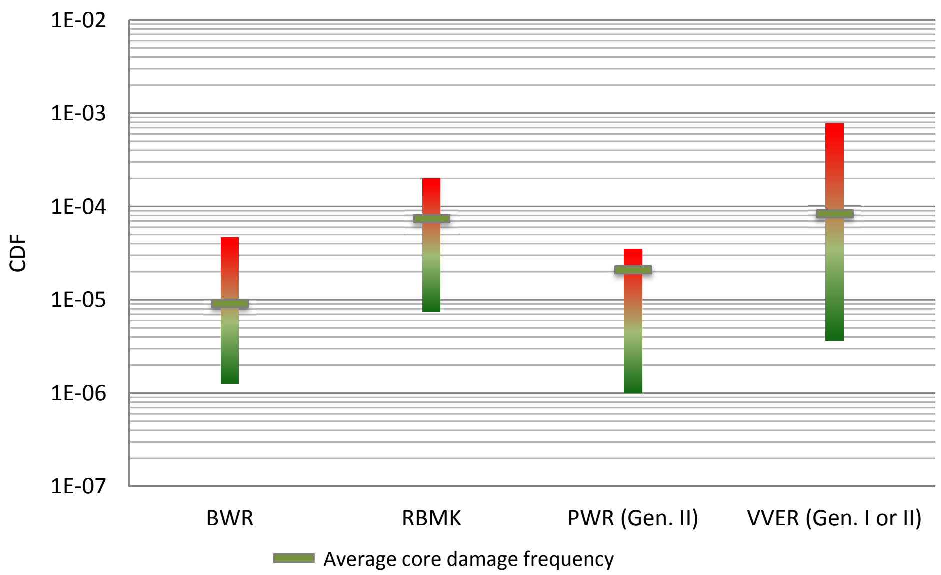

Figure 14: Range of core damage frequencies for NPPs in operation, grouped by reactor type, based on the open literature (132 values).

Europe and are Russian-designed reactors. These power plants were not included in the scenarios shown in Sections 5.6, 5.7, and 5.8. The decision for the introduction or expansion of nuclear power is a highly political topic. Therefore, planning of new units as well as cancelling of planned units may be expected in the coming years. Nevertheless, the units selected here constitute a base for the estimation of future capacities.

5.1.2 Nuclear fuel cycle facilities and research reactors

While Europe is heavily dependent on the import of natural uranium, currently several facilities for the processing of uranium and subsequent production of reactor fuel are in operation. Furthermore, there are reprocessing facilities and off-site spent fuel storage facilities in Europe. These facilities – as listed in Table 15 – were added to the data basis to complete the picture of nuclear facilities in the flexRISK domain. Most of these facilities are located in France (5 facilities), Germany (5), the UK

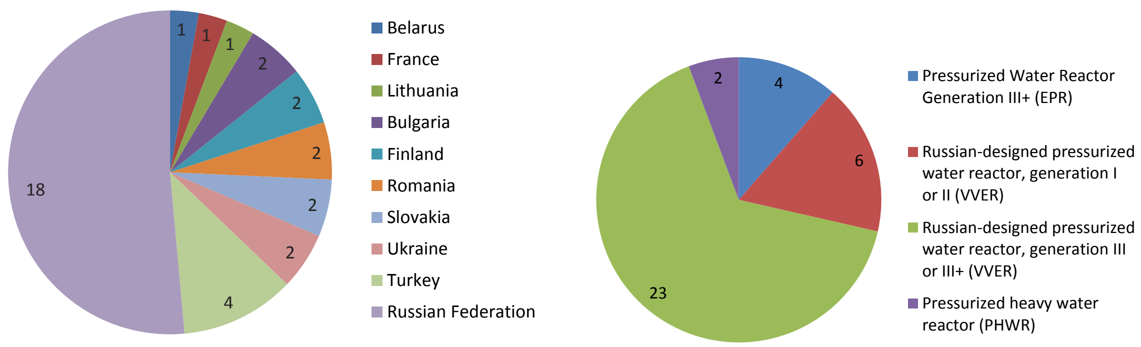

Figure 15: Numbers of planned NPPs by country (left) and by type (right), as evaluated in January 2010.

(4) and the Russian Federation (4)[3]. Their age distribution is given Figure 16. The nuclear fuel-cycle facilities are not included in the accident analysis, as accident scenarios for these facilities are hardly available. It is also assumed that their contribution to the total risk is rather small compared to NPPs.

Table 15: Nuclear fuel cycle facilities documented in flexRISK, listed by country and name.

Enrichment plants (with type)		
France	Eurodif	Gaseous diffusion enrichment plant
Germany	Gronau	Centrifuge enrichment plant
Netherlands	Almelo	Centrifuge enrichment plant
United Kingdom	Capenhurst	Centrifuge enrichment plant
Fuel fabrication (with reactor type for which fuel is manufactured)		
Belgium	Dessel	PWR
France	Marcoule	MOX
France	Romans	PWR
Germany	Lingen	PWR/BWR
Russian Federation	Elektrostal	FBR
Russian Federation	Elektrostal	RBMK
Russian Federation	Elektrostal	VVER
Russian Federation	Elektrostal	U pellets
Romania	Pitesti	PHWR
Spain	Juzbado	PWR/BWR
Sweden	Vasteras	PWR/BWR
United Kingdom	Springfields	GCR/AGR
United Kingdom	Springfields	LWR
Spent nuclear fuel reprocessing facilities		
France	La Hague	
United Kingdom	Sellafield	
Spent fuel storage		
France	Cadarache	
Germany	Ahaus	
Germany	Gorleben	
Germany	Zwischenlager Nord	
Netherlands	Covra	
Sweden	Clab	
Switzerland	Zwilag	

To complete the picture of large nuclear facilities in Europe, the following research reactors with 40 MWth or larger were identified and site locations were included in the data base; accident scenarios

[3]Excluding facilities outside the flexRISK domain.

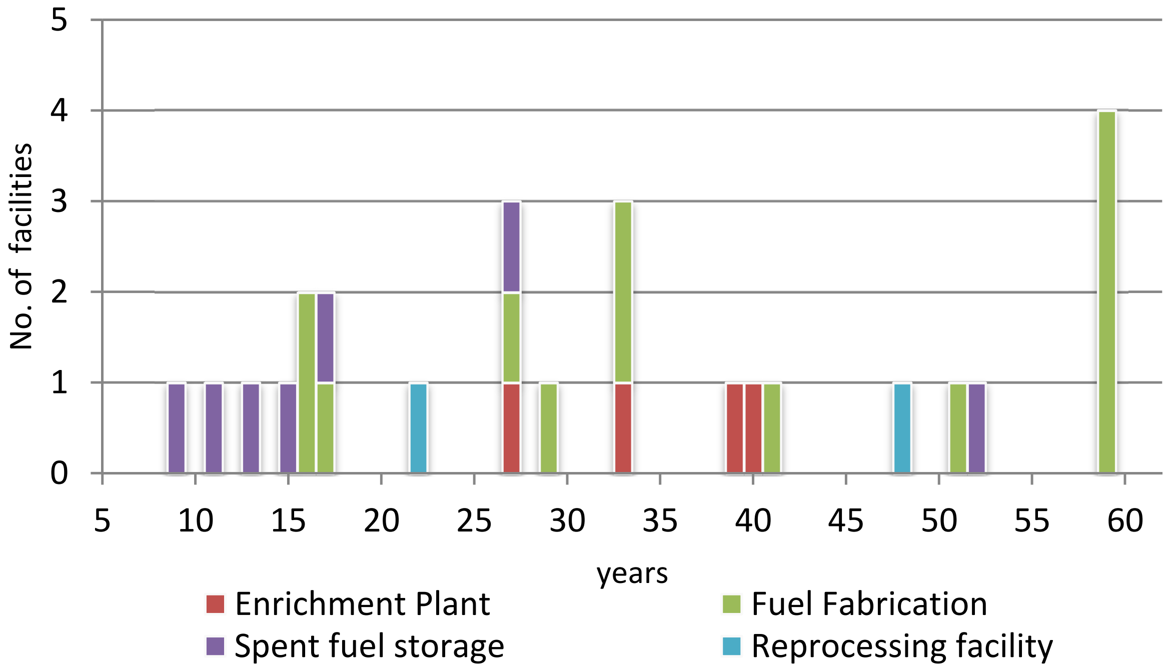

Figure 16: Age distribution of nuclear fuel cycle facilities (in 2012).

or source terms were not identified for the same reasons as for NFC facilities. These large research reactors are:

- Belgium, Mol, BR-2, 100 MWth, tank type reactor, light water cooled and light water & beryllium moderated, operated by SCK CEN, operating since 1961.
- Netherlands, Petten, 45 MWth tank in pool type reactor, light-water cooled and moderated, operating since 1961.
- France, Grenoble, 58.3 MWth high-flux reactor, heavy-water cooled and moderated, operating since 1971.

5.2 Source terms and releases

Source terms are the basis for the dispersion and dose calculations and include the following parameters: :

– release shape (time, duration and height of the release);
– equilibrium core radionuclide inventory;
– release fraction (amount radioactive material released, per nuclide category).

At this point, it has to be stated once more that the work is based on publicly available data, and that information on nuclear installations is not easily accessible in most cases. In order to obtain source terms for each reactor and to be able to handle the large number of reactors, they were grouped into facilities with similar properties. Accident scenarios were derived from available literature. The source term parameters were assigned by expert judgement to reactor groups or single units.

5.2.1 Release shapes

The release shapes used in the dispersion modelling are shown in Table 16. They represent the time sequences of the releases to the environment for accident progressions with similar characteristics.

For different groups of reactors, initially two typical accident progressions and thus release shapes were selected. Typical courses of accidents such as steam generator tube ruptures, station blackouts or ISLOCAs were worked out. For the dispersion calculations, those release shapes were chosen which best fit the accident scenarios for the respective reactor. In this way, only 8 out of 17 release shapes were actually used.

5.2.2 Release fractions and frequencies

Release fractions and frequencies are the most relevant components of the source terms. As not the whole spectrum of possible accidents could be represented in the project, a selection of two accidents was made per plant, and one of these, representing a large release that is not too unlikely, was used for dispersion calculations. A comparison of these accident scenarios has to be done with caution and the necessary expertise. In some cases it can be assumed that they represent rather the upper limit for releases, while in other cases larger releases seem possible.

Figure 17 shows the accident frequencies and corresponding releases of caesium and iodine for all of the accident sequences identified in the project, including those used as well as those not used in the further calculations. The figures depict the generic frequencies used for the groups of reactors. For some units, specific accident frequencies could be identified and were then used instead of the generic ones. Details on release amounts and frequencies can be found in Appendix B. The figures show that there is no clear correlation between release fraction and likelihood of the accident for many of the selected scenarios.

Large releases and rather high frequencies were found for the following reactor types:

– VVER-440:
  Release of 65% of the iodine and caesium inventory with frequencies ranging from 2.5E-5/a (VVER-440/179) to 1E-5/a (VVER-440/213). The release fractions are generic, based on NUREG-1465 (USNRC, 1995), while the frequencies represent fractions of the total CDF (75-80%) or PSA results (Lajtha et al., 2005), respectively.
– VVER-1000 / 187, 302, 338:
  The release fractions of these “small” VVER-1000 units, all situated in states of the former Soviet Union, were the highest ones found in the project. Based on literature available for Kalinin Unit 1 (USNRC, 2005), possible releases of 82% of iodine and 80% of caesium were identified at a frequency of 2.86E-6/a (1.3% of CDF).
– BWR-69:
  All units of this type have been shut down after the Fukushima accidents. For the project,

Table 16: Release shapes used for the flexRISK source terms. $t_{1,2,3}$ denote the beginning of the first phase, the end of the first phase (which is the beginning of the second phase), and the end of the second phase. $h_{1,2}$ denote the lower and upper height of the effective release height interval.

			Phase 1				Phase 2		
No.	Accident	Type	t_1 (s)	t_2 (s)	$h_{1,2}$ (m)		t_3 (s)	$h_{1,2}$ (m)	
I	PWR 1 - Steam generator tube rupture	late	28800	30600	100	300			
II	PWR 2 - Containment failure at time of reactor vessel failure or soon thereafter; core melt accident with failure of containment isolation; or interfacing systems LOCA with containment bypass until reactor vessel failure	early	10800	25200	0	50			
III	VVER 440 - core melt accident, confinement ineffective (reactor pressure vessel failure, CCI)	early	10800	10920	0	50	18120	0	50
IV	BWR 1 - Station blackout, early containment overpressure failure at time of reactor vessel failure (releases from reactor pressure vessel failure and CCI)	early	41400	42300	0	50	56700	0	50
V	BWR 2 - ISLOCA with coolant loss outside containment	early	21800	30800	0	30			
VI	CANDU - core melt, late containment overpressure failure	late	84600	88200	0	50			
VII	RBMK - core power excursion and steam explosion (Chernobyl Unit 4)	early	0	60	1000	3000	432000	50	150
VIII	AGR - Loss of carbon dioxide coolant (depressurisation accident), late core damage and release	late	86400	93600	50	100			

large releases of 61% of iodine and caesium due to containment bypass were evaluated at a frequency of 20% of the CDF (based on Löffler and Sonnenkalb, 2006).

- AGR/MAGNOX:
  Publically available information on gas-cooled reactors is scarce. The source term used is considered to be rather conservative[4], as it requires a large opening in the pre-stressed concrete reactor vessels and a graphite fire extending over a long period. The resulting releases from such a generic accident could be expected to be about 60% for iodine and 40% for caesium. The frequency was assumed to be 1E-6/a, corresponding approximately to the “Basic Safety Limit” (BSL) in the UK Safety Assessment Principles.
- RBMK:
  For a Chernobyl-type accident, a release of 60% of the iodine and 40% of the caesium inventory can be expected (OECD/NEA, 2002). The frequency of such an event is estimated to be on the order of 10% of the CDF (Usburus et al., 2007).
- BWR-72:
  The source terms for a severe accident with large early release from a BWR-72 was derived

[4] In the context of nuclear accident assessments, “conservative” refers to assumptions which rather over- than underestimate the consequences.

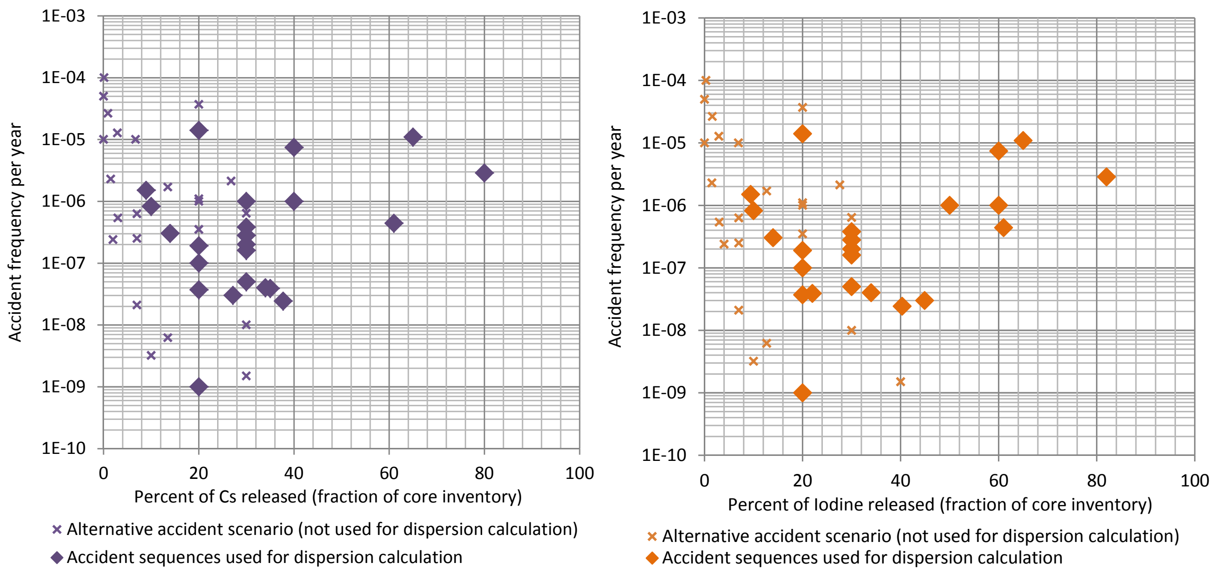

Figure 17: Release fractions of caesium and iodine vs. accident frequencies. The figure shows generic frequencies of the severe accidents selected for the different reactor types. For details on the units see Appendix B.

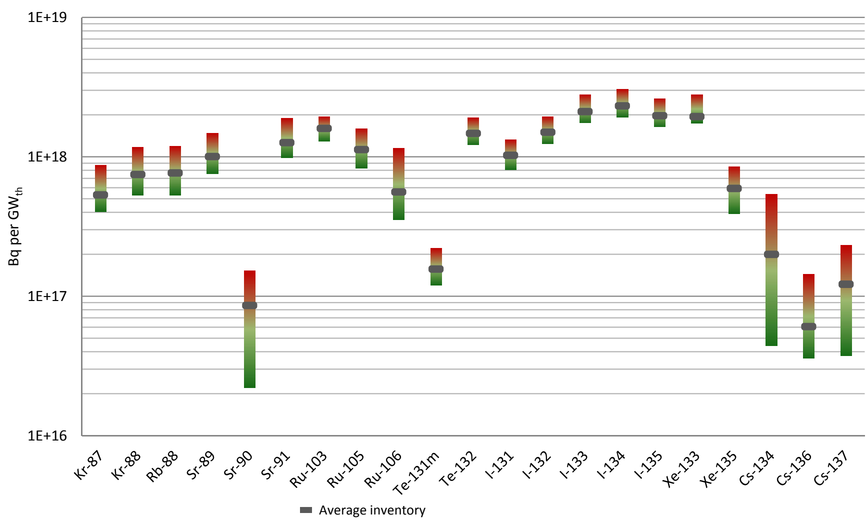

Figure 18: Range of core inventories of different radionuclides per GWth. The range is spanned by the different reactor types. For details on the units refer to Appendix B.

from SSK (2003). With a frequency of 1E-6/a, releases of 50% of iodine and 30% of caesium are expected.

5.2.3 Core inventories

The inventories collected were assigned to the NPPs according to their characteristics (reactor type, thermal power, MOX or U core) and scaled with the ratio of the thermal power rating of the reactor under consideration and the reactor for which the assigned inventory stemmed. Release fractions were applied in agreement with the accident scenario for the calculations. Figure 18 shows the range of the 17 different core inventories collected from available literature. Note that not all of them were appropriate and used further on. Concerning the boiling-water reactors, see the remarks in Section 2.3.3

5.3 Contamination and doses

5.3.1 Interpretation of logarithmic scales

Contamination and dose values vary by orders of magnitude between locations close to the source and far away. Also, the release frequencies differ by orders of magnitude. Therefore, graphical presentation of results needs to use logarithmic dose and contamination scales. Typically, the axes or colour bars are annotated at intervals which correspond to factors of 10, e.g., 1, 10, 100, 1000, etc. Values may also be written in exponential notation, either in the mathematical style ($10^0, 10^1, 10^2, 10^3$, etc.) or in the engineering style (1.E0, 1.E1, 1.E2, 1.E3, etc.; may also look like 1.E01, 1.E02, etc.). Then, the intermediate axis ticks or colours correspond to values such as $10^{1.1}, 10^{1.2}, \ldots, 10^{1.9}$ (in the case of 9 intermediate values; for 4 intermediate values, only $10^{1.2}, 10^{1.4}, 10^{1.6}, 10^{1.8}$ are used). As these values are not immediately clear, and there is no space to annotate them in every figure, Table 17 shows the values for these intermediate intervals.

Table 17: Numerical values which correspond to intermediate intervals in logarithmic scales. Lines corresponding to four intermediate values in bold.

Interval	Sample values			
0	**1.00**	**10.0**	**100.**	(annotated)
1	1.26	12.6	126.	
2	**1.58**	**15.8**	**158.**	
3	2.00	20.0	200.	
4	**2.51**	**25.1**	**251.**	
5	3.16	31.6	316.	
6	**3.98**	**39.8**	**398.**	
7	5.01	50.1	501.	
8	**6.31**	**63.1**	**631.**	
9	7.94	79.4	794.	
10	**10.00**	**100.0**	**1000.**	(annotated)

5.3.2 Contamination patterns and their variability

All the contamination parameters as defined in Section 4.2 have been evaluated. Ready-made plots are available on the flexRISK web site for the weather situations of the year 1995 (see also Section 5.4) and the following parameters:

- total deposition of caesium-137 on the surface,
- total time-integrated concentration of iodine-131 in near-surface air, and
- (for selected sites) gif-movies of the near-instantaneous (3-h averaged) concentration of iodine-131 in near-surface air.

There is a great variety of patterns for the movement of contaminated air and thus the integrated concentrations. For deposition, the complexity of rainfall patterns adds to this, so that deposition patterns are even more complex. Some samples are shown here to illustrate this, and to explain also the interaction with geographic factors such as mountain ranges that influence the climatic conditions.

Sometimes, with – often westerly – winds blowing constantly and over most of Europe in a similar direction, without much precipitation, the simple pattern of a narrow cone of contamination, rather straight-lined, with concentration decreasing steadily, occurs (Fig. 19).

At other times, the transport may be first straight-lined, but then the contaminated air is influenced by turning winds, so it changes direction and widens up (Fig. 20). This effect can be strong, as in the case of Fig. 21, where, after crossing the Pyrenees, the plume spreads over the Iberian peninsula and ultimately over most of Europe, beyond the zoomed domain. For this reason, the coarse domain

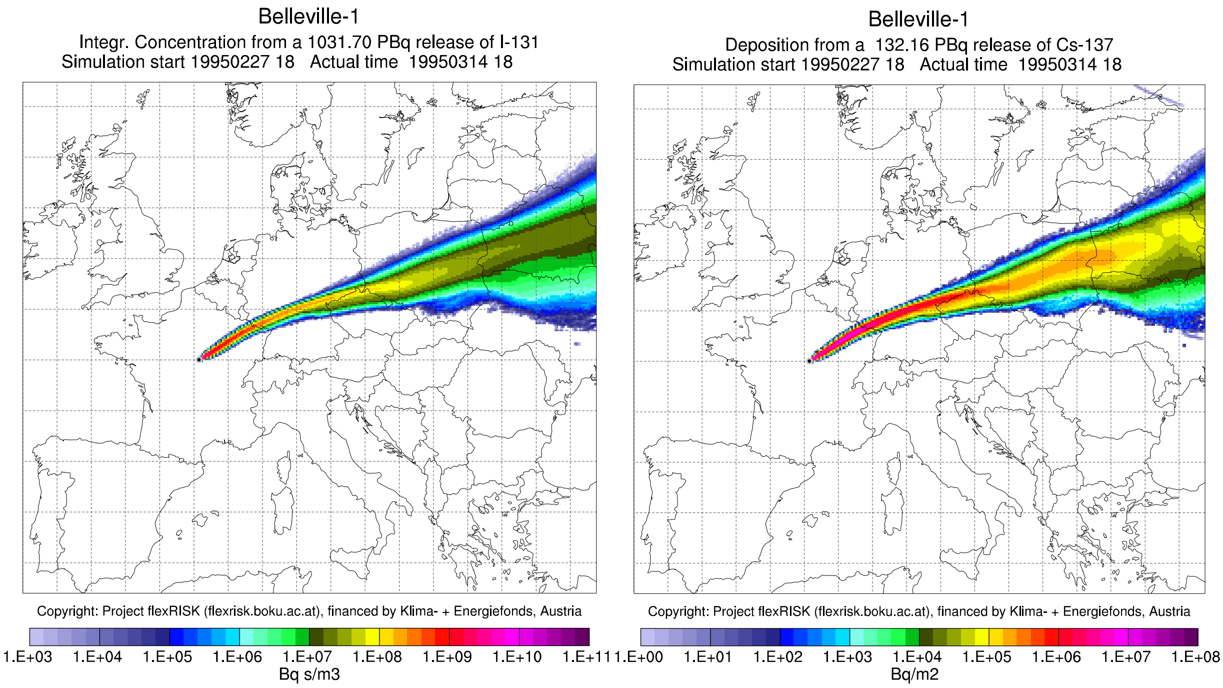

Figure 19: Sample of dispersion patterns for the French NPP site Belleville (left: I-131 concentration, right: Cs-137 deposition) with undisturbed straight transport.

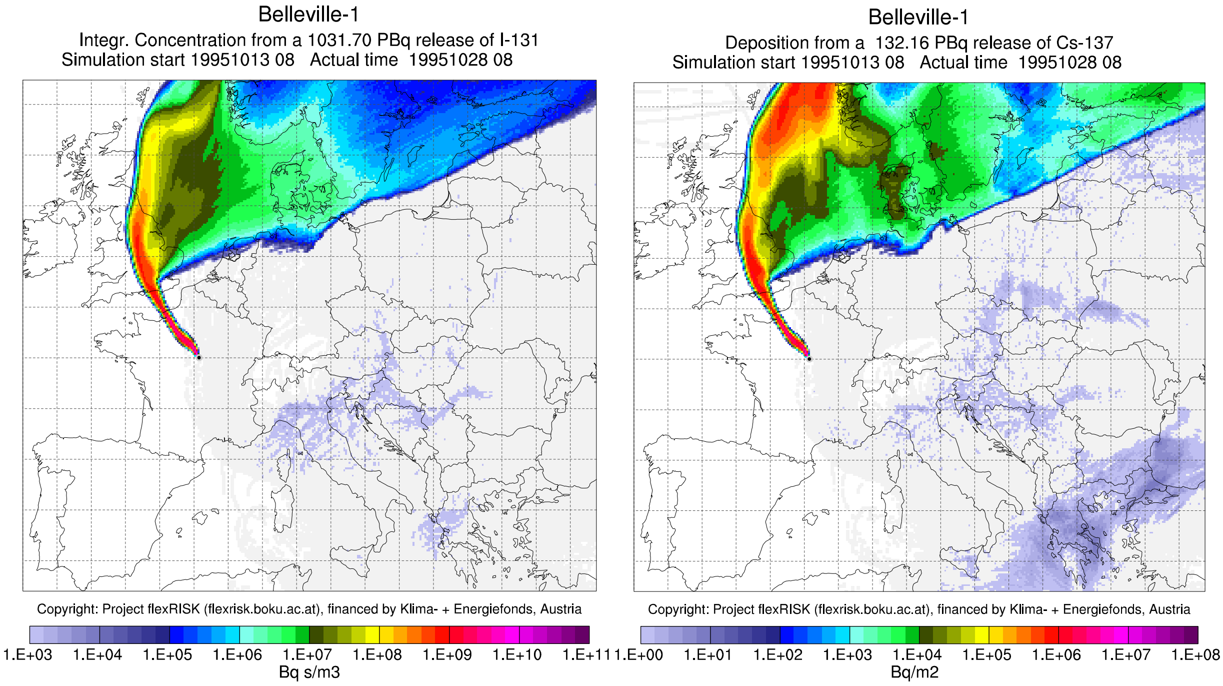

Figure 20: Sample of dispersion pattern with slightly variable transport for the French NPP site Belleville (left: I-131 concentration, right: Cs-137 deposition).

results are shown as well. The comparison between the zoomed and the coarse domain also illustrates the effect of the coarse grid: narrow plumes (like over France) are smeared and their centreline values are considerably reduced. Furthermore, the deposition field is patchy with isolated maxima – an effect of the distribution of precipitation. If one looks closely, it is recognisable that there are maxima on the western side of Sardinia, the Italian peninsula, and the Dinaric coast – for the westerly flow prevailing at that time, this is the windward side, where precipitation is enhanced through orographic lifting. There are other interesting features in this case, such as the detached concentration maximum south of the Cantabrian mountains in the western part of central Spain, probably due to vertical mixing or vertical transports in the lee of the mountains. In the zoomed maps, both concentration and deposition, in regions with very low values, exhibit a kind of lines and small spots. This is a manifestation of the fact that in a Lagrangian particle model, the calculation is done by tracking computational particles: the lines are traces of single particles, and one-grid-cell spots are locations of single particles. This is a normal feature and to be expected. As such spots and traces are naturally associated with very low concentration or deposition (below 100 Bqm^{-2}, no radiological significance), this is not a reason for concern.

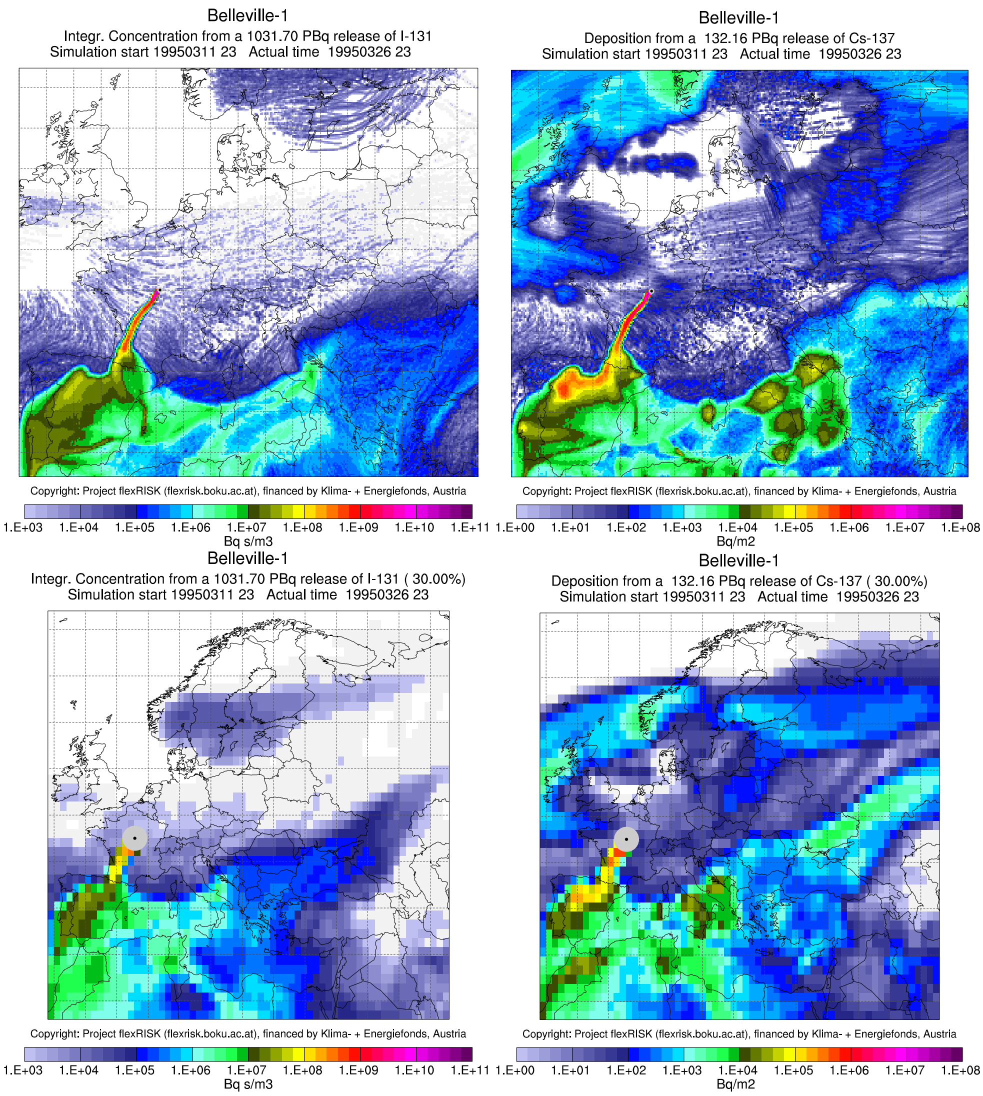

Figure 21: Sample of complex dispersion pattern for the French NPP site Belleville (left: I-131 concentration, right: Cs-137 deposition; top: zoomed domain, bottom: coarse domain).

The transport direction can also easily reverse. Plumes may perform large loops, as Fig. 22 shows, or can go back and forth over almost the same strip of land, which would particularly complicate the accident management, as in Fig. 23. Obviously, the contaminated air first moved from Krümmel near Hamburg eastward to the Polish border, then turned 180 degrees and came back just south of the site, moving to North Holland, and then – now in a more diffused, broad cloud – turned again and passed over the site and its surroundings, including Hamburg. At the western turning point, a part is detached and moves south. It is obvious that such patterns would make evacuations potentially hazardous unless a reliable dispersion forecast were available.

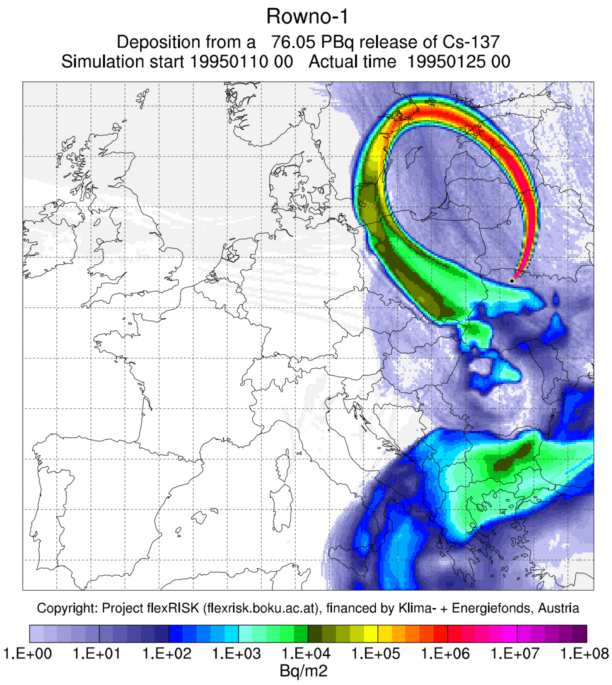

Figure 22: Sample of dispersion pattern with loop.

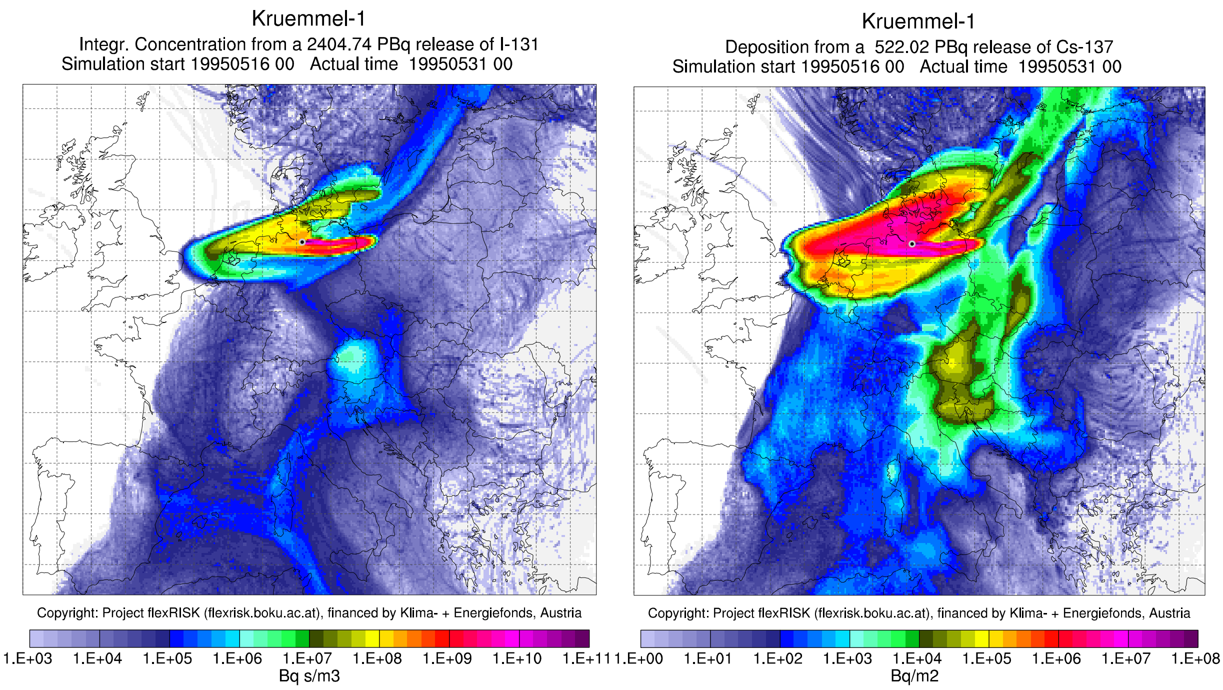

Figure 23: Sample of dispersion pattern with wind reversal (left: I-131 concentration, right: Cs-137 deposition).

5.4 Dose results for each NPP unit and weather situation

For all NPP units, comprehensive results of contamination and dose patterns were evaluated. Ready-made plots are available on the web site for all the weather situations in the year 1995 through a selection menu (Fig. 24).

Fig. 25 gives a sample result, which is obtained in the web interface through the selections

– Dukovany NPP,

Figure 24: Screenshot from the flexRISK web site: Selection menu for contamination and dose results for all units.

- Unit 1,
- weather situation 03-03-1995,
- 30-d effective dose infants, and
- zoomed domain.

Besides the contamination parameters (see Section 5.3.2), the following dose endpoints were evaluated and plotted:

- 7-d thyroid inhalation dose for adults,
- 7-d thyroid inhalation dose for infants,
- 7-d effective dose for adults,
- 7-d effective dose for infants,
- 30-d effective dose for adults,
- 30-d effective dose for infants,
- 1-a effective dose for adults,
- 1-a effective dose for infants,
- 50-a (lifetime) effective dose for adults.

As explained in Table 10, a dose of 30 mSv (30-d effective dose from ground-shine) is the intervention level for temporary relocation. In the above figure, 30 mSv are reached where the red colour changes into violet. In this scenario, it could be necessary to temporarily relocate a part of the Austrian population living in the north-eastern parts of Lower Austria near the border to the Czech Republic.

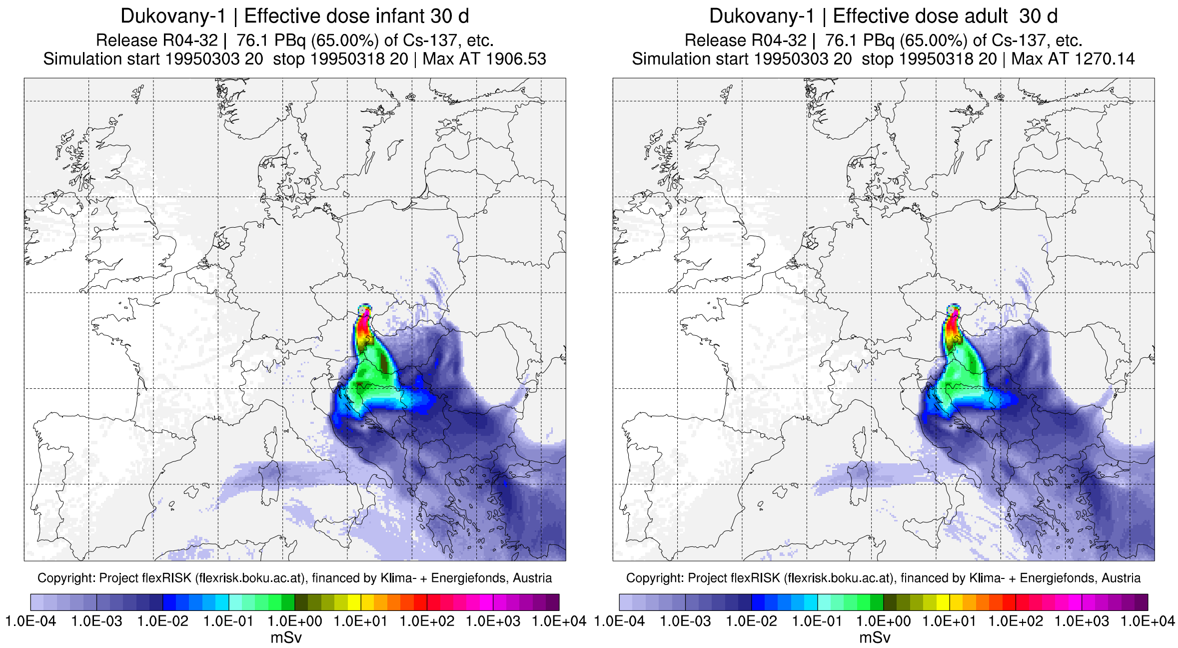

Figure 25: 30-d effective dose for infants from ground-shine, Dukovany NPP Unit 1, weather situation of release starting on 3 March 1995, 20 UTC. Left: for infants, right: for adults.

The maximum dose value for this scenario on Austrian territory is 1,900 mSv, more than 60 times the intervention level of 30 mSv.

For comparison the same scenario is also shown for adults in Fig. 26. Also for adults, the level of 30 mSv is exceeded in this scenario, with a maximum dose of 1,270 mSv in Austria.

5.5 Aggregated risk per NPP unit

If all the weather situations for a single endpoint from a single NPP unit are aggregated, the risk due to this NPP unit can be expressed as probability of exceedance of the chosen contamination or dose level. This probability is based on the weather-related risk, but does not include accident frequencies. For a detailed explanation see Section 4.6.1.

This type of result has been evaluated for a reduced list of endpoint-threshold-combinations:

- weather-related probability of ground contamination with Cs-137>5 kBqm^{-2},
- weather-related probability of ground contamination with Cs-137 >37 kBqm^{-2},
- weather-related probability of ground contamination with Cs-137>185 kBqm^{-2},
- weather-related probability of ground contamination with Cs-137>555 kBqm^{-2},
- weather-related probability of ground contamination with Cs-137>1480 kBqm^{-2},
- average ground contamination with Cs-137,
- weather-related probability of 7-day thyroid dose for infants >10 mSv,
- average 7-d thyroid dose for infants,
- weather-related probability of 1-year effective dose for adults > 2.5 mSv,
- weather-related probability of 1-year effective dose for adults > 25 mSv,
- weather-related probability of 1-year effective dose for adults > 250 mSv,
- average 1-year effective dose for adults.

Figure 27 shows as an example the probabilities of exceedance of a 1-year effective dose for adults of 2.5/25/250 mSv from Dukovany Unit 1. Here, the weather-related probabilities range from 0.0001 to

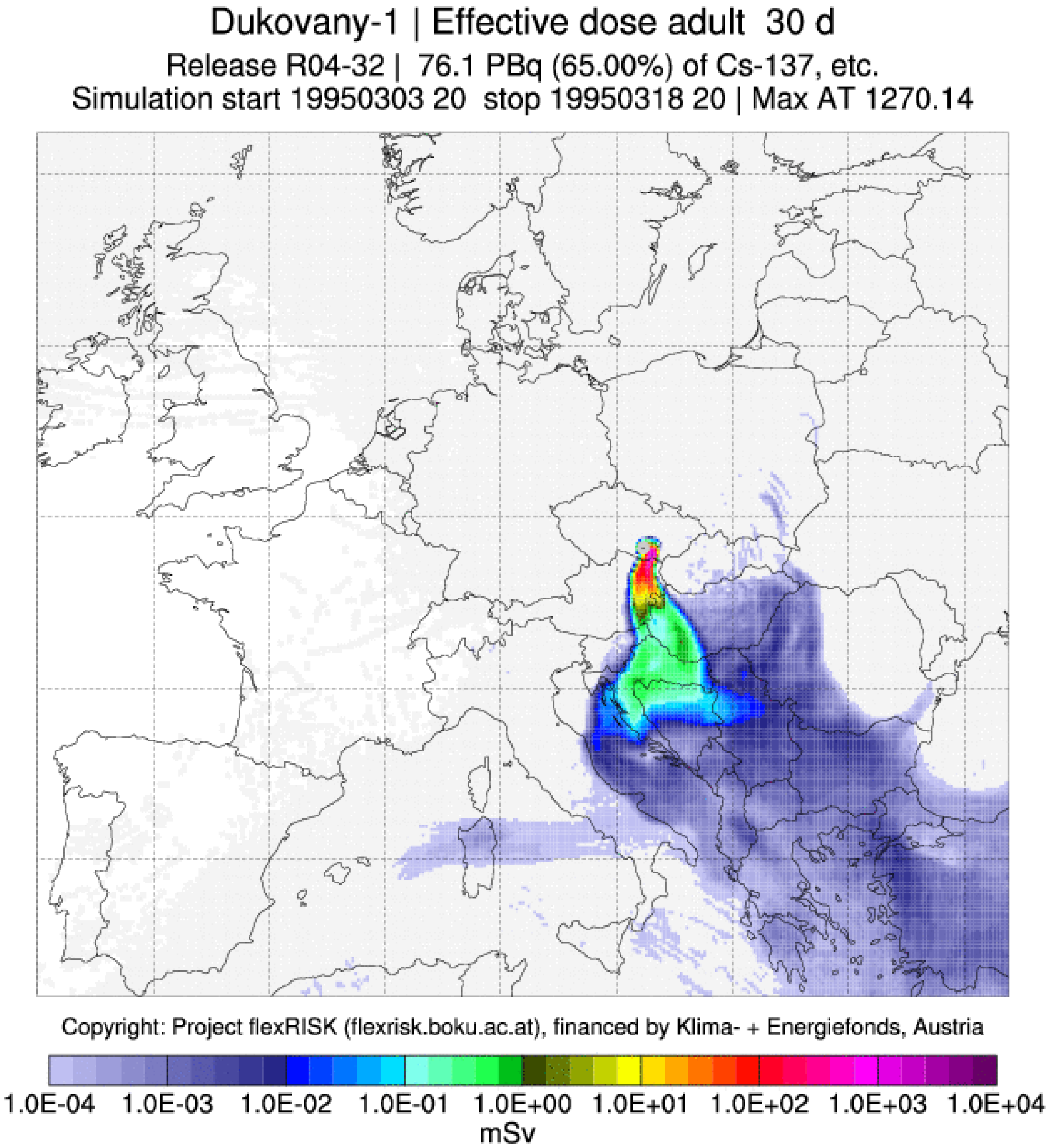

Figure 26: 30-d effective dose for adults from ground-shine, Dukovany NPP Unit 1, weather situation of release starting on 3 March 1995, 20 UTC.

nearly 1. For this example, the maximum probability in Austria was found to be 21% for 2.5 mSv, 13% for 25 mSv, and still 2.4% for 250 mSv. The dose value of 250 mSv in the first year after a nuclear accident was the former Austrian dose level for the so-called "intervention level 4" (BMGKS, 1992). If such a high dose could be expected, intervention measures like evacuation and relocations were considered necessary. Even though only for a small part of the country, the degree of exceedance of this level is not insubstantial.

As explained in Section 4.6.1, also evaluations of the risk just as a function of distance have been carried out, for the Tihange-1 NPP, which may serve as a characteristic sample for Central Europe away from mountains, not at the coast etc. The risk with respect to ground contamination with caesium-137 is shown in Figure 28. Mainly the high percentiles are of interest, the values exceeded in 10% of the cases (90th percentile), in 1% (99th percentile), or in 0.1% (strictly speaking, not a percentile, 99.9% of the values are lower). We can see that the level of 1480 kBq Cs-137 m^{-2} in 5% is

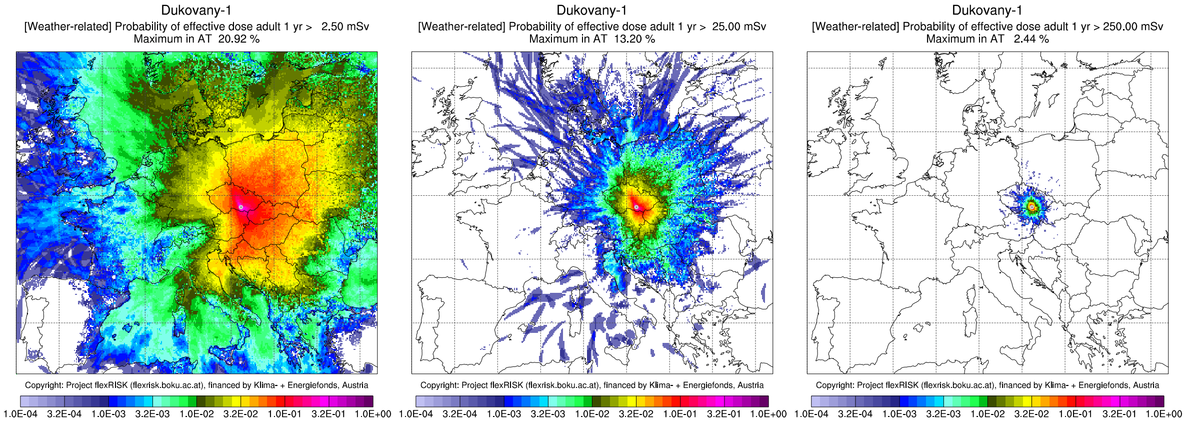

Figure 27: Weather-related probability of exceeding a 1-year effective dose of 2.5 mSv (left), 25 mSv (centre), and 250 mSv (right) for adults from Dukovany-1.

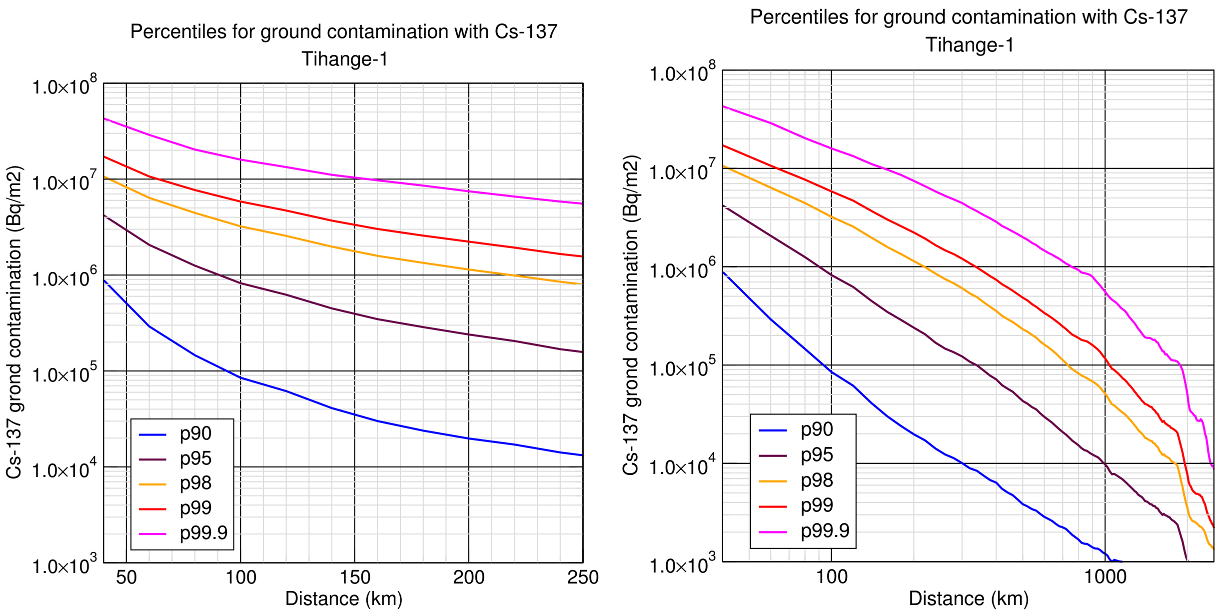

Figure 28: Percentile values for ground contamination with Cs-137 around Tihange-1. Left: First 250 km with linear distance scale. Right: Whole range of 2500 km with logarithmic distance scale.

exceeded up to 75 km, however, in 1% this contamination level can reach almost 300 km. If we look at the 99.9-percentile value, as an estimate for the maximum, it is found that only at a distance of 600 km it falls below the 1480 kBq Cs-137 m^{-2} level, and 185 kBq Cs-137 m^{-2} can still be exceeded up to about 1300 km. A massive contamination of 7000 kBq Cs-137 m^{-2} could occur (with a 0.1% probability) up to distances of 240 km.

With respect to the thyroid dose (Fig. 29), the possibility for exceeding the Austrian intervention level of 10 mSv within 7 days from inhalation of iodine, leading to the recommendation for children to ingest iodine tablets, was investigated. It was found that this level is exceeded with 10% probability at 90 km, but in 800 km there is still a probability of 1%. The 99.9%-value falls below 10 mSv only at a distance of about 1400 km. If we look at the 100 mSv value instead, then it will be exceeded with 10% of probability up to 45 km, with 1% up to 200 km, and with 0.1% at more than 500 km. Even though doses for adults will be somewhat lower, this shows that preparedness with respect to iodine prophylaxis is relevant also for adults.

For the 1-year effective dose, the regions where the value of 2.5 mSv may be exceeded are similar to those of the 10 mSv thyroid dose of infants. It reaches as far as 2000 km, close to the maximum distances that can be found in the zoomed output grid. For the next dose level, 25 mSv (that is

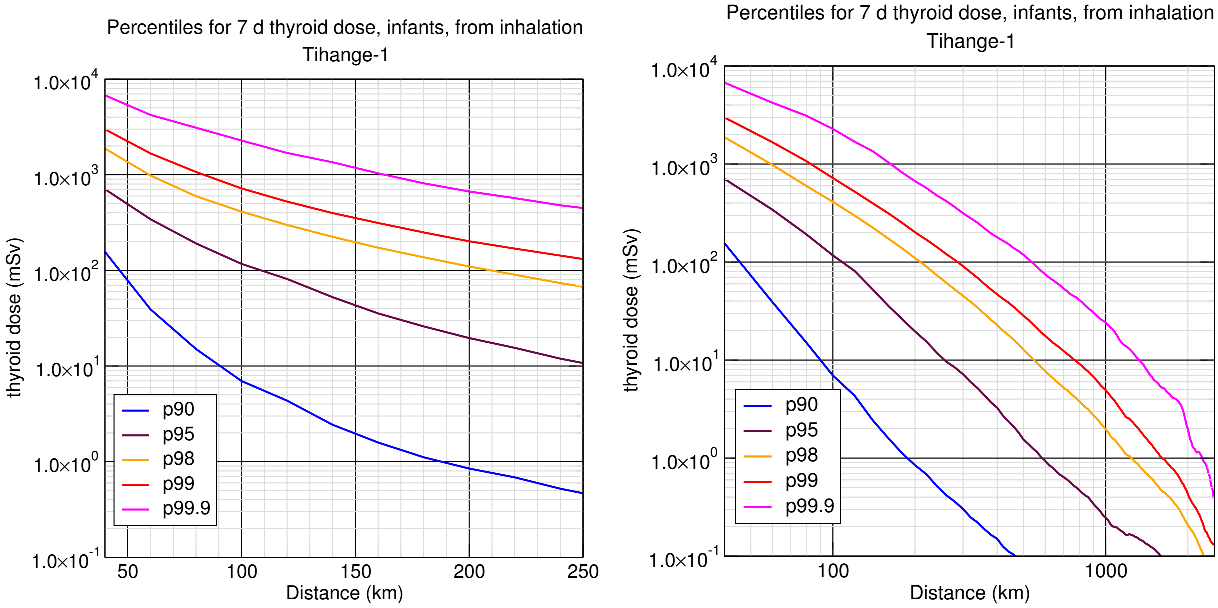

Figure 29: Percentile values for 7-d thyroid inhalation doses for infants around Tihange-1. Left: First 250 km with linear distance scale. Right: Whole range of 2500 km with logarithmic distance scale.

more than the annual maximum for occupational exposure), an exceedance is possible in almost all of Europe, with distances from NPP sites of about 900 km, and even for 1% risk the distance is still about 350 km. For very high doses of more than 250 mSv, the radius is much more restricted, with a risk of 1% at 70 km and 0.1% at 140 km.

Concerning the 7-day doses (all paths) and the 30-day doses (only groundshine), at a distance of 100 km the dose exceeded in 0.1% of all cases is 230 mSv (7 d) or, respectively, 300 mSv (30 d), and at 500 km the values are 20 mSv for 7 d and 35 mSv for 30 d doses.

Thus, we see that a distance of a few hundred kilometres to a nuclear power plant cannot guarantee that there will be no major consequences.

5.5.1 “Seven-day problem” – results

As explained in Section 4.5.2, iodine inhalation doses were calculated both for the first and for the maximum seven-day period. A frequency distribution of the ratios between the former and the latter was calculated, using Mochovce unit 1 and the maximum 7-d inhalation dose in Austria. To avoid cases with spurious doses from marginal parts of the plume, which are expected to behave more irregularly with respect to their temporal appearance and far from practical relevance, a minimum dose threshold of 1 mSv has been applied . The result (Fig. 30) shows that for 65% of the cases, the missed part of the dose is below 20% if only the first 7-d period is considered. However, there are about 10% of the cases with an underestimation of about 85% or more.

5.6 Risk export of NPP countries

The next step of aggregation leads to risk caused by a whole country. In this aggregation step, also the frequencies for the selected accident have been included as explained in Section 4.6. Therefore, the probability values are much lower than for the risk per unit as discussed above.

The list of endpoints considered is the same as for the aggregation of results pertaining to a single NPP unit.

As an example, the risk of exceeding a 7-day thyroid dose of 10 mSv for infants (the Austrian intervention level for iodine prophylaxis in children) from Switzerland is shown in Figures 31 and 32. The

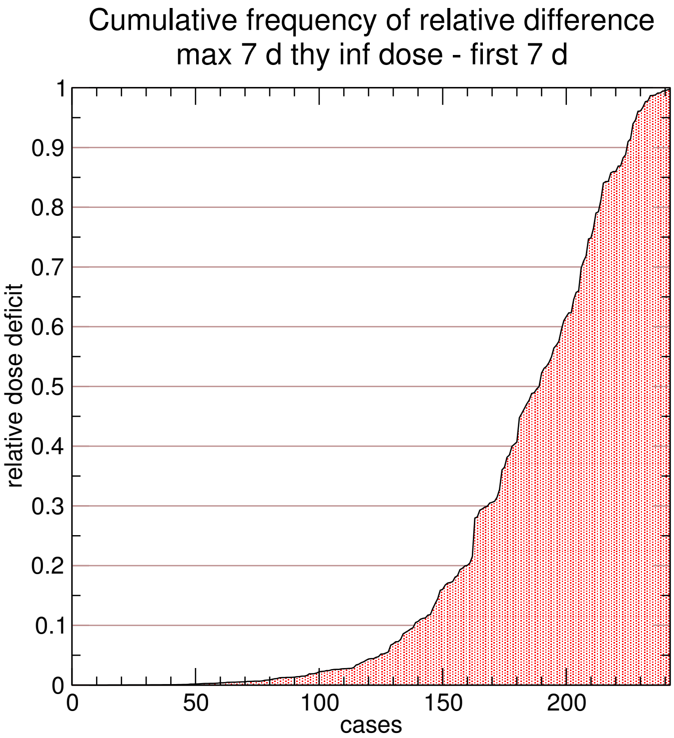

Figure 30: Cumulative frequency distribution of the ratio between the first 7-day thyroid dose and the maximum 7-day thyroid dose in Austria, for Mochovce unit 1, with a threshold of 1 mSv.

scenario is the baseline scenario S1, all NPPs under operation at the beginning of the year 2011 (note that for all countries except Germany and the UK, there is no difference between S1 and S2). From the map (Fig. 31) it can be seen that the risk extends preferably to the Northeast and Southwest, the two prevailing wind directions north of the Alps in Switzerland, where the Swiss NPPs are located. A considerable portion of the risk falls on Southern Germany, some also on France. Also Austria, Czech Republic and Italy are more affected. This redistribution of the risk on different countries is also reflected in the box plot (Fig. 32). However, here the size of the receiving country and how much of it comes under the influence of the potential contamination from Switzerland plays a role. First of all, the highest risk is borne by Switzerland itself. Next comes Germany, where the peak and the upper whisker (95% of country below) are, however, not much lower than in Switzerland, indicating the fact that parts of Germany are exposed to a similar risk than Switzerland. The third in the order of this plot, which follows the 95% value, is France, where values are not only less, but also more spread – the westernmost parts of France don't receive much risk from Swiss NPPs. The maximum and the 95% value for Austria are only a little less than in France, and in fact all the lower values (75%, average, median, 25% etc.) are even higher, as Austria does not have large areas without risk from Switzerland. In Czech Republic it is similar. Italy has a wide span of risks, the peak value in the northwest of the country being even higher than the peak for the Czech Republic, while the far south of the country receives practically no risk at all.

5.7 Overall risk distribution

5.7.1 Contamination risk maps

By combining the risk contributions from all NPPs in the flexRISK domain considered according to the operation scenario (see Section 2.5), an overall map of nuclear risk in Europe is obtained. This can be done for all the endpoints and thresholds available, and it turns out that the geographical patterns depend strongly on the severity of the threshold.

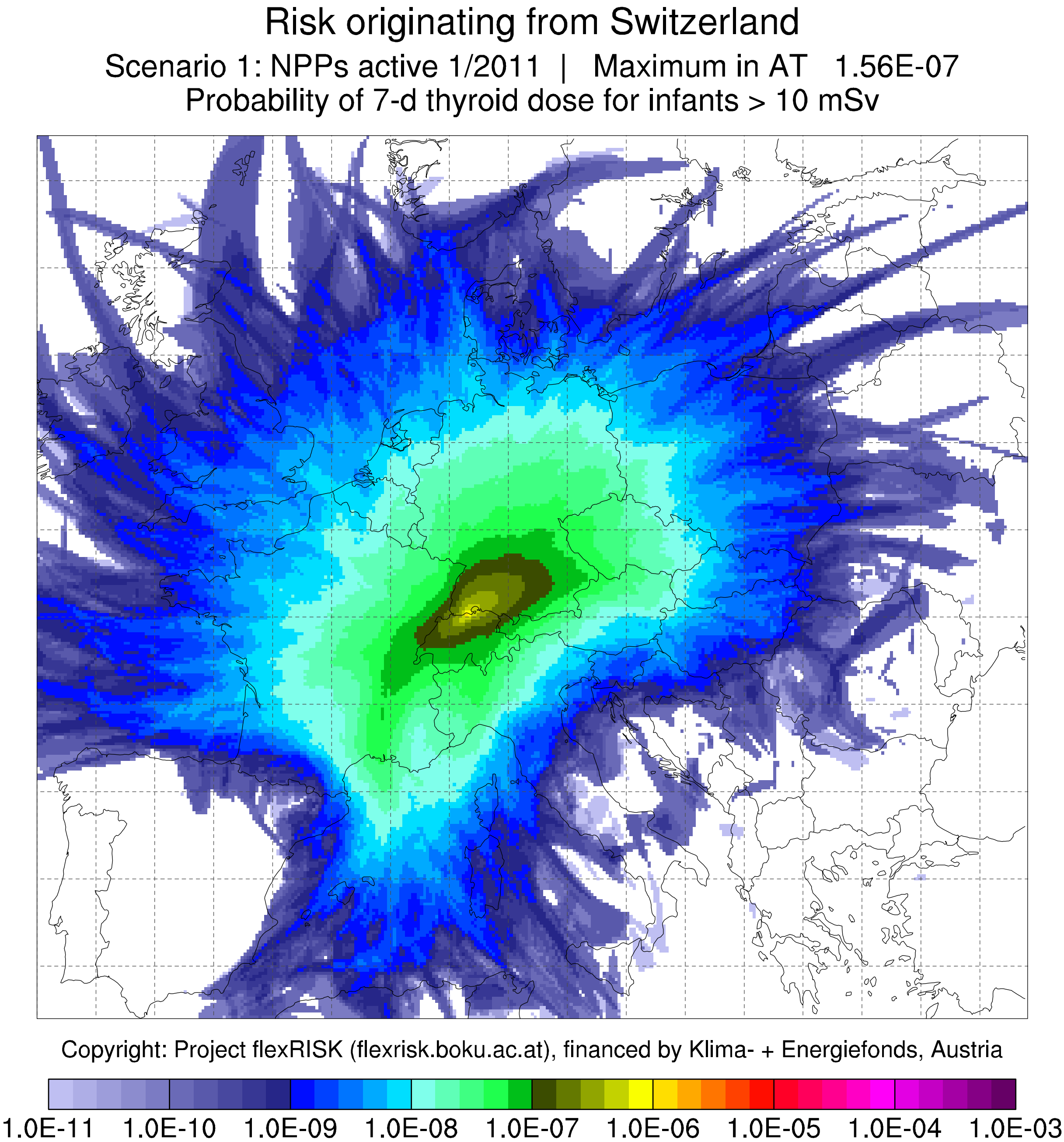

Figure 31: Map of the risk for exceeding a thyroid dose of 10 mSv in 7 days for infants from all NPPs in Switzerland, scenario 1 (all Swiss NPP units in operation in January 2011).

As the ground contamination endpoint has been evaluated with respect to the widest range of thresholds, it will be used to illustrate this point. Figure 33 shows these maps for the zoomed domain, and Fig. 34 for the coarse domain. First of all, one can recognise that for low thresholds the maps are very similar while for higher thresholds, the maxima of risk are lower in the coarse-grid results. This is an effect of the grid resolution, and coarse-grid results should be interpreted keeping in mind that they will be less accurate at higher contamination and dose.

The threshold for low contamination (e.g., 5 kBq Cs-137 m^{-2}, which roughly corresponds to the existing contamination from the nuclear weapon tests in the 1950ies and 60ies) can be exceeded easily in a distance of 1000 km and more. Thus, the influences from the various NPP sites overlap according to prevailing wind directions, and the risk generally increases within Europe from East to West, from about 1E-7 per year at the Algarve in Portugal to a bit over 1E-4 in Belorussia, Ukraine and Russia, with a maximum over Western Russia. Almost all the Mediterranean has a risk on the order of 1E-5, being lowest in Spain together with the Southern and Eastern rim of the Mediterranean Sea

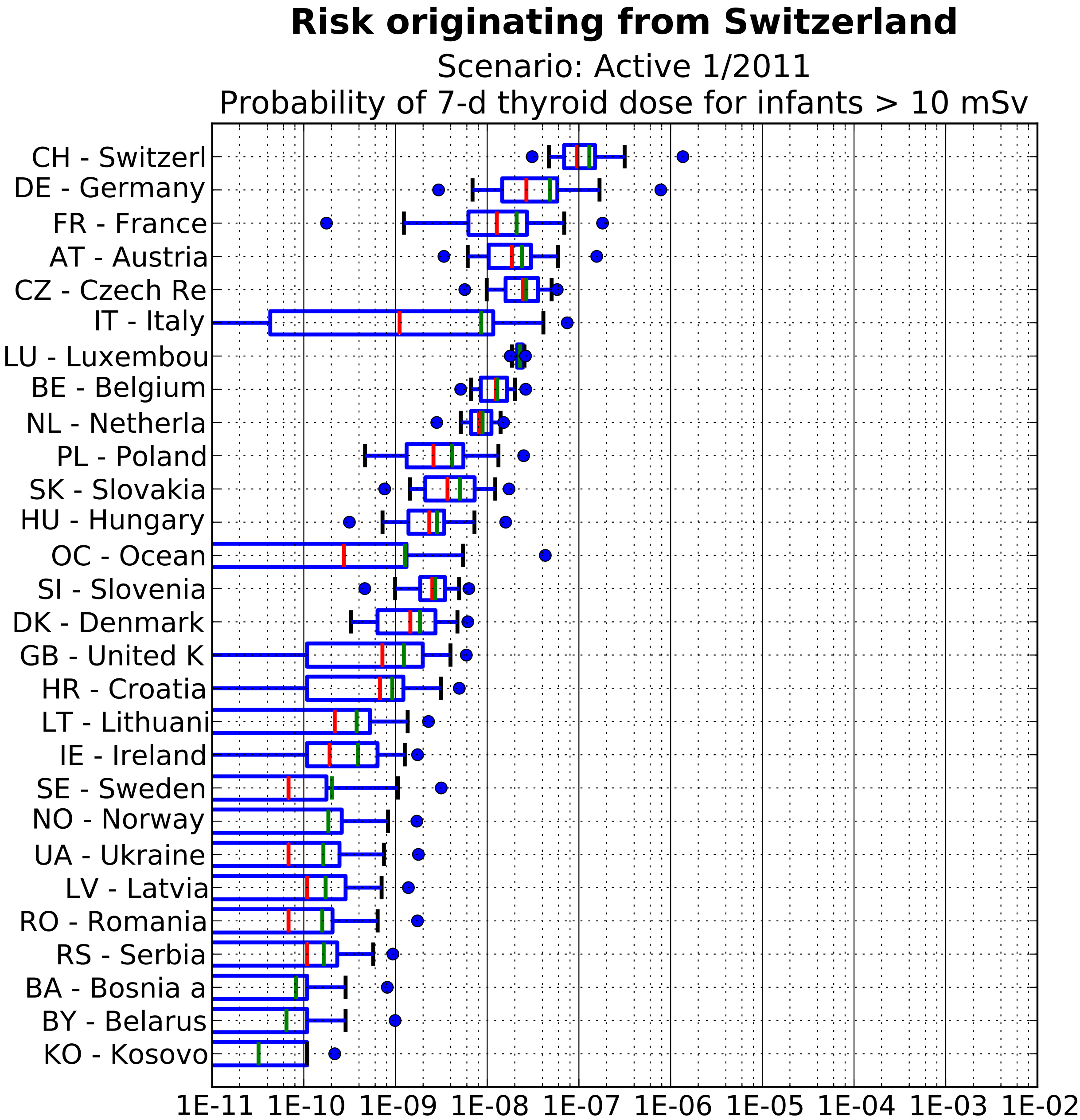

Figure 32: Box plot of the risk caused by the NPPs in Switzerland (scenario 1), risk parameter: exceedance of a thyroid dose of 10 mSv in 7 days for infants. Subdivisions of the logarithmic x-axis refer to factors of 2, 4, 6, 8. The right dot gives the highest reisk found in the country, the left dot the lowest one (may be off-scale). The green line indicates the mean over the country. Box and whiskers represent percentiles, as explained in Section 4.6.2.

(note that Akkuyu on the southern coast of Turkey is not yet considered!) and larger in Italy and more so in Greece. Scandinavia and Ireland are also included in the zone of approx. 1E-5 per year.

On the other hand, the threshold of 1480 kBq Cs-137 m^{-2} is mostly exceeded only within some dozens up to some hundreds of kilometres. Therefore, the density of the NPP sites is clearly visible, modulated by block size, and severity and frequency of releases. Larger areas with a risk exceeding 2E-6 are thus mainly found in parts of France, especially in the Rhône Valley where in addition to an agglomeration of nuclear installations there is channelling of the winds, on the arc Temelín–Dukovany–Bohunice–Mochovce–Paks, around Kozloduy (Bulgaria and Romania), in the northwestern Ukraine and the surroundings of Sosnovy Bor near St. Petersburg. In the large domain, Kola, sites further east in Russia, and Medzamor add to this. Meteorological influences are not only visible in the Rhône Valley,

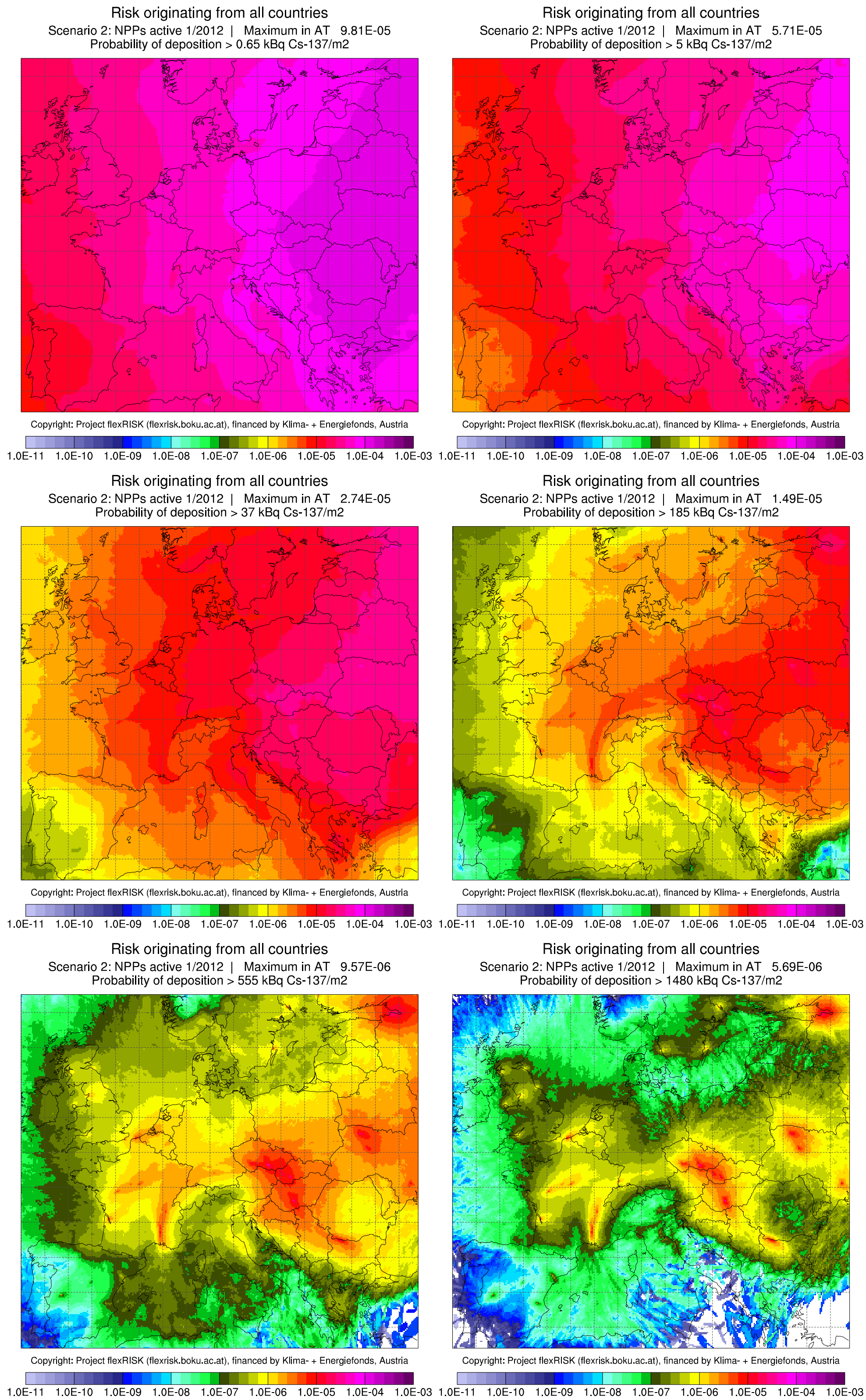

Figure 33: Risk of exceeding a given ground contamination threshold due to contributions from all NPPs operating under Scenario 2, zoomed domain.

they manifest also in a strong gradient across the Alps: while the northern rim of the Alps is exposed to a relatively high risk, this decreases to one tenth and less over the Central and Southern Alps and the Po Basin. The influence of windward-side enhancement of precipitation is not only found on the

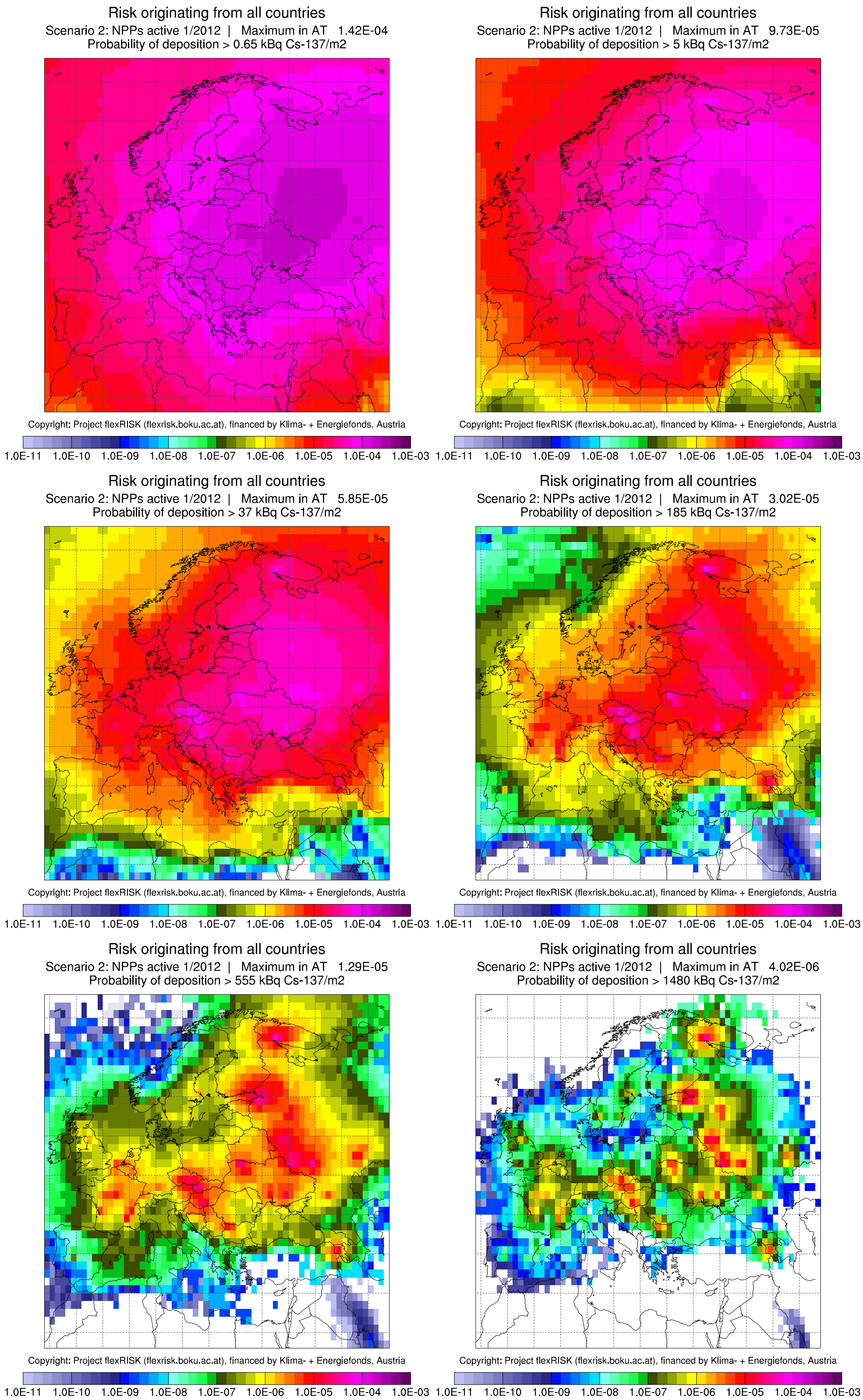

Figure 34: Risk of exceeding a given ground contamination threshold due to contributions from all NPPs operating under Scenario 2, coarse domain.

northern side of the Alps, also the eastern slopes of the Appennines are exposed to increased risk originating from East. Because of the influence of the Rhône Valley and its mistral wind, the risk in the western Mediterranean is markedly higher than in the eastern Mediterranean, even though being clearly lower than in Central Europe. This influence even reaches to the North-African coast.

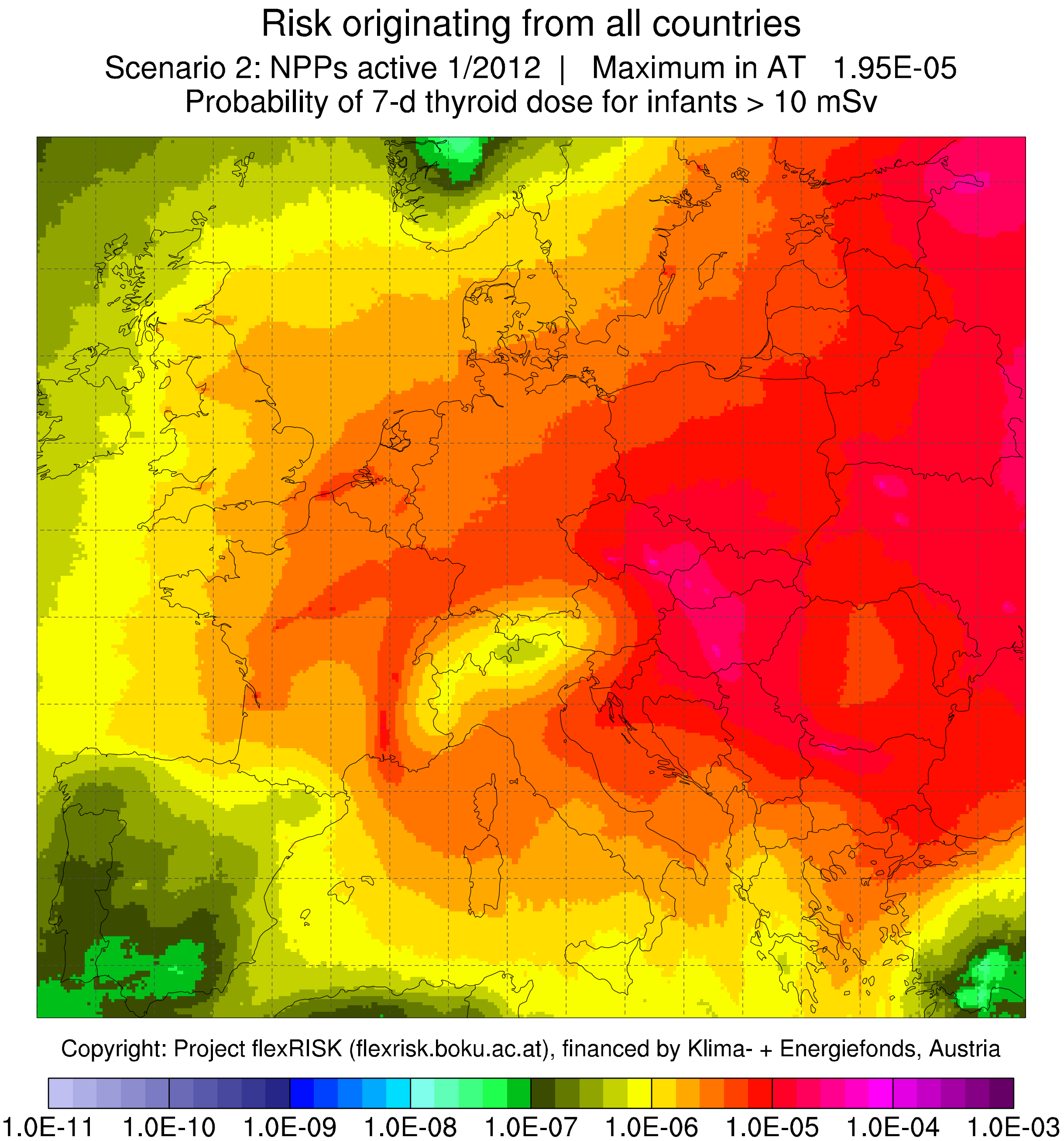

Figure 35: Map of the risk of exceeding a thyroid dose of 10 mSv in 7 days for infants, all NPPs, scenario 2, zoomed domain.

5.7.2 Dose risk maps

As shown in Figure 35, there is chance everywhere in the zoomed domain for exceeding the Austrian intervention level for administering stable iodine to children, based on the 7-day inhalation dose from iodine. However, the risk varies by a factor of more than 100, from 1E-7/a in some parts of southern Europe and Norway to around 1E-5/a in the higher-risk zones of Central and Eastern Europe. Thanks to the fact that winds most of the time go around rather than over mountains, and if they do go over usually there will be wash-out centred around the foothills, the Alps (and to a lesser extent the Carpathian mountains in Romania) form an island of less risk for inhalation-related doses. Once more, the east of Austria is found to be exposed to a relatively high risk compared to other countries.

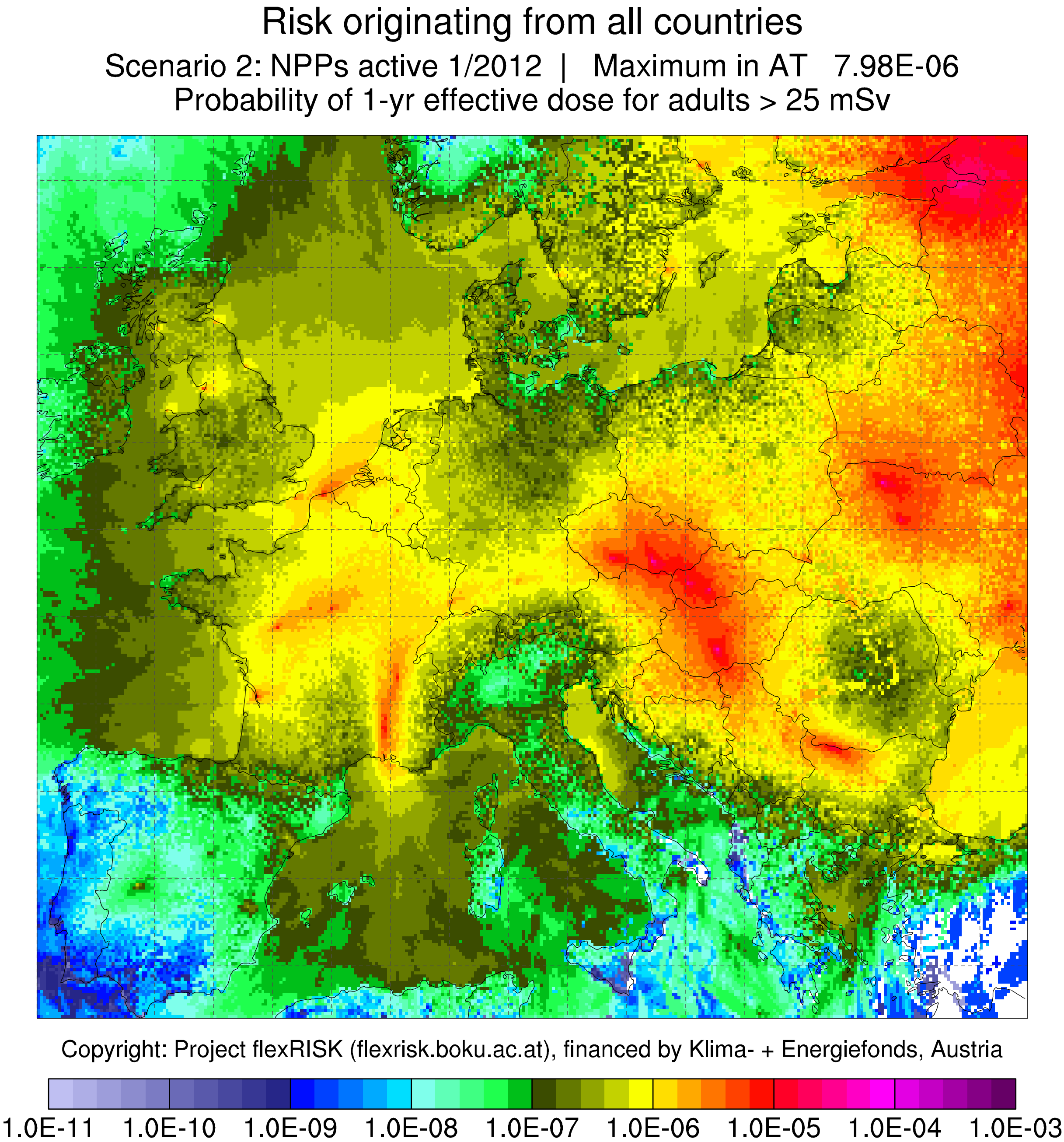

Figure 36: Map of the risk of exceeding an effective dose of 25 mSv in 1 year for adults, all NPPs, scenario 2, zoomed domain.

Serbia is in a similar situation, as are Poland (which is, however, planning for nuclear power itself) and Croatian (being co-owner of the Krsko NPP situated near the Slovenian-Croatian border, thus not really a nuclear-free country).

A map for the risk for exceeding a 1-year effective dose of 25 mSv (Fig. 36) looks different in several aspects. Firstly, this is a comparatively high dose level and the risk is more concentrated to the surroundings and nearby downwind areas of the NPP sites. Secondly, for the 1-year effective dose, the location factors describing the dose reduction due to staying inside buildings (cf. Section 4.3.7) becomes a major factor. They are implemented as a function of population density. Therefore this risk is higher over sea than over land, and over land there is small-scale variability reflecting the variability of population density. For example in Austria, we see a dose minimum in the Inn Valley in Tyrol which is because of the high population density there. Once more the regions already identified as having higher risks are prominent, such as many regions in France with the Rhône Valley as no. 1, Belgium and Southern Germany, as well as Eastern Austria and many parts of Eastern Europe,

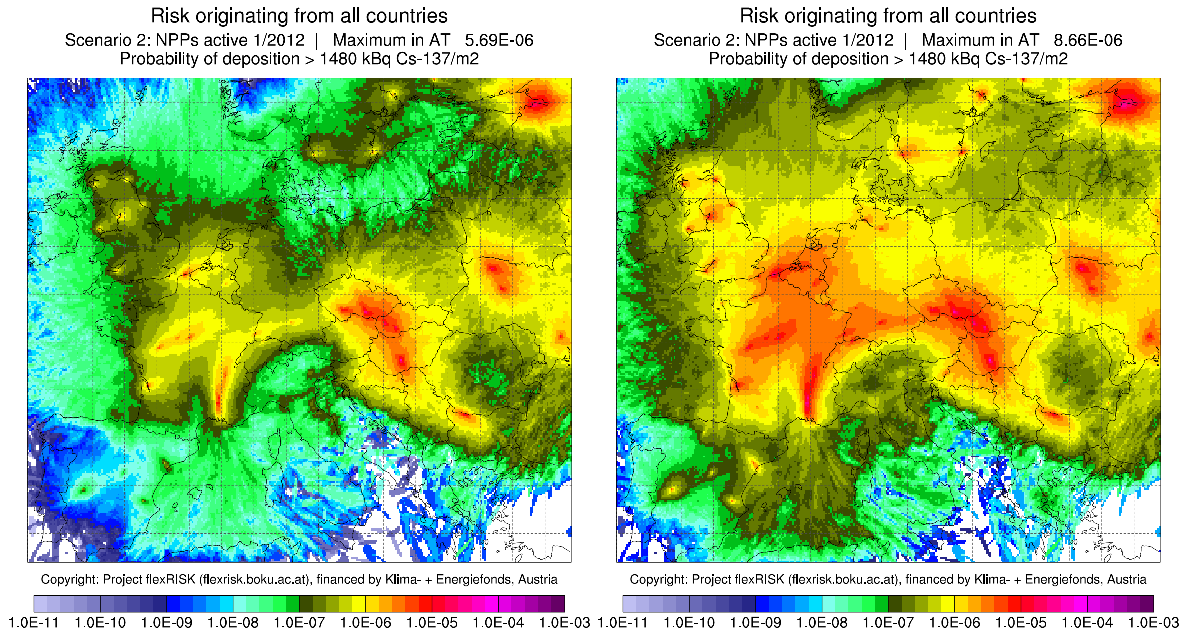

Figure 37: Comparison of risk of exceeding a 1480 kBqm^{-2} ground contamination with ^{137}Cs, all NPPs operating under Scenario 2, for reference release frequencies (left) and reduced range of release frequencies (right).

in the latter case due to the presence of certain VVER and RBMK reactors which were assigned a comparatively high release frequency.

5.7.3 Sensitivity of results to the release frequencies

As noticed several times, the strongest risk maxima are associated with certain types of VVER (pressurised water reactor developed originally in the Soviet Union) and RBMK (graphite-moderated, water-cooled reactor of Soviet design, the “Chernobyl reactor”) reactors. This is a consequence not only of the source term strengths (see Fig. 17) but also, and even more so, of the large release frequencies (see Fig. 14) assigned to them, much higher than those of other reactors. The large-release frequencies span more than three orders of magnitude, from 2.4E-5 for the worst (certain VVER-440 reactors) to 1.0E-9 for the best reactors (German KWU Convoi reactors). It can be questioned how reliable these numbers are, especially considering the inhomogeneity of the probabilistic safety assessments for different plants, and the possibly not fully considered list of relevant events. The present record of large releases from NPPs – at least Chernobyl unit 3 and Fukushima units 1–3 (maybe also unit 4), to a lesser extent the Windscale 1957 event – within only about 10^4 reactor years is, although not statistically robust, a hint that the PSA-based frequency might be too optimistic. In any case, it appears useful to study the sensitivity of the results to this parameter. For this purpose, the release frequencies have been modified so that their range is halved in the logarithmic space, in such a way that the highest value is kept, and that the logarithmic difference of the lower values to this highest value is halved. If these frequencies are used, then the risk in Western Europe would increase strongly and the risk distribution in Europe would not be dominated by VVER and RBMK reactors anymore (Fig. 37). This release frequency scenario is shown purely to illustrate sensitivity, not because we consider it to be necessarily realistic. However, it is obvious that certain results and conclusions strongly depend on the reliability of these data.

5.8 Risk import

Let us now turn to the ranking of the risk originators for a specific receiving country, in this case Austria. As the risk origination is not a continuous function of space, this cannot be displayed as

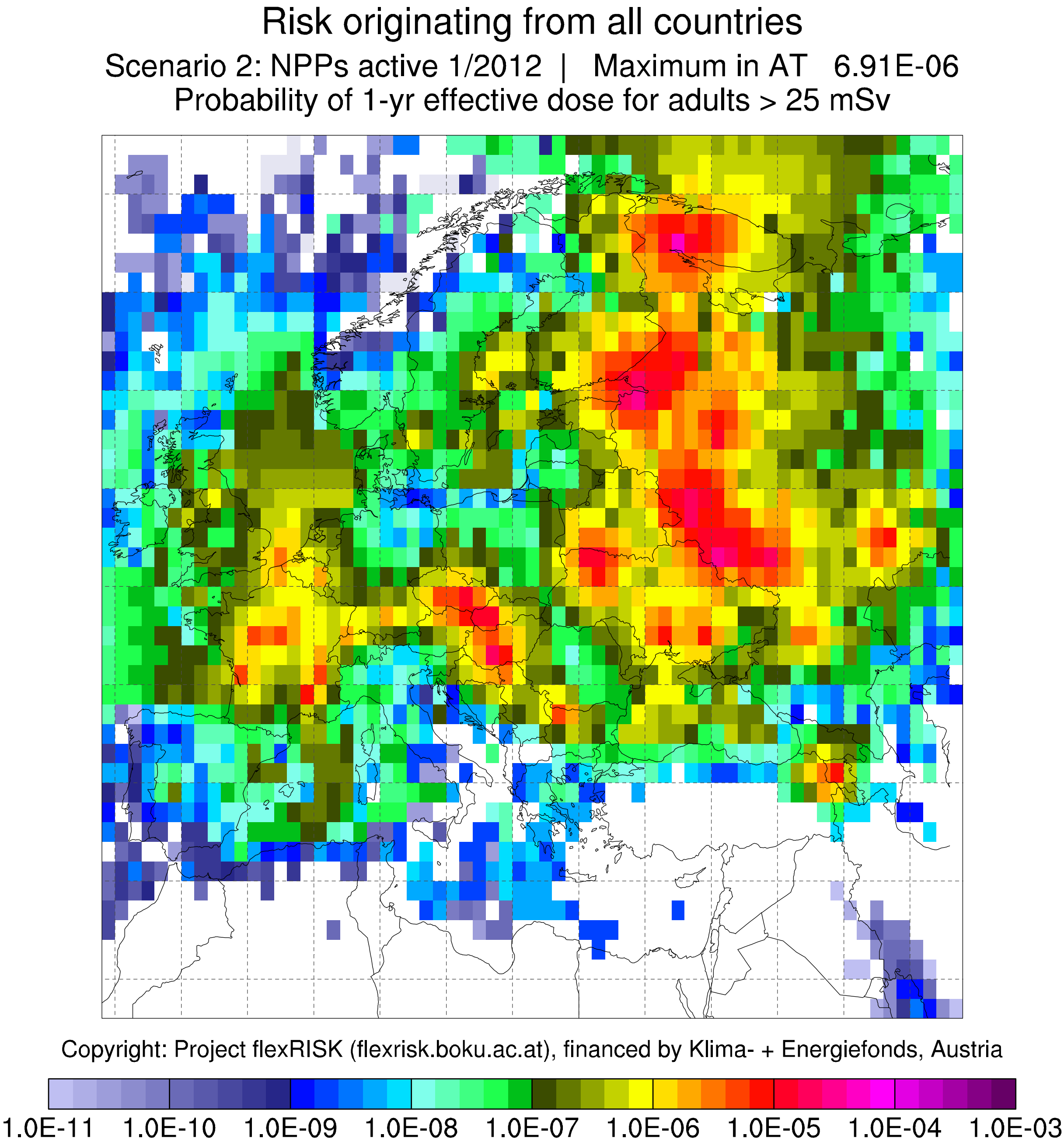

Figure 38: Map of the risk of exceeding an effective dose of 25 mSv in 1 year for adults, all NPPs, scenario 2, coarse domain.

contours on a map. It is presented as a box plot with countries acting as risk sources (Fig. 39). The risk of a thyroid dose exceeding the 10 mSv threshold (intervention level for iodine prophylaxis in children) is dominated by NPPs of the Czech republic. Next comes Slovakia and Hungary, and then in a third group of countries with similar risk, Ukraine, Bulgaria, France and Germany (in this order, in spite of different geographical proximity and wind patterns – an effect of the release frequencies ascribed to different plant types). Russia, Switzerland, Slovenia, Belgium and the UK make the next group, and finally there is some risk also from Sweden, Spain and the Netherlands. The wider the box for a country, maybe starting beyond the lower end of the scale, the more inhomogeneous is the risk from this country within the territory of Austria.

If we look at effective doses for the first year (Fig. 40), the result for the lower threshold is similar to that of the thyroid dose, but with a higher contribution from France, and with less spatial inhomogeneity (bars are less wide). In the case of the higher threshold, the list of risk-contributing countries is shortened and the risk values are lowered, but the order remains the same.

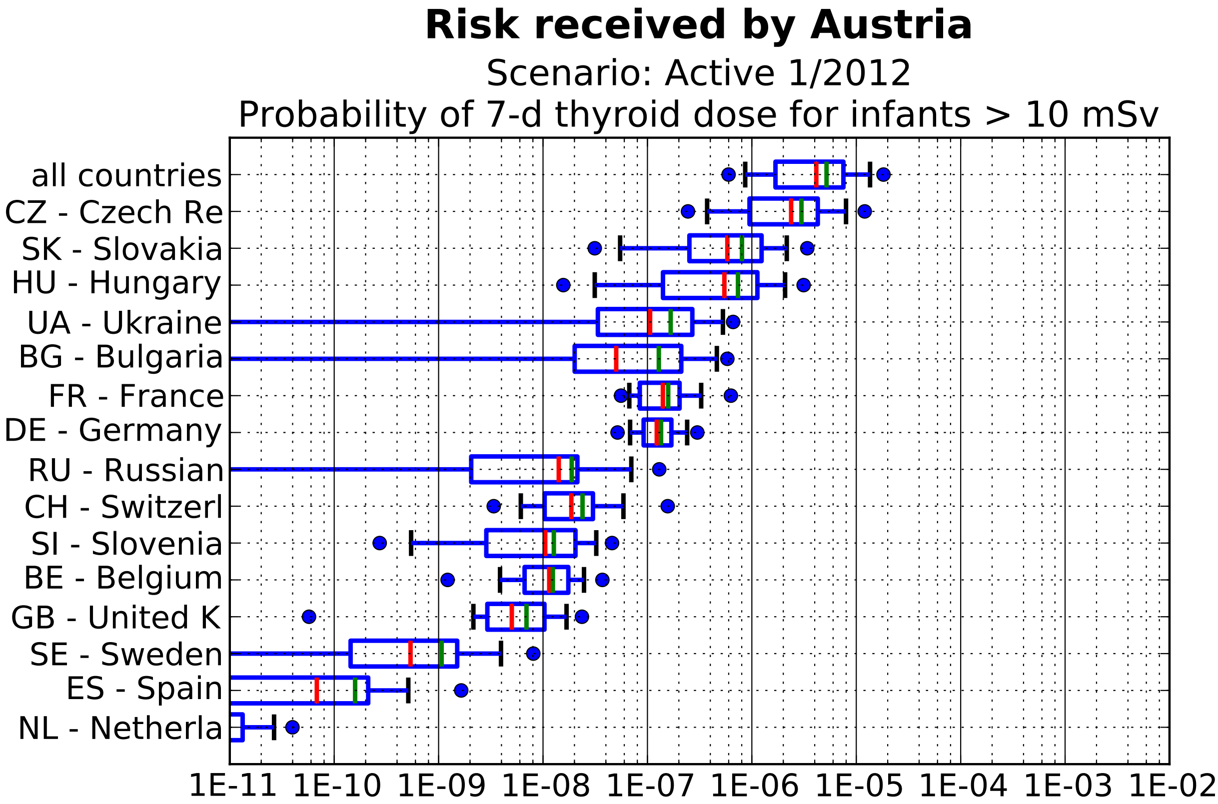

Figure 39: Box plot of the risk sources for Austria (scenario 2), risk parameter: exceedance of a thyroid dose of 10 mSv in 7 days for infants. Explanation of this diagram see Fig. 32 and Section 4.6.2.

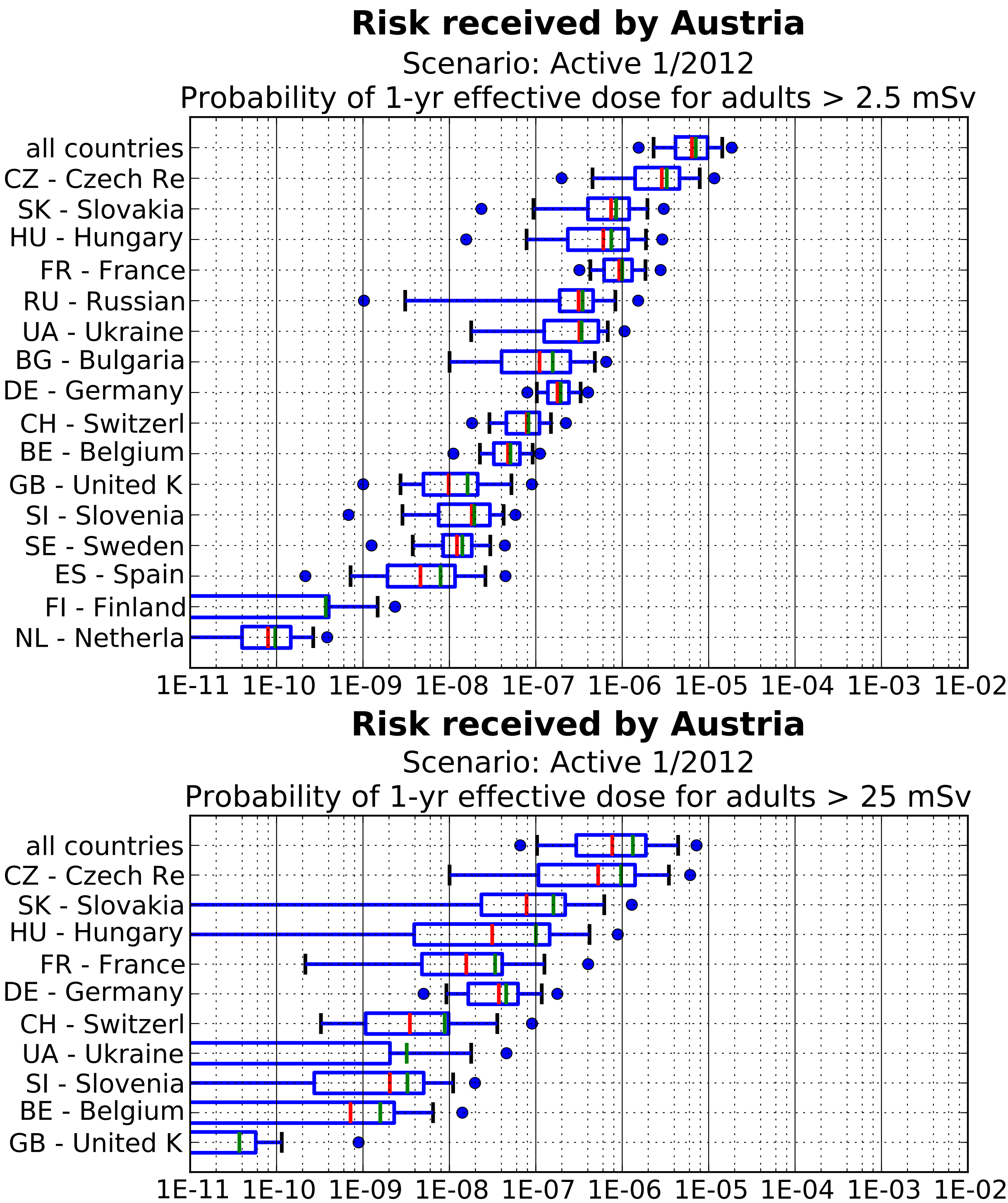

Figure 40: Box plot of the risk sources for Austria (scenario 2), risk parameters: exceedance of an effective dose of 2.5 mSv (top) and 25 mSv (bottom) in 1 year for adults.

6 Conclusions and recommendations

6.1 Conclusions

In flexRISK, long-range consequences of severe accidents in the European nuclear reactor park have been evaluated with respect to contamination as well as various types of radiation doses for a large number of real weather situations. A very rich source of data has been created, and a set of flexible tools has been developed.

For a relevant subset of about 2% of the weather situations (i.e., all those referring to the year 1995), all the single accident results have been visualised and made available on the web. Furthermore, aggregated results have been produced for each NPP unit and for each nuclear-power country, as well as aggregated results with respect to the risk received by country. Percentiles of contamination and doses have been calculated as a function of distance for a selected plant. Aggregated risks on country level which include an estimate of the severe accident frequency have been visualised as maps (country-to-grid) and box plots (country-to-country).

Three reactor park scenarios have been considered: the situation at the beginning of 2011, at the beginning of 2012 (with Fukushima-triggered shutdowns in Germany and a scheduled shut-down in the UK), and a phase-out scenario with plants started up before 1980 considered closed. All plants where construction is going on or definitive decisions and building licenses were in place during the project have already been calculated. They can be added to aggregated results without much additional work if so desired.

All source term and accident frequency data take into account reactor-specific characteristics to the extent that was possible with the data situation found.

From this material, conclusions can be drawn on

1. the general spatial behaviour of the risk;
2. the regions having the highest risks;
3. the regions having the lowest risks;
4. the effectiveness of shutdowns;
5. the risk as a function of distance from the plant;
6. the major factors of uncertainty;
7. the needs for emergency planning.

6.1.1 General spatial behaviour of the risk

Spatial risk patterns depend on the level of damage considered. For low damage thresholds, which typically occur for distances of hundreds of kilometres, or even one- to two-thousand kilometres, the variation of the risk is low and it increases from west to east. For higher damage thresholds, the risk maxima increasingly concentrate in regions around and downwind of the most dangerous plants.

6.1.2 Regions having the highest risks

For high damage thresholds, such as a ground contamination with ^{137}Cs of more than 1480 kBqm^{-2} or one-year effective doses exceeding 25 mSv, main risk areas for scenario 2, plants operating 1/2012, are (roughly from west to east)

- the Rhône valley in France,
- an arc from Czech Republic through Slovakia to Hungary, touching adjacent countries such as Austria,
- the region near Kozloduy (Bulgaria),

– northern Ukraine (Rovno area),
– western Russia,
– the region near Sosnovy Bor / St. Petersburg (Russia).

Within Germany, there is a clear risk increase from north to south.

6.1.3 Regions having the lowest risks

For high damage thresholds, such as a ground contamination with ^{137}Cs of more than 1480 kBqm^{-2} or one-year effective doses exceeding 25 mSv, areas with little risk (again scenario 2, plants operating 1/2012) are

– Ireland,
– the west and south of the Iberian peninsula,
– southern Italy,
– southern Greece,
– non-European parts of the Mediterranean,
– most of Norway and northern Sweden.

6.1.4 Effectiveness of shutdowns

As the risk for higher damage thresholds is concentrated within a few hundred kilometres from a site, closure of nuclear power plants does lead to a relevant reduction of such risk. In the case of regions with several plants, closure of all or at least those plants considered to have a higher accident frequency is able to substantially reduce or even almost remove risk in that region, as Figure 41 shows. The exclusion of virtual all risk by the removal of most of the NPPs in the region of Hamburg (northern Germany) is striking, and the effect of taking out British GCRs or the Fessenheim NPP (France, border to Southern Germany) and Swiss NPPs is also substantial.

6.1.5 Risk as a function of distance from the plant

In general, the contamination risk is not simply a function of the distance only. The shape of the risk depends on the wind and precipitation climatology, and for example, near the Alps it is far from being isotropic (in concentric circles), as Fig. 42 illustrates. In single cases, very complex contamination patterns can occur, as was demonstrated in Section 5.3.2. As a rough guidance, for a site not much influenced by mountains, risk has also been evaluated as a function of distance, combining all directions, in Section 5.5. Summarising a few of these results, it was found that the risk zone, here taken as the distance where the value indicated was exceeded in 1% of all cases (99th percentile),

– extends to 1300 km for a contamination risk of 185 kBqm^{-2} (zone with the right to resettlement after Chernobyl),
– extends to 300 km for a contamination risk of 1480 kBqm^{-2} (priority zone for permanent resettlement after Chernobyl),
– extends to 1500 km for a 7-d thyroid dose for infants of 10 mSv (Austrian intervention level for giving stable iodine to children),
– extends to 300 km for a 7-d thyroid dose for infants of 100 mSv, and
– extends to 85 km for infants for a 7-d thyroid dose of 1000 mSv (roughly corresponding to Austrian intervention level for adults).

These numbers very clearly indicate the long-range and transboundary character of nuclear accident risks.

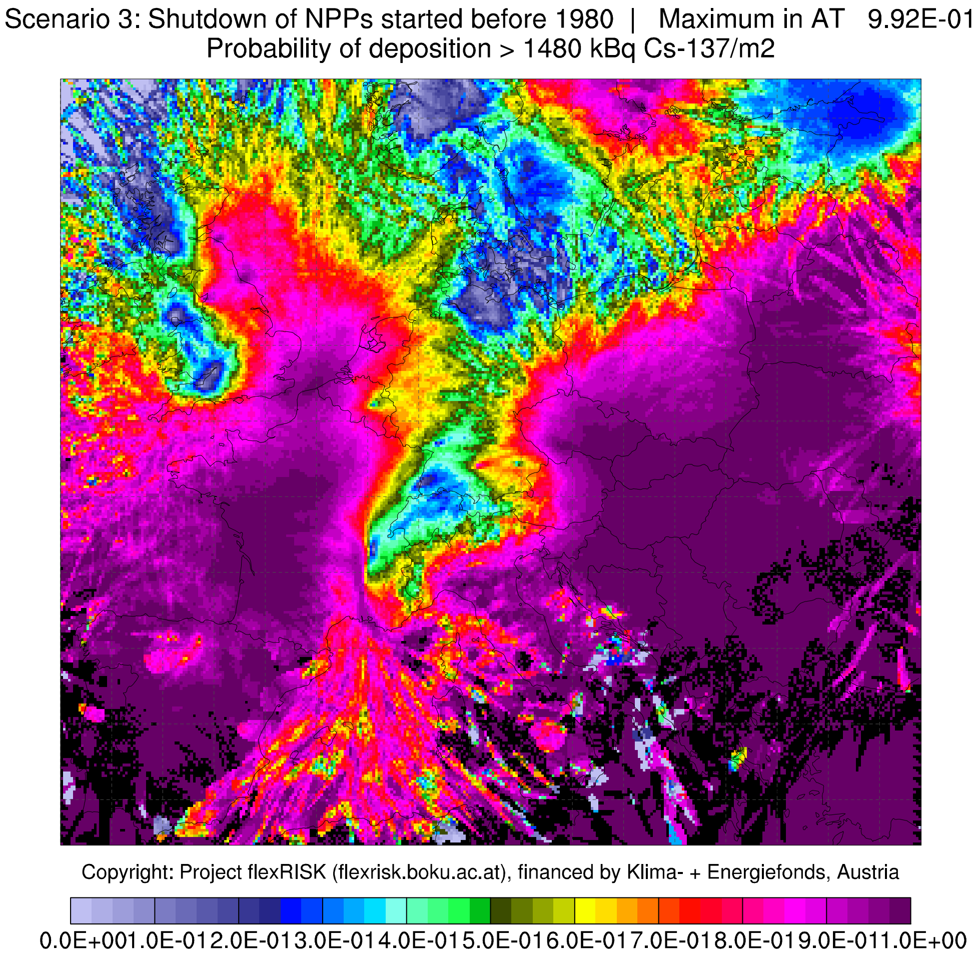

Figure 41: Ratio of risk for exceeding ^{137}Cs deposition of 1480 kBqm^{-2}, scenario 3 (shutdown of pre-1980 NPPs) to scenario 1 (1/2011), all NPPs. The left end of the (linear!) scale points to zero risk left, the right one to 100% of the risk left.

6.1.6 Major factors of uncertainty

The single most important factor of uncertainty for the risk is the accident frequency assigned to different plants, as it varies by more than a factor of 1000, the methodologies applied for different NPPs are not always comparable, and the absolute values may be questioned.

The risk parameter considered (e.g., thyroid or effective dose, and low, medium or higher dose threshold) is also an important influence factor. A generally accepted “overall risk parameter” probably does not exist, the usual approach towards it being inclusion of economic consequences with monetarising all kinds of damage, which is however, not only out of the scope of our project but involves many additional assumptions.

The release fraction is probably the most important uncertainty factor if only a single plant is considered, if the accident frequency is disregarded as we did here.

In the dispersion calculations, the partioning and behaviour of iodine is a relevant uncertainty of this substance, and in general the washout and thus especially ground contamination parameters have to be considered more uncertain than other meteorological processes.

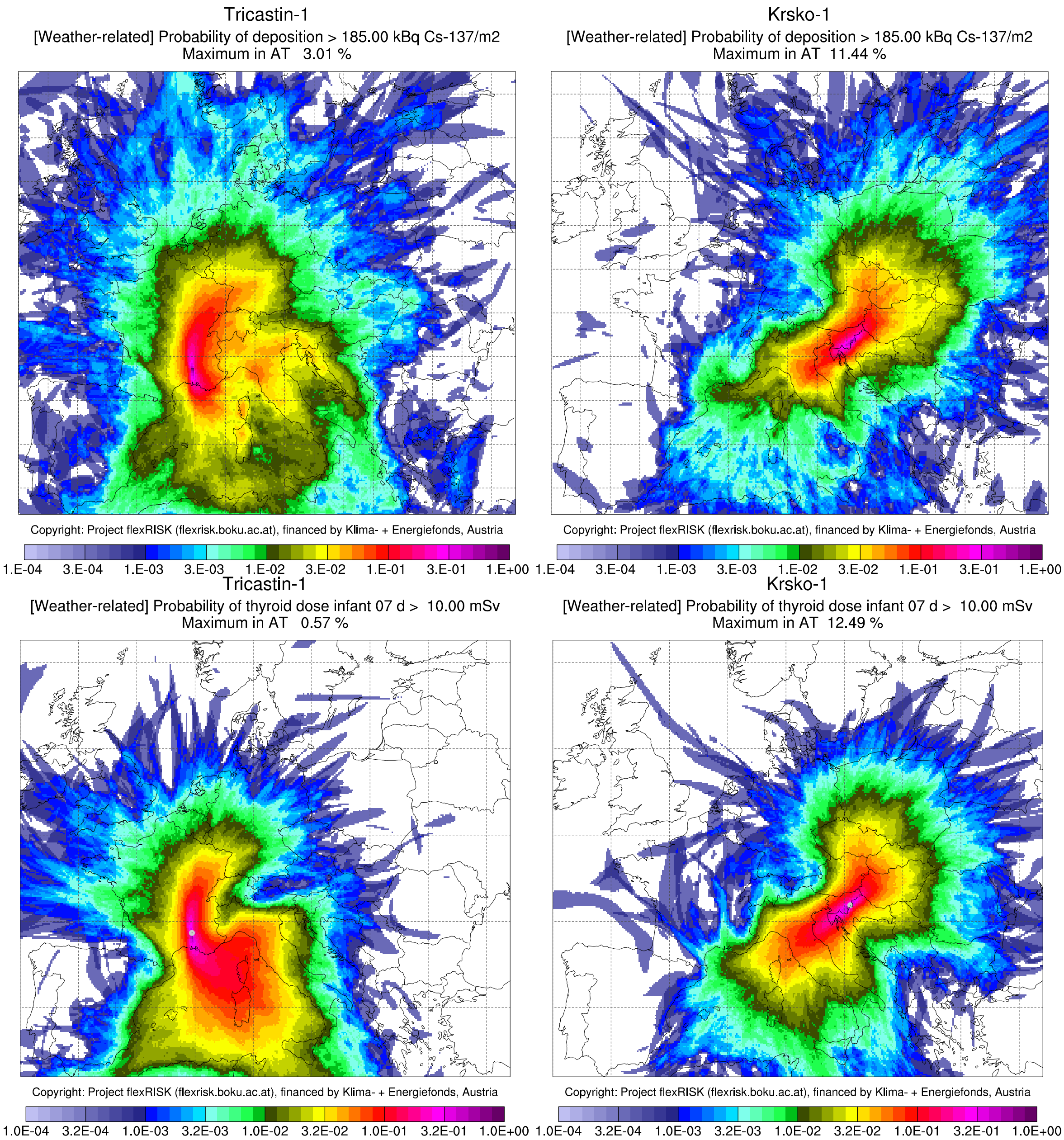

Figure 42: Anisotropic risk distribution at the example of Tricastin-1 (left column) and Krsko (right column). The top row shows the meteorological risk for exceeding 185 kBqm^{-2} ^{137}Cs-deposition, and the bottom row for exceeding 10 mSv thyroid dose in infants. Note the secondary maximum at the Ligurian coast for the deposition risk of Tricastin!

6.1.7 Needs for emergency planning

Iodine prophylaxis

flexRISK results show that Austrian intervention dose levels can be exceeded for 5% to 25% of the weather situations within Austrian territory for accidents in the neighbouring NPPs.

A recent study of the German Federal Office for Radiation Protection BfS (Gering et al., 2012) analysed emergency planning measures in the light of Fukushima experiences for two German NPP sites, Unterweser and Philippsburg. An accident with a release of about 10% of iodine over up to 30 days was assumed. In Germany, an intervention level for iodine prophylaxis of 50 mSv for children is used. Iodine tablets are stored in a radius of 100 km around NPP sites.

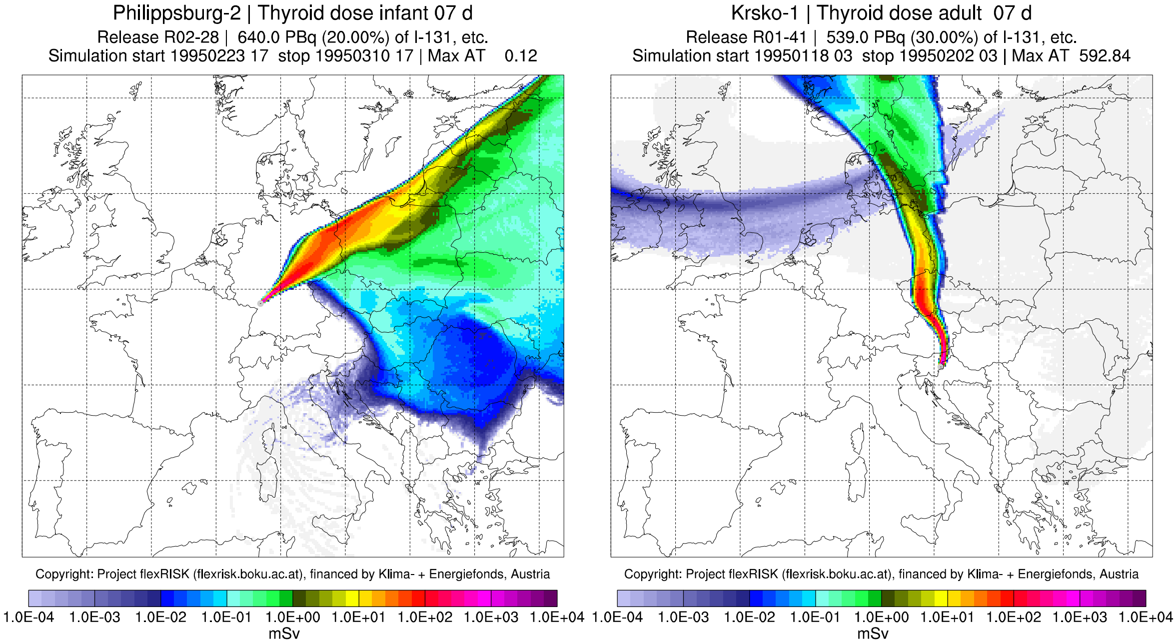

Figure 43: Left: Thyroid dose for infants from a hypothetical accident at Philippsburg-2, release starting 1995-02-23, 17 UTC; right: thyroid dose for adults from a hypothetical accident at Krsko, release starting 1995-01-18, 03 UTC.

Regarding results for Philippsburg it was shown that in nearly all of the BfS scenarios the intervention limit for stable iodine administration was exceeded at distances larger than 100 km, reaching up to 190 km. The conclusion of the authors was that the existing emergency planning was not adequate. Similar conclusions were obtained for other emergency measures such as sheltering and evacuation, and for the Unterweser site.

Thyroid dose results from flexRISK for Philippsburg unit 2 are shown in Figure 43 (left) for a weather situation with severe consequences. The German intervention level of 50 mSv is reached in the grid cells with orange and red colour. This region has a dimension of > 700 km north-south and >950 km east-west, obviously much more than a radius of 100 km around the site. The difference to the BfS results can be explained by the different accident scenarios and source terms. Emergency planning in Germany (and elsewhere) should rethink its politics of the restricted storage of iodine tablets for offsite emergency measures. In Austria, iodine tablets are available for every child in kindergardens and schools (predistributed), and adults can buy them in pharmacies all over the country.

In Austria, for adults above the age of 40 intake of stable iodine tablets is recommended only if thyroid doses above 500 mSv are expected. This dose level would be reached in some of the flexRISK scenarios, as the example of Krsko (Fig. 43, right) shows, with a maximum for Austria of nearly 600 mSv thyroid dose. Regarding these results, iodine prophylaxis has to be re-thought by radiation protection authorities.

These findings are underlined by the maximum thyroid dose values found for each of the coarse grid cells, considering all the NPPs active in scenario 2 in the whole flexRISK domain (Fig. 44). Even if we consider that the worst case out of 2,800 weather situations is a very extreme event, and that results for grid cells containing NPP sites, or those very close, need to be interpreted with care (due to the large cell size, maxima within the cell are underestimated, but not all the cell will reach the value shown), it is quite obvious that intervention limits for children can be exceeded everywhere and those for adults over large areas.

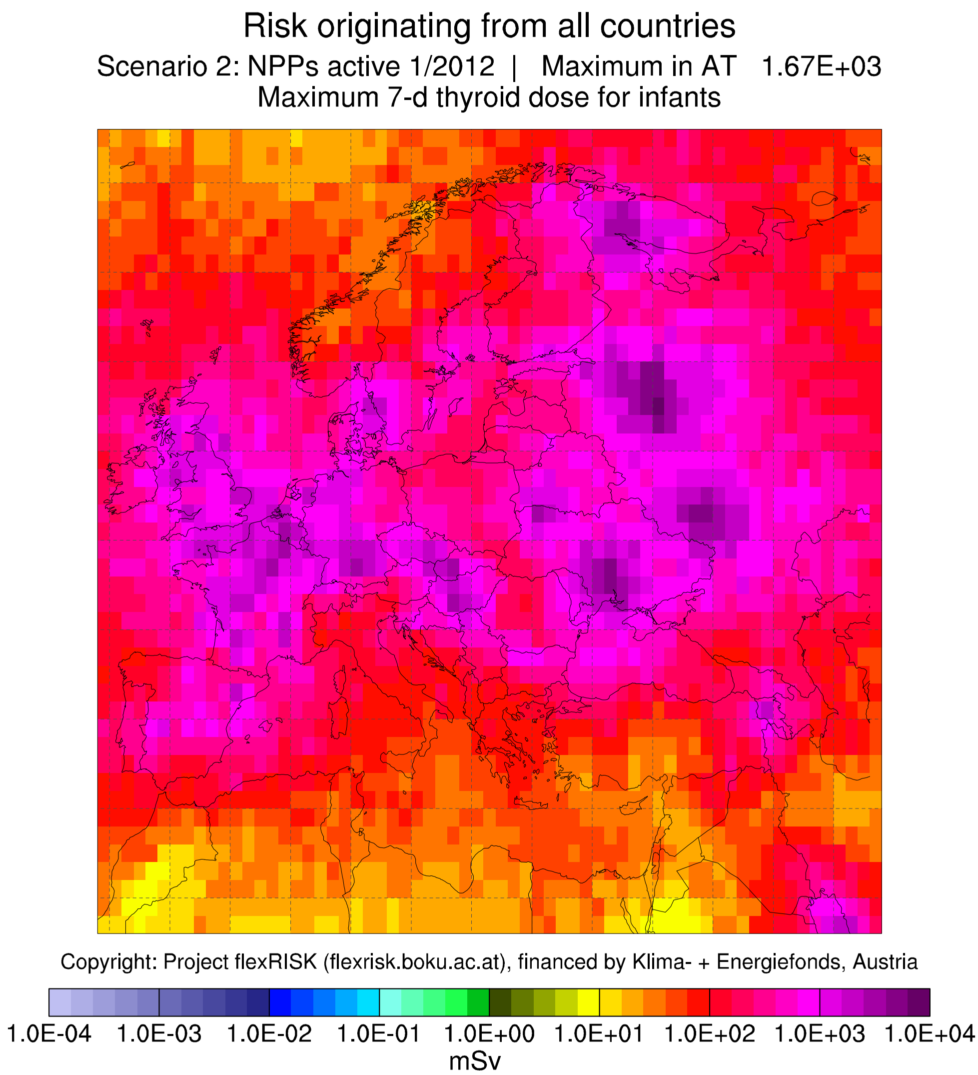

Figure 44: Maximum thyroid dose for infants for all weather situations, all NPP units of scenario 1, coarse domain.

6.2 Recommendations

6.2.1 Emergency preparedness

Europe-wide, rapid distribution or pre-distribution of stable iodine should be prepared all over the country, as done in Austria. This is especially important for children and pregnant women. Stable iodine tablets should be available in schools and other places where children are staying. Furthermore, it should be taken into account that adults above 40 years could receive thyroid doses above intervention levels, therefore iodine tablets for these groups should also be disseminated.

Emergency planning for other intervention measures should also be reviewed in the light of Fukushima experiences, flexRISK and BfS results. flexRISK can provide many examples for complex contamination patterns, even with relatively simple source terms. It should be assessed to which extent emergency plans are based on assumptions which are too much idealised. Specifically, short exposure times such as 2 days or 7 days for defining intervention levels need to be reassessed (this refers also to iodine prophylaxis). Plans for evacuation and temporary relocation need to consider well the actual or expectable contamination patterns, as the experience of Fukushima has demonstrated.

6.2.2 Risk reduction

Risk reduction here refers to shutting down nuclear power plants for effective reduction of the risk of severe consequences of nuclear accidents. Considering that flexRISK addressed – not only, but in the first place – the situation of Austria, there is a clear result that the risk source no. 1 for Austria is Temelín and Dukovany, followed by other VVER sites in neighbouring countries, namely Bohunice, Mochovce and Paks. This result is partly linked to geographical and climatological features, but also to the accident assumptions (release fractions and frequencies). It is thus recommended to conduct in-depth studies on the technical aspects of these reactors and to update the results from flexRISK, should such studies lead to modification of the accident assumptions. flexRISK results show clearly that there are good reasons for Austria to continue efforts for the technical assessment of these NPPs and corresponding consequences on a political level.

Other plants which deserve special attention are Gundremmingen (Germany) and Fessenheim (France), and then Krsko (Slovenia) as well as the Swiss NPPs. While the shut-down of Isar-1 (Germany) in 2011 has eliminated a major risk source for Austria, Isar-2 (and to a lesser amount Neckarwestheim-2) continue to provide a possibility for high contamination in Austria. However, these plants have been assigned a rather low accident frequency. It might be worthwhile to assess the reliability of this finding.

The fact that there are NPPs not mentioned above should not be interpreted as meaning that they don't create a contribution to the risk of Austria. The above statements only refer to the most important steps to be taken.

6.2.3 Research and development needs

Apart from applications and extensions which can be based on the existing data set as created in flexRISK, listed in Section 6.3, work in flexRISK identified issues which deserve more research and development.

Wet deposition is a very important process with respect to consequences of nuclear accidents. Experience from the flexRISK shows that the implementation of this process in FLEXPART and in general its parameterisation needs to be evaluated more and improved, on the base of first developments made during flexRISK. Similarly, both dry and wet deposition properties of iodine should be reviewed, whereby the partitioning of this species to gaseous and aerosol-bound forms should receive special attention. Available data from Fukushima and other accidents need to be compared to usual source term / modelling assumptions. Furthermore, international efforts for a long-range tracer experiment with an aerosol tracer have to be considered (Stohl et al., 2012; Galmarini et al., 2011). When such improvements are available in FLEXPART, the dispersion runs and evaluations of flexRISK could be repeated and differences assessed.

A desirable refinement for dispersion models to be applied to nuclear accidents, although it would probably not be used for a climatological calculation as in flexRISK for computation reasons, is the *consideration of gas-to-aerosol transformation during the transport process*, for the case of iodine as well as for decay chains involving noble gas radionuclides.

With respect to the accident scenarios, it would be desirable *to investigate more in depth the spectrum of accidents with their release frequencies and release fractions* for the plants with the highest risks in the countries near Austria, i.e. VVER reactors. A closer examination might, however, also be useful for plants near Austria which were assigned low large-release frequencies, in order check whether these results are sufficiently reliable, e.g. with respect to external event consideration. The outcome of such studies could be used for risk assessment in two different ways. The simpler one would just repeat evaluations with possibly adjusted numbers. The more complex one would consider a larger spectrum of accident sequences, instead of just a single one, for those plants which are considered to have the most impact on Austria (or any other country of interest, respectively).

6.3 Possible applications and extensions for the future

6.3.1 Applications

Assessment of new nuclear energy projects: The toolkit created in flexRISK allows to determine the impact of any new plant or project quickly, provided a suitable source term and frequency are given. On a typical machine available at BOKU-Met, using 4 cores (in order not to block the whole machine), it would take about 10 days to perform the set of 2800 dispersion calculations. Including dose calculations, visualisation and evaluation of output, results would be deliverable within weeks. Using more computing power, or with a quick-look of fewer weather situations, this could of course be shortened.

In the following, a non-exhaustive list of further applications and developments is given that might be of interest.

Risk measure for a country: So far, the frequency exceeded over a certain fraction of a country has been evaluated for the situation that dose or contamination is over a given threshold in a spot. Other measures are also possible, for example the frequency with which a given fraction of the country is contaminated above a threshold (i.e., how often would, e.g., 50% of the country receive a contamination or dose over the threshold. This is interesting as for smaller countries, a high contamination over major parts of the country is possible which would have quite severe effects on economy and everyday life. One could compare different country-wide risk measures in order to arrive at a useful single parameter which then would be the base for import–export considerations.

Further scenarios: Obviously, further reactor park scenarios and phasing-out options could be defined and investigated. A more systematic comparison of the effects of these scenarios with respect to different risk parameters would also be useful.

Statistical evaluation: From a statistical point of view, the available data set is interesting as it has non-trivial properties. In general, the distribution of contamination and doses is L-shaped. In contrast to standard statistical models for extreme-value problems, there should be a physical upper bound, as for example for contamination, the total material emitted could be deposited on a finite area only. It would be interesting to study the properties of these distributions and their relationship with both mean and exceedance frequencies / percentiles, keeping in mind that they will vary with distance and region. A desirable application that could be developed on this base would be a method for spatially smoothing fields that represent high values, including statistical variability.

Risk minimisation scenarios: The possibility exists to rank NPP units for the minimisation of a given risk parameter and a given region, so that taking number 1 out of service will give the largest risk reduction, number 2 the second-largest, and so on. In this way it can be determined which units should go out of operation to substantially reduce the risk in the most efficient way. However, it has to be kept in mind that release frequencies are an important factor of uncertainty for the ranking of risk contributions, and such an analysis would probably only be a preliminary step in a process where a detailed technical assessment of the plants on the shutdown list would need to follow. After this, another iteration of the risk minimisation can be done.

6.3.2 Additional calculation endpoints

There are more possible endpoints of interest which could be computed and analysed in the future, based on the already existing contamination and dose data.

Contamination of milk

Milk contaminated with radioactive iodine can contribute considerably to the thyroid dose if it is not identified and eliminated from food chain. Contamination with radioactive caesium has also been a major, long-lasting concern after Chernobyl. As transfer factors are relatively high, milk contamination is typically an important consequence, both for emergency management (need to measure quickly a large quantity of milk samples) and economically (usually, milk that has high content of iodine is also contaminated by caesium, so that making products like cheese or milk powder which could be stored until iodine has decayed is not a viable solution). From the results of deposition of I-131 as reference nuclide, the iodine contamination of locally produced milk could be calculated with the use of transfer factors. Then, resulting values could be compared with maximum permitted levels for radioactive contamination of food, e.g. those recommended by the European Community and the levels that were applied in the aftermath of Chernobyl in Austria. By estimating the total consumption of milk (considering various intervention levels or not) in a given time period, the resulting ingestion doses can be assessed, or, assuming that contaminated milk will be screen out, the period for which milk would not be fit for consumption could be calculated. Such an evaluation would need to take into account the temporal evolution of contamination and thus pose certain computational demands.

Collective doses and health consequences

As gridded population data are available, it will not be difficult to calculate collective doses for the pathways considered, and resulting health effects. However, applicable dose periods with their associated location factors and dose coefficients need further attention. It should also be noted that there are major differences in opinion concerning values for risk factors relating doses to morbidity and mortality. This endpoint is also interesting because it is linearly related to the source terms (linear dose-effect relationship and linear release-dose relationship) – at least as long as emergency measures with intervention levels (which constitute non-linear influences) would not be considered. Thus, it would be easy to produce results for source terms scaled by a given factor from those used here.

6.3.3 Economic consequences

With the gridded results, and considering that high-resolution land-use data are easily available, an assessment of economic consequences appears possible. However, this requires another interdisciplinary project. A thorough discussion on the kind of consequences to be included in such an assessment would be required; not all of them are readily quantifiable.

Glossary and list of acronyms

AECL Atomic Energy of Canada, Limited.

AGR Advanced Gas-Cooled Reactor, carbon dioxide cooled, graphite moderated.

Base-load The share of the overall load in an electrical grid which remains constant for a given time frame (day, week, month or year).

Becquerel The becquerel (abbreviation Bq) is the SI derived unit of radioactivity, defined as the activity of a quantity of radioactive material in which one nucleus decays per second. It is therefore equivalent to s^{-1}. The older unit of radioactivity was the Curie (Ci), equivalent to 3.7E10 Bq or 37 GBq. In a fixed mass of radioactive material, the number of becquerels changes with time. Sometimes, amounts of radioactive material are given after adjustment for some period of time. $\boxed{W}$

Often used quantities are kBq for ground contamination and PBq for nuclear reactor inventories:
kBq = Kilobecquerel = E3 Bq = 1,000 Bq
PBq = Petabecquerel = E15 Bq = 1,000,000,000,000,000 Bq

Blackout Station blackout describes the loss of alternating current (AC) in a nuclear power plant. If the direct current (DC) supply for the emergency systems is also lost, it is referred to as "total station blackout".

Burnup In the field of nuclear energy conversion, the burnup is the amount of thermal energy that has been produced per mass unit of fuel. Usually it is expressed in Gigawatt-days per ton of heavy metal. In contrast to fossil fuel, the fuel in nuclear reactors cannot be converted "in one go" since the fuel undergoes changes during its use in the reactor which require the fuel elements to be exchanged.

BWR Boiling Water Reactor.

Bypass, Containment Bypass A containment bypass involves a direct release of radioactive material to the environment that bypasses the containment atmosphere. Examples include PWR steam generator tube ruptures (SGTR), which allow radionuclides to be released through the secondary system, or interfacing systems loss-of-coolant accidents (ISLOCA), which allow radionuclides to be released through a breach in a system outside the containment that interfaces with the reactor coolant system (RCS). $\boxed{N}$

CANDU Canadian Deuterium-Uranium Reactor (heavy water cooled and moderated, natural uranium fuelled) (Atomic Energy of Canada, Limited).

CCI Core-concrete interaction. In an accident with core melt and failure of the RPV, the molten core may relocate to the basemat of the containment. The resulting molten core – concrete interaction (CCI or MCCI) is important for the further accident progression and release pattern. For more details, see `http://en.wikipedia.org/wiki/Corium_(nuclear_reactor)`.

CDF Core Damage Frequency.

Containment The large concrete and steel shell around a reactor whose purpose is to contain any radioactivity that might escape from the reactor itself. **Primary containment:** The principal structure of a reactor unit that acts as a pressure retaining barrier, after the fuel cladding and reactor coolant pressure boundary, for controlling the release of radioactive material into the environment. It includes containment structure, its access openings, penetrations and other associated components used to effect isolation of the containment atmosphere. **Secondary Containment:** The structure surrounding the primary containment that acts as a further barrier.

Decay constant The inverse of the time after which the activity of a radionuclide has decayed to $1/e$ of its initial value. It is related to the half-life by the relation $\lambda = \frac{\ln 2}{T_{1/2}}$.

ECMWF European Centre for Medium-Range Weather Forecasts (`http://www.ecmwf.int/`).

EPR European Pressurized Reactor (Areva NP), pressurized light water cooled and moderated.

ERA-40 ECMWF re-analysis of the global atmosphere and surface conditions for the period September 1957 – August 2002 (originally only 40 years).

ERA-Interim ERA-Interim is the latest global atmospheric reanalysis produced by the European Centre for Medium-Range Weather Forecasts (ECMWF) which will cover the period from 1989 to 2013. It has higher horizontal and vertical resolution, better data assimilation and a more recent model system than the ERA-40.

Espoo-Convention The Espoo-Convention regulates licensing procedures for technical plants which can lead to cross-boarder environmental impacts.

EURATOM European Atomic Energy Community.

Fast Breeder Reactor The fast breeder or fast breeder reactor (FBR) is a reactor where fission is triggered by fast neutrons (as opposed to thermal neutrons in conventional reactors), designed to breed new fuel by producing more fissile material through neutron capture than it consumes. The FBR is one possible type of breeder reactor.

FLEXPART Lagrangian particle model used in flexRISK (web site: `http://transport.nilu.no/flexpart/`, will change to `http://flexpart.eu/`).

GCR Gas-cooled reactor.

GW Gigawatt: 1 GW = 1,000 Megawatt.

GWe Gigawatt of electrical power, is a measure used to describe the power output of electric power plants. For thermodynamic reasons, the electrical power output of a nuclear power plant is on the order of one third of its thermal power.

GWth Gigawatt of thermal power, measure of the primary power production rate in electric power plants.

Half-life Time in which the activity of a radionuclide decays to half of its initial value. See also *Decay constant*.

IAEA International Atomic Energy Agency.

IEA International Energy Agency.

ISLOCA An Interfacing Systems Loss-Of-Coolant Accident (ISLOCA) is a breach in a system that interfaces with the reactor coolant system (RCS) and could cause a loss-of-coolant accident, if the breach is not isolated from the RCS. Such a breach could be caused if valves fail to isolate the RCS from an interfacing system not designed for the high RCS pressures. When portions of an interfacing system are located outside the containment, particular concern arises. $\boxed{N}$

LEU Low-enriched Uranium.

Leukaemia Leukemia (or leukaemia) is a cancer of the blood or bone marrow characterized by an abnormal proliferation of blood cells, usually white blood cells (leukocytes). It is part of the broad group of diseases called hematological neoplasms. $\boxed{W}$

Light Water Reactor A light water reactor or LWR is a thermal nuclear reactor that uses ordinary water, also called light water, as its neutron moderator. This differentiates it from a heavy water reactor, which uses heavy water as a neutron moderator. In practice all LWRs are also water cooled.

LOCA Loss-of-Coolant-Accident: these are accidents in which cooling water is lost from the primary cooling system as a result of a pipe rupture or blockage. A LOCA could lead to overheating of the core and a meltdown.

LPDM Lagrangian particle dispersion model. A dispersion model where transport and diffusion of trace substances in the atmosphere are simulated by tracking computational particles.

LRF Large Release Frequency. The frequency of large releases from nuclear installations.

MAGNOX A design of gas-cooled reactors using a magnesium-based alloy for the fuel tubes.

MOX Mixed oxide or MOX fuel is a blend of plutonium and natural uranium, reprocessed uranium, or depleted uranium which behaves similarly (though not identically) to the low enriched uranium feed for which most nuclear reactors were designed. MOX fuel is an alternative to low enriched uranium (LEU) fuel used in the light water reactors that presently dominate nuclear power generation. It is also a way of disposing of surplus weapons-grade plutonium, which otherwise would have to be handled as a nuclear waste product, difficult to store and posing nuclear proliferation risks. $\boxed{W}$

MW Megawatt: 1 MW = 1,000,000 Watt.

MWe Megawatt electrical power (see **GWe**).

MWth Megawatt thermal power.

NEA Nuclear Energy Agency (see **GWth**).

NFC Nuclear fuel cycle. NFC facilities relevant in flexRISK are mainly fuel fabrication plants and reprocessing plants.

NPP Nuclear Power Plant.

Nuclear Reprocessing Nuclear reprocessing separates any usable elements (e.g., uranium and plutonium) from fission products and other materials in spent nuclear reactor fuels. Usually, the goal is to recycle the reprocessed uranium or place these elements in new mixed oxide fuel (MOX), but some reprocessing is done to obtain plutonium for weapons. It is the process that partially closes the loop in the nuclear fuel cycle.

PHWR Pressurized Heavy Water Reactor.

PDS Plant Damage State: State of the NPP at the moment of core damage, affecting the further accident progression and the macro-consequences.

RCS Reactor Coolant System: The system used to remove energy from the reactor core and transfer that energy either directly or indirectly to the steam turbine.

PSA Probabilistic Safety Assessment.

PUREX Process PUREX is a nuclear reprocessing method which is the de facto standard aqueous method based on liquid-liquid extraction for the recovery of uranium and plutonium from used nuclear fuel. It extracts in uranium, plutonium, and the fission products into separate streams. This process can be used to recover weapon-grade materials as well as reprocessed uranium from spent nuclear reactor fuel, and as such, its component chemicals are monitored. PUREX is an acronym standing for Plutonium and Uranium Recovery by Extraction. $\boxed{N}$

PWR Pressurized Water Reactor.

Radiotoxicity Measure of how nocuous a radio nuclide is to health. The type and energy of rays, absorption in the organism, residence time in the body, etc. influence the degree of radiotoxicity of a radionuclide.

RCS Reactor coolant system.

RISKMAP Predecessor project of flexRISK in the 1990ies (`http://www.umweltbundesamt.at/fileadmin/site/umweltthemen/kernenergie/Riskmap/Deutsch/main.htm`).

RBMK High Power Channel-type Reactor (Russian acronym for Reactor Bolshoi Moschnosti Kanalynyi).

RPV Reactor Pressure Vessel, a stainless steel vessel that encloses the fuel assemblies and is filled by pressurised coolant.

RODOS In case of a nuclear accident in Europe, the Real-time On-line Decision Support system for off-site emergency management in Europe (RODOS) provides consistent and comprehensive information on the present and future radiological situation, the extent and the benefits and drawbacks of emergency actions and countermeasures, and methodological support for taking decisions on emergency response strategies. Main users of the system are those responsible at local, regional, national and supra-national levels for off-site emergency management. The application of the system for training and exercises was a further important consideration in its development.

SGTR Steam Generator Tube Rupture: Damage at the steam generator resulting in a primary-to-secondary-side leakage.

Spent fuel storage Interim or planned final storage facility for spent fuel from NPPs.

Source Receptor Sensitivity, SRS The source-receptor sensitivity describes the sensitivity of a receptor element for an atmospheric trace substance to a source element through atmospheric transport.

Steam Generator A boiler in which hot coolant from a reactor raises steam to turn a turbine generator.

VVER Pressurized light water cooled and moderated reactor (Russian acronym for Voda-Vodyanoi Energetichesky Reaktor).

WHO World Health Organization.

WNA World Nuclear Association.

$\boxed{W}$ indicates entries which are partly or fully quoted from Wikipedia (http://en.wikipedia.org/). These entries are licensed under the Creative Commons Attribution/Share-Alike License[1].

$\boxed{N}$ indicates entries which are partly or fully quoted from http://www.nuce.boun.edu.tr/.

$\boxed{E}$ indicates entries which are partly or fully quoted from http://www.euronuclear.org/.

[1] See http://creativecommons.org/licenses/by-sa/3.0/.

Acknowledgements

This project was financed by the Climate- and Energy Fund of the Austrian Federal Government (Klima- und Energiefonds der Bundesregierung) in the framework of the programme “NEW ENERGIES 2020”, project number 822051.

The members of the Advisory Group, Stefano Galmarini, Peter Hofer, Karl Kienzl, Alfred Körblein, and Rianne Teule, provided valuable suggestions in several workshops and through personal contacts. We thank them very much. They are, however, not responsible – neither as a group nor as individuals – for the decisions of the project team with respect to source terms, model set-up, parameterisations and coefficients, etc. The responsability for the project results is born exclusively by the project team.

Dispersion and dose calculations were carried out in the Vienna Scientific Cluster (VSC) computing centre. This possibility and the highly effective support by its staff (Jan Zabloudil, Markus Stöhr, Bernhard Hermann) are gratefully acknowledged.

Access to ECMWF data was granted through the Special project “Modelling of tracer transport”.

We thank ZAMG (Matthias Langer) for making the TAMOS code available, Philipp Sutter (ÖÖI) for the web design and programming, Andrea Wallner (ÖÖI) for literature research, Theresa Gorgas and David Leidinger (BOKU-Met) for programming support, and Anne Philipp for proofreading.

References

AG Proben (2010), Probenahmeplan. Organisation und Durchführung von Probenahmen bei großräumiger radioaktiver Kontamination. Erarbeitet von der AG Proben des Staatlichen Krisen- und Katastrophenschutzmanagements (SKKM), Stand 5. Oktober 2010. URL: `http://www.lebensministerium.at/umwelt/strahlenatom/strahlenschutz/notfallplanung/notfallvorsorge.html`.

Andreev, I., H. Gohla, M. Hittenberger, P. Hofer, W. Kromp, H. Kromp-Kolb, W. Rehm, P. Seibert, and G. Wotawa (1999), Riskmap – Erstellung einer Karte des nuklearen Risikos für Europa. Riskmap – Creation of a Map of the Nuclear Risk for Europe. URL: `http://www.umweltbundesamt.at/umweltschutz/kernenergie/akw/riskmap/`.

Andreev, I., M. Hittenberger, P. Hofer, W. Kromp-Kolb, P. Seibert, and G. Wotawa (1998), Risks due to beyond design base accidents of nuclear power plants in Europe – the methodology of Riskmap. *J. Hazardous Materials* **61**, 257–262.

AREVA (2009), US EPR final safety analysis and environmental report. URL: `http://adamswebsearch2.nrc.gov/idmws/ViewDocByAccession.asp?AccessionNumber=ML092450768`.

Arnold, D., P. Seibert, H. Nagai, G. Wotawa, P. Skomorowski, K. Baumann-Stanzer, E. Polreich, M. Langer, A. Jones, M. Hort, S. Andronopoulos, J. G. Bartzis, E. Davakis, P. Kaufmann, and A. Vargas (2013), Lagrangian models for nuclear studies: Examples & applications. In: J. C. Lin, D. Brunner, C. Gerbig, A. Stohl, A. Luhar, and P. Webley (eds.), *Lagrangian Modeling of the Atmosphere*, vol. 26 of *AGU Geophysical Monograph*, American Geophysical Union. doi:10.1029/2012GM001294.

Baklanov, A., A. Mahura, D. Jaffe, L. Thaning, R. Bergman, and R. Andres (1998), Atmospheric transport patterns and possible consequences after a nuclear accident in North-West Russia. In: *The 11th World Clear Air and Environment Congress, Durban, South Africa, 14-18 September*, vol. 2, pp. 14–18.

Baklanov, A., A. Mahura, D. Jaffe, L. Thaning, R. Bergman, and R. Andres (2002), Atmospheric transport patterns and possible consequences for the European North after a nuclear accident. *J. Environ. Radioactivity* **60**(1-2), 23–48.

BKA (1988), Die Auswirkungen des Reaktorunfalls in Tschernobyl auf Österreich. Beiträge 2/88, Bundeskanzleramt, Sektion VII, Wien.

BMGKS (1992), Rahmenempfehlungen für die Festlegung und Durchführung von Maßnahmen zum Schutz der Bevölkerung vor ionisierender Strahlung in Fällen großräumiger radioaktiver Verunreinigung. 3. erweiterte Auflage, Forschungsberichte des Bundesministeriums für Gesundheit, Sport und Konsumentenschutz, Sektion III, 3/92. URL: `http://www.lebensministerium.at/filemanager/download/7869/`.

Brisbois, J., J. M. Lanore, A. Villemeur, J. Berger, and J. M. de Guio (1991), Probabilistic safety assessment of French 900 and 1,300 MWe nuclear plants. EA Report DES/025 presented at the conference on “Nuclear Safety: The Way Ahead”, Brussels, Belgium. URL: `http://www.iaea.org/inis/collection/NCLCollectionStore/_Public/23/017/23017323.pdf`.

Busby, C., R. Bertell, I. Schmitz-Feuerhake, M. Scott Cato, and A. Yablokov (eds.) (2010), *2010 Recommendations of the ECRR. The Health Effects of Ionising Radiation Exposure at Low Doses and Low Dose Rates for Radiation Protection Purposes: Regulators’ Edition*. European Committee on Radiation Risk and Green Audit, Aberystwyth. URL: `http://www.euradcom.org/2011/ecrr2010.pdf`.

CEC (1995), ExternE. Externalities of energy. vol. 1 (summary report). Publication No. EUR16520EN, CEC DG XII, Luxembourg.

Christy, M. and K. F. Eckerman (1987), Specific absorbed fractions of energy at various ages from internal photon sources. 1. Methods. ORNL/TM-8381/V1; cited in: Health Canada (1999).

CIESIN (1995), Gridded Population of the World, Version 3 (GPWv3). Palisades, NY: Socioeconomic Data and Applications Center (SEDAC), Columbia University. Center for International Earth Science Information Network (CIESIN), Columbia University; and Centro Internacional de Agricultura Tropical (CIAT). URL: `http://sedac.ciesin.columbia.edu/gpw`.

Dee, D. P., S. M. Uppala, A. J. Simmons, P. Berrisford, P. Poli, S. Kobayashi, U. Andrae, M. A. Balmaseda, G. Balsamo, P. Bauer, P. Bechtold, A. C. M. Beljaars, L. van de Berg, J. Bidlot, N. Bormann, C. Delsol, R. Dragani, M. Fuentes, A. J. Geer, L. Haimberger, S. B. Healy, H. Hersbach, E. V. Hólm, L. Isaksen, P. Kållberg, M. Köhler, M. Matricardi, A. P. McNally, B. M. Monge-Sanz, J.-J. Morcrette, B.-K. Park, C. Peubey, P. de Rosnay, C. Tavolato, J.-N. Thépaut, and F. Vitart (2011), The ERA-Interim reanalysis: configuration and performance of the data assimilation system. *Q. J. Royal Meteorol. Soc.* **137**, 553–597. URL: http://dx.doi.org/10.1002/qj.828, doi:10.1002/qj.828.

Eckerman, K. F. and R. W. Leggett (1996), DCFPAK: Dose coefficent data file package for Sanida National laboratory. ORNL/TM-13347, Oak Ridge National Laboratory. URL: http://ordose.ornl.gov/downloads.html.

ENSI (2009), Sicherheitstechnische Stellungnahme zur periodischen Sicherheitsüberprüfung des Kernkraftwerks Leibstadt. ENSI 12/1300. URL: http://www.ensi.ch/fileadmin/deutsch/files/psue_KKL-2009.pdf.

Entergy (2006), License renewal application, Pilgrim nuclear power station. URL: http://www.nrc.gov/reactors/operating/licensing/renewal/applications/pilgrim/environ-report_attach-e.pdf.

Entergy (2007), Indian Point 3 – Applicant's environmental report, operating license renewal stage, Attachment E, "Severe accident mitigation alternatives analysis". URL: http://www.nrc.gov/reactors/operating/licensing/renewal/applications/indian-point/ipec-er-attachments_c-e.pdf.

EURATOM (1996), Council Directive 96/29/Euratom of 13 May 1996 laying down basic safety standards for the protection of the health of workers and the general public against the dangers arising from ionizing radiation. OJ L 159, 29.6.1996, p. 1–114. URL: http://eur-lex.europa.eu/smartapi/cgi/sga_doc?smartapi!celexplus!prod!DocNumber&type_doc=Directive&an_doc=1996&nu_doc=29&lg=en.

European Commmission (1995), PC COSYMA Version 2.0 User Guide. Publication No. EUR 16240 EN.

Forster, C., A. Stohl, and P. Seibert (2007), Parameterization of convective transport in a Lagrangian particle dispersion model and its evaluation. *J. Climate Appl. Meteorol.* **46**, 403–422. URL: http://journals.ametsoc.org/doi/abs/10.1175/JAM2470.1, doi:10.1175/JAM2470.1.

Galmarini, S., A. Stohl, and G. Wotawa (2011), Fund experiments on atmospheric hazards. *Nature* **473**(7347), 285. URL: http://dx.doi.org/10.1038/473285d.

Gering, F., B. Gerich, E. Wirth, and G. Kirchner (2012), Analyse der Vorkehrungen für den anlageninternen Notfallschutz für deutsche Kernkraftwerke basierend auf den Erfahrungen aus dem Unfall in Fukushima. Fachbereich Strahlenschutz und Umwelt, Bundesamt für Strahlenschutz, Salzgitter.

Health Canada (1999), Recommendations on dose coefficients for assessing doses from accidental radionuclide releases to the environment. Prepared by a Joint Working Group of Radiation Protection Bureau, Health Canada, Atomic Energy Control Board, Atomic Energy of Canada Limited, March 1999. URL: http://www.hc-sc.gc.ca/ewh-semt/pubs/radiation/dose/index-eng.php.

Himanen, R. and H. Sjövall (2004), An integrated approach to living level 2 PSA. CSNI International Workshop on Level 2 PSA and Severe Accident Management, Köln, Germany. URL: http://www.oecd-nea.org/nsd/workshops/psa/Level2_Workshop_%20papers_presentations/Session%201%20Presentation%202.ppt.

Hofer, P., P. Seibert, I. Andreev, H. Gohla, and H. Kromp-Kolb (2000), Risks due to severe accidents of nuclear power plants in Europe – the methodology of Riskmap. In: *Transitions Towards a Sustainable Europe. Ecology–Economy–Policy*, 3rd Biennial Conference of the European Society for Ecological Economics, Vienna. URL: http://www.wu.ac.at/project/esee2000/PapersPDF/C316.pdf.

HSK (1999), Periodische Sicherheitsüberprüfung KKW Gösgen. URL: http://www.ensi.ch/fileadmin/deutsch/files/psu_kkg.pdf.

HSK (2007), Sicherheitstechnische Stellungnahme zur periodischen Sicherheitsüberprüfung des Kernkraftwerks Mühleberg: Zusammenfassung, Ergebnisse und Bewertung. HSK 11/1100. URL: http://www.umweltbundesamt.at/fileadmin/site/umweltthemen/kernenergie/Muehleberg/psu_muehleberg_2007.pdf.

IAEA (2008), Chernobyl: Looking back to go forward – Proceedings of an international conference organized by the IAEA on behalf of the Chernobyl Forum, held in Vienna on 6-7. September 2005. IAEA Proceedings Series, Vienna. URL: http://www-pub.iaea.org/MTCD/publications/PDF/Pub1312_web.pdf.

IAEA (2009), Energy, electricity and nuclear power estimates for the period up to 2030. IAEA Reference data series No.1, Vienna.

IAEA (2010a), Development and application of level 1 probabilistic safety assessment for nuclear power plants, Specific Safety Guide SSG-3. URL: http://www-pub.iaea.org/MTCD/publications/PDF/Pub1443_web.pdf.

IAEA (2010b), Development and application of level 2 probabilistic safety assessment for nuclear power plants, Specific Safety Guide SSG-4. URL: http://www-pub.iaea.org/MTCD/publications/PDF/Pub1430_web.pdf.

IAEA (2011a), Criteria for use in preparedness and response for a nuclear or radiological emergency. IAEA Safety Standards, General Safety Guide No. GSG-2, jointly sponsored by the FAO, IAEA, ILO, PAHO, WHO, Vienna.

IAEA (2011b), Database on Nuclear Power Reactors. Last accessed 14 June 2011. URL: http://pris.iaea.org/pris/.

ICRP (1977), Recommendations of the ICRP. Annuals of the ICRP l(3). ICRP Publication 26. Pergamon Press, Oxford, UK.

ICRP (1991), Recommendations of the International Commission on Radiological Protection. Annals of the ICRP 21(1-3). ICRP Publication 60. Pergamon Press, Oxford.

ICRP (1995), Age-dependent doses to the members of the public from intake of radionuclides: Part 4, inhalation dose coefficients. Annals of the ICRP 25(3-4). ICRP Publication 71.

ICRP (1996), The ICRP database of dose coefficients: Workers and members of the public. An Extension of ICRP Publications 68 and 72, Prepared by the “Task Group on Dose Calculations” of Committee 2 of the ICRP, CD-Rom, Pergamon.

ICRP (2007), The 2007 recommendations of the International Commission on Radiological Protection. Annals of the ICRP. Publication 103. Editor J. Valentin. Elsevier.

ICRP (2011), Fukushima nuclear power plant accident. ICRP ref: 4847-5603-4313, press release from March 21, 2011. URL: http://www.icrp.org/docs/fukushima%20nuclear%20power%20plant%20accident.pdf.

IEA/NEA, O. (2010), Technology roadmap nuclear energy. URL: http://www.iea.org/publications/freepublications/publication/nuclear_roadmap.pdf.

IRSN and CEA (2007), Research and development with regard to severe accidents in pressurised water reactors: Summary and outlook. IRSN-2007/83, CEA-2007/351. URL: http://www.irsn.fr/FR/Larecherche/publications-documentation/Publications_documentation/BDD_publi/DSR/SAGR/Documents/rapport_RetD_AG_VA.pdf.

Ivkov, I. (2010), Key features of the MIR.1200 (AES-2006) design and current stage of Leningrad NPP-2 construction. International Topical Meeting on VVER-2010 – Experience and Perspectives, Prague, Czech Republic.

Jackson, P. C. (1996), Age-dependent doses to members of the public from intake of radionuclides: Part 5, compilation of ingestion and inhalation dose coefficients (ICRP Publication 72). *Physics in Medicine and Biology* **41**(12), 2807.

Jacob, P. (1991), Externe Strahlenexposition nach der Ablagerung künstlicher Radionuklide. *Atomwirtschaft* **36**, 328–331.

KEMA (1987), Ernstige reactorongevallen opnieuw bezien, de bronterm. Energieonderzoek Centrum Nederland (ECN), ECN-PB-87-13. URL: http://www.iaea.org/inis/collection/NCLCollectionStore/_Public/20/029/20029496.pdf.

Khatib-Rahbar, M. (2001), Level-2 probabilistic safety assessment: Fundamentals & methods. Energy Research, Inc., paper and presentation at PSA 2001, Rockville MD USA.

Lajtha, G., A. Bareith, E. Holló, Z. Karsa, P. Siklóssy, and Z. Téchy (2005), Uncertainty of the Level 2 PSA for NPP Paks. OECD NEA Workshop on Evaluation of Uncertainties in Relation to Severe Accidents and Level-2 Probabilistic Safety Analysis, NEA-6053, November 2005, Aix-en-Provence, France. URL: http://www.nea.fr/nsd/reports/2007/nea6053/Session-IV-Applications-to-Uncertainty-Assessment-in-Level-2-PSA/Presentation-18_Lajtha-et-al.pdf.

Large, J. (2007), Assessments of the radiological consequences of releases from existing and proposed EPR/PWR nuclear power plants in France. Report No. R3150-3, prepared for Greenpeace France, Large & Associates Consulting Engineers, U.K.

Lebensministerium (2007), Verordnung des Bundesministers für Land- und Forstwirtschaft, Umwelt und Wasserwirtschaft über Interventionen bei radiologischen Notstandssituationen und bei dauerhaften Strahlenexpositionen (Interventionsverordnung – IntV). Bundesgesetz BGBl. II Nr. 145/2007, ausgegeben am 26. Juni 2007. URL: http://www.lebensministerium.at/umwelt/strahlen-atom/strahlenschutz/rechtsvorschriften/intV.html.

Lelieveld, J., D. Kunkel, and M. G. Lawrence (2012), Global risk of radioactive fallout after major nuclear reactor accidents. *Atmos. Chem. Phys.* **12**(9), 4245–4258. URL: http://www.atmos-chem-phys.net/12/4245/2012/.

Lembrechts, J., H. Slaper, D. W. Pearce, and A. Howarth (2000), Technical report on nuclear accidents and other major accidents in Europe: An integrated economic and environmental assessment. RIVM Report 481505013.

Löffler, H. and M. Sonnenkalb (2006), Methods and results of a PSA Level 2 for a German BWR of the 900 MWe class. EUROSAFE 2006, 13-14 November 2006 (Paris). URL: http://www.eurosafe-forum.org/products/data/5/pe_429_24_1_seminar1_02_2006_.pdf.

Meyer, G. and E. Stokke (1997), Description of Sizewell B nuclear power plant. OECD Halden Reactor Project, Halden Norway, Report NKS/RAK-2(97)TR-C4, prepared for the Nordic Nuclear Safety Research Project.

Mück, K., M. Suda, M. Gerzabek, and B. Kunsch (1991), Ingestion dose response to the deposition date in the first year after radionuclide deposition. *Radiation Protection Dosimetry* **42**, 103–114.

Müller, H., F. Gering, and G. Pröhl (2003), Model description of the terrestrial food chain and dose module FDMT in RODOS PV6.0. RODOS(RA3)-TN(03)06, GSF.

NEK (2007), Belene nuclear power plant, project progress. Presentation to European Commission DG Energy and Transport. URL: http://belene-npp.com/uploads/file/12/belene_ec-final.pdf.

OECD/NEA (2002), Chernobyl – assessment of radiological impacts. URL: http://www.oecd-nea.org/rp/reports/2003/nea3508-chernobyl.pdf.

OECD/NEA (2007a), Recent developments in Level 2 PSA and severe accident management. NEA/CSNI/R(2007)16, Organisation for Economic Co-operation and Development (OECD), Paris, November 2007. URL: http://www.olis.oecd.org/olis/2007doc.nsf/ENGDATCORPLOOK/NT00004822/\protect\T1\textdollarFILE/JT03236099.PDF.

OECD/NEA (2007b), Use and development of probabilistic safety assessment. NEA/CSNI/R(2007)12. URL: http://www.nea.fr/html/nsd/docs/2007/csni-r2007-12.pdf.

Päsler-Sauer, J. (2007), Model description of the early countermeasures module EmerSim - in RODOS PV 6.0 Final. RODOS(RA3)-TN(04)-03, Forschungszentrum Karlsruhe.

Rigina, O. and A. Baklanov (2001), Regional radiation risk and vulnerability assessment by integration of mathematical modelling and GIS-analysis. *Journal of Environment International* **27**(6), 1–20.

Russian Federation (2007), Fulfillment of commitments resulting from the Convention on Nuclear Safety: Fourth review meeting.

Seibert, P. (2012), Interactive comment on "Comment on 'Global risk of radioactive fallout after nuclear reactor accidents by J. Lelieveld et al. (2012)' by J. Lelieveld et al.". *Atmos. Chem. Phys. Disc.* **12**, C6678–C6681. URL: `http://www.atmos-chem-phys-discuss.net/12/C6678/2012/`.

Seibert, P., D. Arnold, H. Kromp-Kolb, and N. Arnold (2012), Interactive comment on "Global risk of radioactive fallout after nuclear reactor accidents" by J. Lelieveld et al. *Atmos. Chem. Phys. Disc.* **11**, C14351–C14359. URL: `http://www.atmos-chem-phys-discuss.net/11/C14351/2012/`.

Shevchik, V. E. and V. L. Gurachevsky (2006), National Report Belarus: 20 years after the Chernobyl catastrophe: The consequences in the Republic of Belarus and their overcoming. Committee on the Problems of the Consequences of the Catastrophe at the Chernobyl NPP under the Belarussian Council of Ministers, Minsk. URL: `http://chernobyl.undp.org/english/nat_rep.shtml`.

Siltanen, S., T. Routamo, H. Tuomisto, and P. Lundström (2005), Severe accident management at the Loviisa NPP – application of integrated ROOAM and PSA Level 2. OECD NEA Workshop on Evaluation of Uncertainties in Relation to Severe Accidents and Level-2 Probabilistic Safety Analysis, NEA-6053, Aix-en-Provence, France. URL: `http://www.nea.fr/nsd/reports/2007/nea6053/Session-IV-Applications-to-Uncertainty-Assessment-in-Level-2-PSA/Paper-19_Siltanen-et-al.pdf`.

Sinyak, Y. (1995), Nuclear energy in Eastern Europe and the Former Soviet Union: How safe and how much? International Institute for Applied Systems Analysis (IIASA), Laxenburg, Austria.

Sinyak, Y. (1996), Nuclear energy in Eastern Europe and the former Soviet Union: How safe and how much? *Fuel and Energy Abstracts* **37**(2), 107–107. URL: `http://www.ingentaconnect.com/content/els/01406701/1996/00000037/00000002/art87631`.

Slaper, H. and R. O. Blaauboer (1995), Probilistic risk assessment for accidental releases from nuclear power plants in Europe: Methods and results. In: *Environmental Impact of Radioactive Releases, Proceedings of an International Symposium, Vienna, 8-12 May 1995*, IAEA.

Slaper, H., R. O. Blaauboer, and G. J. Eggink (1994), Risks of potential accidents of nuclear power plants in Europe. RIVM report 74030001, Bilthoven, the Netherlands. URL: `http://www.rivm.nl/bibliotheek/rapporten/743030002.pdf`.

Smith, F. (1998), Estimating the statistics of risk from a hazardous source at long range. *Atmos. Environ.* **16**(16), 2775–2791.

SSK (2003), Berichte der Strahlenschutzkommission, 2003: Leitfaden für den Fachberater Strahlenschutz der Katastrophenschutzleitung bei kerntechnischen Notfällen. Heft 37, ISBN 3-437-11639-8.

SSK (2008), Radiologische Grundlagen für Entscheidungen über Maßnahmen zum Schutz der Bevölkerung bei unfallbedingten Freisetzungen von Radionukliden. Empfehlung der Strahlenschutzkommission. Redaktionelle Überarbeitung der gleichnamigen Veröffentlichung aus dem Jahr 1999. Stand 21.09.2008.

Stohl, A., C. Forster, A. Frank, P. Seibert, and G. Wotawa (2005), Technical note: The Lagrangian particle dispersion model FLEXPART version 6.2. *Atmos. Chem. Phys.* **5**, 2461–2474. URL: `http://www.atmos-chem-phys.net/5/2461/2005/`.

Stohl, A., M. Hittenberger, and G. Wotawa (1998), Validation of the Lagrangian particle dispersion model Flexpart against large-scale tracer experiment data. *Atmos. Environ.* **32**(24), 4245–4264.

Stohl, A., P. Seibert, G. Wotawa, D. Arnold, J. F. Burkhart, S. Eckhardt, C. Tapia, A. Vargas, and T. J. Yasunari (2012), Xenon-133 and caesium-137 releases into the atmosphere from the Fukushima Dai-ichi nuclear power plant: determination of the source term, atmospheric dispersion, and deposition. *Atmospheric Chemistry and Physics* **12**(5), 2313–2343. URL: http://www.atmos-chem-phys.net/12/2313/2012/, doi:10.5194/acp-12-2313-2012.

Stohl, A., H. Sodemann, E. S., A. Frank, P. Seibert, and G. Wotawa (2010), The Lagrangian particle dispersion model FLEXPART version 8.2. 32 pp. URL: http://flexpart.eu/downloads/26.

STUK (2010), Finnish report on nuclear safety: Finnish 5th National Report as referred to in Article 5 of the Convention on Nuclear Safety. URL: http://www.stuk.fi/julkaisut/stuk-b/stuk-b120.pdf.

Teller, A. (2007), Deployment of nuclear, AREVA strategic marketing. International Energy Agency Workshop on Technology Learning & Deployment, Paris, France, 11-12 June 2007. URL: http://www.iea.org/Textbase/work/2007/learning/Teller.pdf.

UBA (2002), Verfahren Betriebsbewilligung AKW Beznau II. URL: http://www.umweltbundesamt.at/fileadmin/site/umweltthemen/kernenergie/Beznau/Bericht_BEZNAU_gesamt.pdf.

UK-EPR (2011), Fundamental safety overview, Volume 2: Design and safety, Chapter R: Probabilistic safety assessment. URL: http://www.epr-reactor.co.uk/ssmod/liblocal/docs/V3/Volume%202%20-%20Design%20and%20Safety/2.R%20-%20Probabilistic%20Safety%20Assessment/2.R.2%20-%20Level%202%20Probabilistic%20Safety%20Assessment%20%28PSA%29%20-%20v2.pdf.

Usburus, E., A. Kaliatka, J. Augutis, S. Rimkevicius, E. Urbonavicius, and V. Kopustinskas (2007), Safety analysis of beyond design basis accidents in RBMK-1500 reactors. Annals of Nuclear Energy.

USNRC (1995), NUREG-1465, Accident source terms for light-water reactor nuclear power plants. URL: http://www.osti.gov/bridge/servlets/purl/29438-tMxVzu/webviewable/.

USNRC (2004), PWR source term release fractions. CNRO-2004-00050. URL: http://adamswebsearch2.nrc.gov/IDMWS/ViewDocByAccession.asp?AccessionNumber=ML042290395.

USNRC (2005), Kalinin VVER-1000 nuclear power station unit 1 PRA (beta project). NUREG/IA-0212, Vol. 1. URL: http://adamswebsearch2.nrc.gov/idmws/doccontent.dll?library=PU_ADAMS^PBNTAD01&ID=061090845.

WNA (2010), WNA nuclear century outlook data. Last accessed July 2010. URL: http://www.world-nuclear.org/outlook/nuclear_century_outlook.html.

WNA (2011), World Nuclear Association reactor database. Last accessed 14 June 2011. URL: http://world-nuclear.org/NuclearDatabase/.

Appendices

Appendix A: Base data of nuclear facilities

Explanation of the scenarios (x marks scenarios where the NPP unit is considered):

Scenario 1: Reactors in operation 1/2011

Scenario 2: Reactors in operation 1/2012

Scenario 3: Reactors in operation 1/2011 with shutdown of NPPs started before 1980

Site name - unit	Type	Startup	Expected shutdown	Power (MWth)	Scenario 1	2	3
Ahaus	Spent fuel and high level waste storage	1997	na	na			
Akkuyu-1	Gidropress 4-loop VVER 1200/491	2016	2076	3200			
Akkuyu-2	Gidropress 4-loop VVER 1200/491	2017	2077	3200			
Akkuyu-3	Gidropress 4-loop VVER 1200/491	2018	2078	3200			
Akkuyu-4	Gidropress 4-loop VVER 1200/491	2019	2079	3200			
Almaraz-1	Westinghouse 3-loop	1981	2020	2696	x	x	x
Almaraz-2	Westinghouse 3-loop	1983	2020	2696	x	x	x
Almelo	Centrifuge enrichment plant	1973	na	na			
Asco-1	Westinghouse 3-loop	1983	2023	2695	x	x	x
Asco-2	Westinghouse 3-loop	1985	2025	2695	x	x	x
Balakovo-1	Gidropress 4-loop VVER 1000/320	1985	2015	3000	x	x	x
Balakovo-2	Gidropress 4-loop VVER 1000/320	1987	2017	3000	x	x	x
Balakovo-3	Gidropress 4-loop VVER 1000/320	1988	2018	3000	x	x	x
Balakovo-4	Gidropress 4-loop VVER 1000/320	1993	2023	3000	x	x	x
Belene-1	Gidropress 4-loop VVER 1000/446	2017	2077	3100			
Belene-2	Gidropress 4-loop VVER 1000/446	2018	2078	3100			
Belleville-1	Framatome 4-loop P4-Type	1987	2027	3817	x	x	x
Belleville-2	Framatome 4-loop P4-Type	1988	2028	3817	x	x	x
Beznau-1	Westinghouse 2-loop	1969	2019	1130	x	x	
Beznau-2	Westinghouse 2-loop	1971	2021	1130	x	x	
Biblis-1	KWU 4-loop	1974	2011	3517	x		
Biblis-2	KWU 4-loop	1976	2011	3733	x		
Blayais-1	Framatome 3-loop CP1-Type	1981	2041	2785	x	x	x
Blayais-2	Framatome 3-loop CP1-Type	1982	2043	2785	x	x	x
Blayais-3	Framatome 3-loop CP1-Type	1983	2043	2785	x	x	x
Blayais-4	Framatome 3-loop CP1-Type	1983	2043	2785	x	x	x
Bohunice-3	Gidropress 6-loop VVER 440/213	1984	2025	1375	x	x	x
Bohunice-4	Gidropress 6-loop VVER 440/213	1985	2025	1375	x	x	x
Borssele-1	KWU 2-loop	1973	2034	1366	x	x	
Brokdorf-1	KWU 4-loop (Pre Convoi)	1986	2033	3900	x	x	x
Brunsbuettel-1	Siemens BWR/69	1976	2011	2292	x		
Bugey-2	Framatome 3-loop CP0-Type	1978	2039	2785	x	x	
Bugey-3	Framatome 3-loop CP0-Type	1978	2039	2785	x	x	
Bugey-4	Framatome 3-loop CP0-Type	1979	2039	2785	x	x	
Bugey-5	Framatome 3-loop CP0-Type	1979	2040	2785	x	x	
Bushehr-1	Gidropress 4-loop VVER 1000/446	2011	2071	3200	x	x	x
Cadarache	Spent fuel and high level waste storage	1960	na	na			
Capenhurst	Centrifuge enrichment plant	1972	na	na			
Cattenom-1	Framatome 4-loop P4-Type	1987	2046	3817	x	x	x
Cattenom-2	Framatome 4-loop P4-Type	1988	2047	3817	x	x	x
Cattenom-3	Framatome 4-loop P4-Type	1990	2050	3817	x	x	x
Cattenom-4	Framatome 4-loop P4-Type	1991	2051	3817	x	x	x
Cernavoda-1	AECL CANDU-6	1996	2056	2180	x	x	x
Cernavoda-2	AECL CANDU-6	2007	2067	2180	x	x	x
Cernavoda-3	AECL CANDU-6	2016	2076	2180			
Cernavoda-4	AECL CANDU-6	2017	2077	2180			
Chinon-B1	Framatome 3-loop CP2-Type	1982	2044	2785	x	x	x
Chinon-B2	Framatome 3-loop CP2-Type	1983	2044	2785	x	x	x
Chinon-B3	Framatome 3-loop CP2-Type	1986	2047	2905	x	x	x
Chinon-B4	Framatome 3-loop CP2-Type	1987	2048	2905	x	x	x
Chooz-B1	Framatome 4-loop N4-Type	1996	2056	4270	x	x	x
Chooz-B2	Framatome 4-loop N4-Type	1997	2057	4270	x	x	x
Civaux-1	Framatome 4-loop N4-Type	1997	2057	4270	x	x	x
Civaux-2	Framatome 4-loop N4-Type	1999	2059	4270	x	x	x
Clab	Spent fuel and high level waste storage	1985	na	na			

Cofrentes-1	General Electric BWR/6 Mark III	1984	2034	3000	x	x	x
Covra	Spent fuel and high level waste storage	2003	na	na			
Cruas-1	Framatome 3-loop CP2-Type	1983	2044	2785	x	x	x
Cruas-2	Framatome 3-loop CP2-Type	1984	2045	2785	x	x	x
Cruas-3	Framatome 3-loop CP2-Type	1984	2044	2785	x	x	x
Cruas-4	Framatome 3-loop CP2-Type	1984	2045	2785	x	x	x
Dampierre-1	Framatome 3-loop CP1-Type	1980	2040	2785	x	x	x
Dampierre-2	Framatome 3-loop CP1-Type	1980	2041	2785	x	x	x
Dampierre-3	Framatome 3-loop CP1-Type	1981	2041	2785	x	x	x
Dampierre-4	Framatome 3-loop CP1-Type	1981	2041	2785	x	x	x
Dessel	Fuel fabrication facility	1961	na	na			
Doel-1	Westinghouse 2-loop	1974	2025	1311	x	x	
Doel-2	Westinghouse 2-loop	1975	2025	1311	x	x	
Doel-3	Westinghouse 3-loop	1982	2022	3064	x	x	x
Doel-4	Westinghouse 3-loop	1985	2025	2988	x	x	x
Dukovany-1	Gidropress 6-loop VVER 440/213	1985	2045	1375	x	x	x
Dukovany-2	Gidropress 6-loop VVER 440/213	1986	2046	1375	x	x	x
Dukovany-3	Gidropress 6-loop VVER 440/213	1986	2046	1375	x	x	x
Dukovany-4	Gidropress 6-loop VVER 440/213	1987	2047	1375	x	x	x
Dungeness-B1	Advanced Gas Cooled Reactor	1983	2018	1500	x	x	x
Dungeness-B2	Advanced Gas Cooled Reactor	1985	2018	1500	x	x	x
Elektrostal	Fuel fabrication facility	1953	na	na			
Elektrostal	Fuel fabrication facility	1953	na	na			
Elektrostal	Fuel fabrication facility	1953	na	na			
Elektrostal	Fuel fabrication facility	1953	na	na			
Emsland-1	KWU 4-loop (Convoi)	1988	2037	3850	x	x	x
Eurodif	Gaseous diffusion enrichment plant	1979	na	na			
Fennovoima-1	AREVA EPR	2018	2078	4300			
Fessenheim-1	Framatome 3-loop CP0-Type	1977	2037	2660	x	x	
Fessenheim-2	Framatome 3-loop CP0-Type	1977	2037	2660	x	x	
Flamanville-1	Framatome 4-loop P4-Type	1985	2046	3817	x	x	x
Flamanville-2	Framatome 4-loop P4-Type	1986	2047	3817	x	x	x
Flamanville-3	AREVA EPR	2016	2072	4300			
Forsmark-1	ABB-Atom BWR	1980	2040	2928	x	x	x
Forsmark-2	ABB-Atom BWR	1981	2041	2928	x	x	x
Forsmark-3	ABB-Atom BWR 75	1985	2045	3300	x	x	x
Goesgen-1	KWU 3-loop	1979	2029	3002	x	x	
Golfech-1	Framatome 4-loop P4-Type	1990	2051	3817	x	x	x
Golfech-2	Framatome 4-loop P4-Type	1993	2054	3817	x	x	x
Gorleben	Spent fuel and high level waste storage	1995	na	na			
Grafenrheinfeld-1	KWU 4-loop (Pre Convoi)	1981	2028	3765	x	x	x
Gravelines-1	Framatome 3-loop CP1-Type	1980	2040	2785	x	x	x
Gravelines-2	Framatome 3-loop CP1-Type	1980	2040	2785	x	x	x
Gravelines-3	Framatome 3-loop CP1-Type	1980	2041	2785	x	x	x
Gravelines-4	Framatome 3-loop CP1-Type	1981	2041	2785	x	x	x
Gravelines-5	Framatome 3-loop CP1-Type	1984	2045	2785	x	x	x
Gravelines-6	Framatome 3-loop CP1-Type	1985	2045	2785	x	x	x
Grenoble-1	High flux research reactor	1971	na	58.3			
Grohnde-1	KWU 4-loop (Pre Convoi)	1984	2032	3850	x	x	x
Gronau	Centrifuge enrichment plant	1985	na	na			
Gundremmingen-B	Siemens BWR/72	1984	2032	3840	x	x	x
Gundremmingen-C	Siemens BWR/72	1984	2033	3840	x	x	x
Hartlepool-A1	Advanced Gas Cooled Reactor	1984	2019	1500	x	x	x
Hartlepool-A2	Advanced Gas Cooled Reactor	1984	2019	1500	x	x	x
Heysham-A1	Advanced Gas Cooled Reactor	1983	2019	1510	x	x	x
Heysham-A2	Advanced Gas Cooled Reactor	1984	2019	1510	x	x	x
Heysham-B1	Advanced Gas Cooled Reactor	1988	2023	1600	x	x	x
Heysham-B2	Advanced Gas Cooled Reactor	1988	2023	1600	x	x	x
Hinkley Point-B1	Advanced Gas Cooled Reactor	1976	2016	1660	x	x	
Hinkley Point-B2	Advanced Gas Cooled Reactor	1976	2016	1660	x	x	
Hunterston-B1	Advanced Gas Cooled Reactor	1976	2016	1500	x	x	
Hunterston-B2	Advanced Gas Cooled Reactor	1977	2017	1500	x	x	
Isar-1	Siemens BWR/69	1977	2011	2575	x		
Isar-2	KWU 4-loop (Convoi)	1988	2034	3850	x	x	x
Juzbado	Fuel fabrication facility	1985	na	na			
Kaliningrad-1	Gidropress 4-loop VVER 1200/491	2016	2076	3200			
Kaliningrad-2	Gidropress 4-loop VVER 1200/491	2018	2078	3200			

Kalinin-1	Gidropress 4-loop VVER 1000/338	1984	2014	3200	x	x	x
Kalinin-2	Gidropress 4-loop VVER 1000/338	1986	2016	3200	x	x	x
Kalinin-3	Gidropress 4-loop VVER 1000/320	2004	2034	3200	x	x	x
Kalinin-4	Gidropress 4-loop VVER 1000/320	2010	2070	3200	x	x	x
Kalinin-2-1	Gidropress 4-loop VVER 1200	2017	2077	3200			
Kalinin-2-2	Gidropress 4-loop VVER 1200	2017	2077	3200			
Kalinin-2-3	Gidropress 4-loop VVER 1200	2019	2079	3200			
Kalinin-2-4	Gidropress 4-loop VVER 1200	2020	2080	3200			
Khmelnitskiy-1	Gidropress 4-loop VVER 1000/320	1987	2032	3200	x	x	x
Khmelnitskiy-2	Gidropress 4-loop VVER 1000/320	2004	2050	3200	x	x	x
Khmelnitskiy-3	Gidropress 4-loop VVER 1000/446	2016	2076	3200			
Khmelnitskiy-4	Gidropress 4-loop VVER 1000/446	2017	2077	3200			
Kola-1	Gidropress 6-loop VVER 440/230	1973	2018	1375	x	x	
Kola-2	Gidropress 6-loop VVER 440/230	1975	2019	1375	x	x	
Kola-3	Gidropress 6-loop VVER 440/213	1981	2026	1375	x	x	x
Kola-4	Gidropress 6-loop VVER 440/213	1984	2029	1375	x	x	x
Kozloduy-5	Gidropress 4-loop VVER 1000/320	1987	2037	3200	x	x	x
Kozloduy-6	Gidropress 4-loop VVER 1000/320	1991	2041	3200	x	x	x
Krsko-1	Westinghouse 2-loop	1981	2023	1994	x	x	x
Kruemmel-1	Siemens BWR/69	1983	2011	3690	x		x
Kursk-1	RBMK-1000 (1st Gen.)	1976	2021	3200	x	x	
Kursk-2	RBMK-1000 (1st Gen.)	1979	2024	3200	x	x	
Kursk-3	RBMK-1000 (2rd or 3rd Gen.)	1983	2013	3200	x	x	x
Kursk-4	RBMK-1000 (2rd or 3rd Gen.)	1985	2015	3200	x	x	x
La Hague-1	Spent nuclear fuel reprocessing facility	1990	na	na			
Leibstadt-1	General Electric BWR/6 Mark III	1984	2022	3600	x	x	x
Leningrad-1	RBMK-1000 (1st Gen.)	1973	2018	3200	x	x	
Leningrad-2	RBMK-1000 (1st Gen.)	1975	2020	3200	x	x	
Leningrad-3	RBMK-1000 (2rd or 3rd Gen.)	1979	2024	3200	x	x	x
Leningrad-4	RBMK-1000 (2rd or 3rd Gen.)	1981	2025	3200	x	x	x
Leningrad-II-1	Gidropress 4-loop VVER 1200/491	2013	2073	3200			
Leningrad-II-2	Gidropress 4-loop VVER 1200/491	2014	2074	3200			
Leningrad-II-3	Gidropress 4-loop VVER 1200/491	2016	2076	3200			
Leningrad-II-4	Gidropress 4-loop VVER 1200/491	2019	2079	3200			
Lingen	Fuel fabrication facility	1979	na	na			
Loviisa-1	Gidropress 6-loop VVER 440/311	1977	2027	1500	x	x	
Loviisa-2	Gidropress 6-loop VVER 440/311	1980	2030	1500	x	x	x
Marcoule	Fuel fabrication facility	1995	na	na			
Medzamor-2	Gidropress 6-loop VVER 440/230	1979	2016	1375	x	x	
Mochovce-1	Gidropress 6-loop VVER 440/213	1989	2028	1375	x	x	x
Mochovce-2	Gidropress 6-loop VVER 440/213	1999	2039	1375	x	x	x
Mochovce-3	Gidropress 6-loop VVER 440/213	2012	2062	1375			
Mochovce-4	Gidropress 6-loop VVER 440/213	2013	2063	1375			
Mol	High flux research reactor	1961	na	100			
Muehleberg-1	General Electric BWR/4 Mark I	1971	2034	1097	x	x	
Neckarwestheim-1	KWU 3-loop	1976	2011	2497	x		
Neckarwestheim-2	KWU 4-loop (Convoi)	1989	2036	3850	x	x	x
Nogent-1	Framatome 4-loop P4-Type	1987	2048	3817	x	x	x
Nogent-2	Framatome 4-loop P4-Type	1988	2049	3817	x	x	x
Zwischenlager Nord	Spent fuel and high level waste storage	1999	na	na			
Novovoronezh-3	Gidropress 6-loop VVER 440/179	1971	2016	1375	x	x	
Novovoronezh-4	Gidropress 6-loop VVER 440/179	1972	2017	1375	x	x	
Novovoronezh-5	Gidropress 4-loop VVER 1000/187	1980	2035	3200	x	x	x
Novovoronezh-II-1	Gidropress 4-loop VVER 1200/392 M	2012	2072	3200			
Novovoronezh-II-2	Gidropress 4-loop VVER 1200/392 M	2013	2073	3200			
Oldbury-A1	MAGNOX Reactor	1967	2011	730	x		
Oldbury-A2	MAGNOX Reactor	1968	2012	660	x	x	
Olkiluoto-1	ABB-Atom BWR 75	1978	2039	2500	x	x	
Olkiluoto-2	ABB-Atom BWR 75	1980	2042	2500	x	x	x
Olkiluoto-3	AREVA EPR	2013	2073	4300			
Oskarshamn-1	ABB-Atom BWR	1971	2031	1375	x	x	
Oskarshamn-2	ABB-Atom BWR	1974	2034	1800	x	x	
Oskarshamn-3	ABB-Atom BWR 75	1985	2045	3300	x	x	x
Ostrovets-1	Gidropress 4-loop VVER 1200/491	2016	2076	3200			
Paks-1	Gidropress 6-loop VVER 440/213	1982	2032	1485	x	x	x
Paks-2	Gidropress 6-loop VVER 440/213	1984	2034	1375	x	x	x
Paks-3	Gidropress 6-loop VVER 440/213	1986	2036	1375	x	x	x

Paks-4	Gidropress 6-loop VVER 440/213	1987	2037	1375	x	x	x
Paluel-1	Framatome 4-loop P4-Type	1984	2045	3817	x	x	x
Paluel-2	Framatome 4-loop P4-Type	1984	2045	3817	x	x	x
Paluel-3	Framatome 4-loop P4-Type	1985	2046	3817	x	x	x
Paluel-4	Framatome 4-loop P4-Type	1986	2026	3817	x	x	x
Penly-1	Framatome 4-loop P4-Type	1990	2050	3817	x	x	x
Penly-2	Framatome 4-loop P4-Type	1992	2052	3817	x	x	x
Petten-1	High flux research reactor	1961	2015	45			
Philippsburg-1	Siemens BWR/69	1979	2011	2575	x		
Philippsburg-2	KWU 4-loop (Pre Convoi)	1984	2032	3950	x	x	x
Pitesti	Fuel fabrication facility	1983	na	na			
Ringhals-1	ABB-Atom BWR	1974	2034	2540	x	x	
Ringhals-2	Westinghouse 3-loop	1974	2034	2660	x	x	
Ringhals-3	Westinghouse 3-loop	1981	2041	3160	x	x	x
Ringhals-4	Westinghouse 3-loop	1982	2042	2775	x	x	x
Romans	Fuel fabrication facility	1979	na	na			
Rowno-1	Gidropress 6-loop VVER 440/213	1980	2030	1375	x	x	x
Rowno-2	Gidropress 6-loop VVER 440/213	1981	2031	1375	x	x	x
Rowno-3	Gidropress 4-loop VVER 1000/320	1986	2032	3000	x	x	x
Rowno-4	Gidropress 4-loop VVER 1000/320	2004	2050	3000	x	x	x
Sellafield-1	Spent nuclear fuel reprocessing facility	1964	na	na			
Sizewell-B	Westinghouse 4-loop	1995	2035	3425	x	x	x
S. Maria de Garona-1	General Electric BWR/3 Mark I	1971	2013	1381	x	x	
Smolensk-1	RBMK-1000 (2rd or 3rd Gen.)	1982	2028	3200	x	x	x
Smolensk-2	RBMK-1000 (2rd or 3rd Gen.)	1985	2015	3200	x	x	x
Smolensk-3	RBMK-1000 (2rd or 3rd Gen.)	1990	2020	3200	x	x	x
South Ukraine-1	Gidropress 4-loop VVER 1000/302	1982	2027	3000	x	x	x
South Ukraine-2	Gidropress 4-loop VVER 1000/338	1985	2030	3000	x	x	x
South Ukraine-3	Gidropress 4-loop VVER 1000/320	1989	2034	3000	x	x	x
Springfields	Fuel fabrication facility	1996	na	na			
Springfields	Fuel fabrication facility	1996	na	na			
St. Alban-1	Framatome 4-loop P4-Type	1985	2046	3817	x	x	x
St. Alban-2	Framatome 4-loop P4-Type	1986	2047	3817	x	x	x
St. Laurent-B1	Framatome 3-loop CP2-Type	1981	2043	2785	x	x	x
St. Laurent-B2	Framatome 3-loop CP2-Type	1981	2043	2785	x	x	x
Temelin-1	Gidropress 4-loop VVER 1000/320	2002	2032	3000	x	x	x
Temelin-2	Gidropress 4-loop VVER 1000/320	2003	2032	3000	x	x	x
Tihange-1	Framatome 3-loop CP0-Type	1975	2025	2873	x	x	
Tihange-2	Westinghouse 3-loop	1982	2022	3064	x	x	x
Tihange-3	Westinghouse 3-loop	1985	2025	3000	x	x	x
Torness Point-1	Advanced Gas Cooled Reactor	1988	2023	1623	x	x	x
Torness Point-2	Advanced Gas Cooled Reactor	1989	2023	1623	x	x	x
Tricastin-1	Framatome 3-loop CP1-Type	1980	2040	2785	x	x	x
Tricastin-2	Framatome 3-loop CP1-Type	1980	2040	2785	x	x	x
Tricastin-3	Framatome 3-loop CP1-Type	1981	2041	2785	x	x	x
Tricastin-4	Framatome 3-loop CP1-Type	1981	2041	2785	x	x	x
Trillo-1	KWU 3-loop	1988	2028	3010	x	x	x
Tsentral-1	Gidropress 4-loop VVER 1200/392 M	2018	2078	3200			
Tsentral-2	Gidropress 4-loop VVER 1200/392 M	2019	2079	3200			
Tsentral-3	Gidropress 4-loop VVER 1200/392 M	2019	2079	3200			
Tsentral-4	Gidropress 4-loop VVER 1200/392 M	2020	2080	3200			
Unterweser-1	KWU 4-loop	1978	2011	3900	x		
Vandellos-2	Westinghouse 3-loop	1987	2027	2941	x	x	x
Vasteras	Fuel fabrication facility	1971	na	na			
Visaginas-1	AREVA EPR	2020	2080	4300			
Volgodonsk-1	Gidropress 4-loop VVER 1000/320	2001	2030	3000	x	x	x
Volgodonsk-2	Gidropress 4-loop VVER 1000/320	2010	2070	3000	x	x	x
Volgodonsk-3	Gidropress 4-loop VVER 1000/320	2014	2074	3000	x	x	x
Volgodonsk-4	Gidropress 4-loop VVER 1000/320	2017	2077	3000	x	x	x
Wylfa-1	MAGNOX Reactor	1971	2012	1920	x	x	
Wylfa-2	MAGNOX Reactor	1971	2012	1920	x	x	
Zaporoshje-1	Gidropress 4-loop VVER 1000/320	1984	2030	3000	x	x	x
Zaporoshje-2	Gidropress 4-loop VVER 1000/320	1985	2031	3000	x	x	x
Zaporoshje-3	Gidropress 4-loop VVER 1000/320	1986	2032	3000	x	x	x
Zaporoshje-4	Gidropress 4-loop VVER 1000/320	1987	2033	3000	x	x	x
Zaporoshje-5	Gidropress 4-loop VVER 1000/320	1989	2034	3000	x	x	x
Zaporoshje-6	Gidropress 4-loop VVER 1000/320	1995	2041	3000	x	x	x

Zwilag	Spent fuel and high level waste storage	2001	na	na

Appendix B: List of source terms

The Table below lists the absolute releases and the corresponding release fractions for one key nuclide of each nuclide group, the accident type (letters refer to the accident sequences of Appendix C), and the release frequency (Rel. freq.).

Site-unit	Xe-133		I-131		Cs-137		Te-132		Sr-90		Ru-106		Type	Rel. freq.
	PBq	fraction	PBq	fraction	PBq	fraction	PBq	fraction	PBq	fraction	PBq	fraction		(a^{-1})
Akkuyu-1	6014	0.800	731	0.200	54	0.200	417	0.080	6	0.030	56	0.040	T	1.0E-7
Akkuyu-2	6014	0.800	731	0.200	54	0.200	417	0.080	6	0.030	56	0.040	T	1.0E-7
Akkuyu-3	6014	0.800	731	0.200	54	0.200	417	0.080	6	0.030	56	0.040	T	1.0E-7
Akkuyu-4	6014	0.800	731	0.200	54	0.200	417	0.080	6	0.030	56	0.040	T	1.0E-7
Almaraz-1	4968	1.000	729	0.300	93	0.300	413	0.120	14	0.060	106	0.080	V	2.0E-7
Almaraz-2	4968	1.000	729	0.300	93	0.300	413	0.120	14	0.060	106	0.080	V	2.0E-7
Asco-1	6273	1.000	912	0.300	109	0.300	524	0.120	16	0.060	126	0.080	V	2.0E-7
Asco-2	6273	1.000	912	0.300	109	0.300	524	0.120	16	0.060	126	0.080	V	2.0E-7
Balakovo-1	5638	0.800	685	0.200	51	0.200	391	0.080	6	0.030	53	0.040	S	1.4E-5
Balakovo-2	5638	0.800	685	0.200	51	0.200	391	0.080	6	0.030	53	0.040	S	1.4E-5
Balakovo-3	5638	0.800	685	0.200	51	0.200	391	0.080	6	0.030	53	0.040	S	1.4E-5
Balakovo-4	5638	0.800	685	0.200	51	0.200	391	0.080	6	0.030	53	0.040	S	1.4E-5
Belene-1	7282	1.000	1589	0.449	72	0.272	82	0.016	7	0.036	61	0.045	Q	3.0E-8
Belene-2	7282	1.000	1589	0.449	72	0.272	82	0.016	7	0.036	61	0.045	Q	3.0E-8
Belleville-1	7034	1.000	1032	0.300	132	0.300	585	0.120	19	0.060	150	0.080	D	5.0E-8
Belleville-2	7034	1.000	1032	0.300	132	0.300	585	0.120	19	0.060	150	0.080	D	5.0E-8
Beznau-1	2203	1.000	275	0.300	44	0.300	189	0.120	5	0.060	69	0.080	U	4.9E-7
Beznau-2	2203	1.000	275	0.300	44	0.300	189	0.120	5	0.060	69	0.080	U	4.9E-7
Biblis-1	5706	0.800	684	0.200	56	0.200	395	0.080	6	0.030	52	0.040	N	1.0E-9
Biblis-2	6056	0.800	726	0.200	60	0.200	419	0.080	7	0.030	55	0.040	N	1.0E-9
Blayais-1	5429	1.000	677	0.300	108	0.300	465	0.120	12	0.060	169	0.080	D	1.6E-6
Blayais-2	5429	1.000	677	0.300	108	0.300	465	0.120	12	0.060	169	0.080	D	1.6E-6
Blayais-3	5132	1.000	753	0.300	96	0.300	427	0.120	14	0.060	109	0.080	D	1.6E-6
Blayais-4	5132	1.000	753	0.300	96	0.300	427	0.120	14	0.060	109	0.080	D	1.6E-6
Bohunice-3	3230	1.000	1021	0.650	76	0.650	672	0.300	10	0.120	3	0.005	P	1.1E-5
Bohunice-4	3230	1.000	1021	0.650	76	0.650	672	0.300	10	0.120	3	0.005	P	1.1E-5

Site-unit	Xe-133		I-131		Cs-137		Te-132		Sr-90		Ru-106		Type	Rel. freq.
	PBq	fraction	PBq	fraction	PBq	fraction	PBq	fraction	PBq	fraction	PBq	fraction		(a^{-1})
Borssele-1	2153	0.800	264	0.200	32	0.200	149	0.080	3	0.030	28	0.040	L	3.7E-8
Brokdorf-1	6082	0.800	632	0.200	101	0.200	434	0.080	9	0.030	118	0.040	N	1.0E-9
Brunsbuettel-1	4753	1.000	1494	0.610	324	0.610	1063	0.310	40	0.120	23	0.010	J	7.6E-7
Bugey-2	5132	1.000	753	0.300	96	0.300	427	0.120	14	0.060	109	0.080	D	1.6E-6
Bugey-3	5132	1.000	753	0.300	96	0.300	427	0.120	14	0.060	109	0.080	D	1.6E-6
Bugey-4	5132	1.000	753	0.300	96	0.300	427	0.120	14	0.060	109	0.080	D	1.6E-6
Bugey-5	5132	1.000	753	0.300	96	0.300	427	0.120	14	0.060	109	0.080	D	1.6E-6
Bushehr-1	7517	1.000	1641	0.449	74	0.272	85	0.016	7	0.036	63	0.045	Q	3.0E-8
Cattenom-1	7034	1.000	1032	0.300	132	0.300	585	0.120	19	0.060	150	0.080	D	5.0E-8
Cattenom-2	7034	1.000	1032	0.300	132	0.300	585	0.120	19	0.060	150	0.080	D	5.0E-8
Cattenom-3	7034	1.000	1032	0.300	132	0.300	585	0.120	19	0.060	150	0.080	D	5.0E-8
Cattenom-4	7034	1.000	1032	0.300	132	0.300	585	0.120	19	0.060	150	0.080	D	5.0E-8
Cernavoda-1	5024	1.000	288	0.100	8	0.100	398	0.100	0	0.010	1	0.001	H	8.2E-7
Cernavoda-2	5024	1.000	288	0.100	8	0.100	398	0.100	0	0.010	1	0.001	H	8.2E-7
Cernavoda-3	5024	1.000	288	0.100	8	0.100	398	0.100	0	0.010	1	0.001	H	8.2E-7
Cernavoda-4	5024	1.000	288	0.100	8	0.100	398	0.100	0	0.010	1	0.001	H	8.2E-7
Chinon-B1	5429	1.000	677	0.300	108	0.300	465	0.120	12	0.060	169	0.080	D	1.6E-6
Chinon-B2	5429	1.000	677	0.300	108	0.300	465	0.120	12	0.060	169	0.080	D	1.6E-6
Chinon-B3	5663	1.000	706	0.300	113	0.300	485	0.120	13	0.060	177	0.080	D	1.6E-6
Chinon-B4	5663	1.000	706	0.300	113	0.300	485	0.120	13	0.060	177	0.080	D	1.6E-6
Chooz-B1	7869	1.000	1154	0.300	148	0.300	654	0.120	21	0.060	168	0.080	D	5.0E-8
Chooz-B2	7869	1.000	1154	0.300	148	0.300	654	0.120	21	0.060	168	0.080	D	5.0E-8
Civaux-1	7869	1.000	1154	0.300	148	0.300	654	0.120	21	0.060	168	0.080	D	5.0E-8
Civaux-2	7869	1.000	1154	0.300	148	0.300	654	0.120	21	0.060	168	0.080	D	5.0E-8
Cofrentes-1	6221	1.000	449	0.140	97	0.140	628	0.140	0	0.000	0	0.000	G	3.0E-7
Cruas-1	5132	1.000	753	0.300	96	0.300	427	0.120	14	0.060	109	0.080	D	1.6E-6
Cruas-2	5132	1.000	753	0.300	96	0.300	427	0.120	14	0.060	109	0.080	D	1.6E-6
Cruas-3	5132	1.000	753	0.300	96	0.300	427	0.120	14	0.060	109	0.080	D	1.6E-6
Cruas-4	5132	1.000	753	0.300	96	0.300	427	0.120	14	0.060	109	0.080	D	1.6E-6

Site-unit	Xe-133		I-131		Cs-137		Te-132		Sr-90		Ru-106		Type	Rel. freq.
	PBq	fraction	PBq	fraction	PBq	fraction	PBq	fraction	PBq	fraction	PBq	fraction		(a^{-1})
Dampierre-1	5429	1.000	677	0.300	108	0.300	465	0.120	12	0.060	169	0.080	D	1.6E-6
Dampierre-2	5429	1.000	677	0.300	108	0.300	465	0.120	12	0.060	169	0.080	D	1.6E-6
Dampierre-3	5429	1.000	677	0.300	108	0.300	465	0.120	12	0.060	169	0.080	D	1.6E-6
Dampierre-4	5429	1.000	677	0.300	108	0.300	465	0.120	12	0.060	169	0.080	D	1.6E-6
Doel-1	2416	1.000	354	0.300	45	0.300	201	0.120	7	0.060	52	0.080	U	3.8E-7
Doel-2	2556	1.000	319	0.300	51	0.300	219	0.120	6	0.060	80	0.080	U	3.8E-7
Doel-3	5973	1.000	745	0.300	119	0.300	512	0.120	13	0.060	186	0.080	V	2.0E-7
Doel-4	5825	1.000	726	0.300	116	0.300	499	0.120	13	0.060	182	0.080	V	2.0E-7
Dukovany-1	3230	1.000	1021	0.650	76	0.650	672	0.300	10	0.120	3	0.005	P	1.1E-5
Dukovany-2	3230	1.000	1021	0.650	76	0.650	672	0.300	10	0.120	3	0.005	P	1.1E-5
Dukovany-3	3230	1.000	1021	0.650	76	0.650	672	0.300	10	0.120	3	0.005	P	1.1E-5
Dukovany-4	3230	1.000	1021	0.650	76	0.650	672	0.300	10	0.120	3	0.005	P	1.1E-5
Dungeness-B1	3042	1.000	875	0.600	48	0.400	211	0.100	1	0.010	4	0.007	B	1.0E-6
Dungeness-B2	3042	1.000	875	0.600	48	0.400	211	0.100	1	0.010	4	0.007	B	1.0E-6
Emsland-1	6246	0.800	749	0.200	62	0.200	432	0.080	7	0.030	57	0.040	N	1.0E-9
Fennovoima-1	7924	1.000	852	0.220	174	0.350	1647	0.300	47	0.130	6	0.003	C	3.9E-8
Fessenheim-1	4902	1.000	719	0.300	92	0.300	408	0.120	13	0.060	105	0.080	D	1.6E-6
Fessenheim-2	4902	1.000	719	0.300	92	0.300	408	0.120	13	0.060	105	0.080	D	1.6E-6
Flamanville-1	7034	1.000	1032	0.300	132	0.300	585	0.120	19	0.060	150	0.080	D	5.0E-8
Flamanville-2	7034	1.000	1032	0.300	132	0.300	585	0.120	19	0.060	150	0.080	D	5.0E-8
Flamanville-3	7924	1.000	852	0.220	174	0.350	1647	0.300	47	0.130	6	0.003	C	3.9E-8
Forsmark-1	3461	0.570	294	0.094	61	0.089	170	0.039	2	0.004	8	0.003	A	1.5E-6
Forsmark-2	3461	0.570	294	0.094	61	0.089	170	0.039	2	0.004	8	0.003	A	1.5E-6
Forsmark-3	3901	0.570	332	0.094	68	0.089	192	0.039	2	0.004	9	0.003	A	1.5E-6
Goesgen-1	4682	0.800	486	0.200	78	0.200	334	0.080	7	0.030	91	0.040	M	1.9E-7
Golfech-1	7034	1.000	1032	0.300	132	0.300	585	0.120	19	0.060	150	0.080	D	5.0E-8
Golfech-2	7034	1.000	1032	0.300	132	0.300	585	0.120	19	0.060	150	0.080	D	5.0E-8
Grafenrheinfeld-1	5871	0.800	610	0.200	97	0.200	419	0.080	8	0.030	114	0.040	N	1.0E-9
Gravelines-1	5429	1.000	677	0.300	108	0.300	465	0.120	12	0.060	169	0.080	D	1.6E-6
Gravelines-2	5429	1.000	677	0.300	108	0.300	465	0.120	12	0.060	169	0.080	D	1.6E-6

Site-unit	Xe-133		I-131		Cs-137		Te-132		Sr-90		Ru-106		Type	Rel. freq. (a^{-1})
	PBq	fraction	PBq	fraction	PBq	fraction	PBq	fraction	PBq	fraction	PBq	fraction		
Gravelines-3	5429	1.000	677	0.300	108	0.300	465	0.120	12	0.060	169	0.080	D	1.6E-6
Gravelines-4	5429	1.000	677	0.300	108	0.300	465	0.120	12	0.060	169	0.080	D	1.6E-6
Gravelines-5	5429	1.000	677	0.300	108	0.300	465	0.120	12	0.060	169	0.080	D	1.6E-6
Gravelines-6	5429	1.000	677	0.300	108	0.300	465	0.120	12	0.060	169	0.080	D	1.6E-6
Grohnde-1	6004	0.800	624	0.200	99	0.200	429	0.080	8	0.030	117	0.040	N	1.0E-9
Gundremmingen-B	7486	1.000	1555	0.500	149	0.300	535	0.100	0	0.001	0	0.000	K	1.0E-6
Gundremmingen-C	7486	1.000	1555	0.500	149	0.300	535	0.100	0	0.001	0	0.000	K	1.0E-6
Hartlepool-A1	3042	1.000	875	0.600	48	0.400	211	0.100	1	0.010	4	0.007	B	1.0E-6
Hartlepool-A2	3042	1.000	875	0.600	48	0.400	211	0.100	1	0.010	4	0.007	B	1.0E-6
Heysham-A1	3062	1.000	881	0.600	48	0.400	212	0.100	1	0.010	4	0.007	B	1.0E-6
Heysham-A2	3062	1.000	881	0.600	48	0.400	212	0.100	1	0.010	4	0.007	B	1.0E-6
Heysham-B1	3245	1.000	934	0.600	51	0.400	225	0.100	1	0.010	4	0.007	B	1.0E-6
Heysham-B2	3245	1.000	934	0.600	51	0.400	225	0.100	1	0.010	4	0.007	B	1.0E-6
Hinkley Point-B1	3366	1.000	969	0.600	53	0.400	233	0.100	1	0.010	4	0.007	B	1.0E-6
Hinkley Point-B2	3366	1.000	969	0.600	53	0.400	233	0.100	1	0.010	4	0.007	B	1.0E-6
Hunterston-B1	3042	1.000	875	0.600	48	0.400	211	0.100	1	0.010	4	0.007	B	1.0E-6
Hunterston-B2	3042	1.000	875	0.600	48	0.400	211	0.100	1	0.010	4	0.007	B	1.0E-6
Isar-1	5340	1.000	1678	0.610	364	0.610	1194	0.310	44	0.120	25	0.010	J	7.8E-7
Isar-2	6004	0.800	624	0.200	99	0.200	429	0.080	8	0.030	117	0.040	N	1.0E-9
Kaliningrad-1	6014	0.800	731	0.200	54	0.200	417	0.080	6	0.030	56	0.040	T	1.0E-7
Kaliningrad-2	6014	0.800	731	0.200	54	0.200	417	0.080	6	0.030	56	0.040	T	1.0E-7
Kalinin-1	7442	0.990	2996	0.820	218	0.800	2450	0.470	113	0.570	169	0.120	R	2.9E-6
Kalinin-2	7442	0.990	2996	0.820	218	0.800	2450	0.470	113	0.570	169	0.120	R	2.9E-6
Kalinin-3	6014	0.800	731	0.200	54	0.200	417	0.080	6	0.030	56	0.040	S	1.4E-5
Kalinin-4	6014	0.800	731	0.200	54	0.200	417	0.080	6	0.030	56	0.040	S	1.4E-5
Kalinin-2-1	6014	0.800	731	0.200	54	0.200	417	0.080	6	0.030	56	0.040	T	1.0E-7
Kalinin-2-2	6014	0.800	731	0.200	54	0.200	417	0.080	6	0.030	56	0.040	T	1.0E-7
Kalinin-2-3	6014	0.800	731	0.200	54	0.200	417	0.080	6	0.030	56	0.040	T	1.0E-7
Kalinin-2-4	6014	0.800	731	0.200	54	0.200	417	0.080	6	0.030	56	0.040	T	1.0E-7
Khmelnitskiy-1	6014	0.800	731	0.200	54	0.200	417	0.080	6	0.030	56	0.040	S	1.4E-5
Khmelnitskiy-2	6014	0.800	731	0.200	54	0.200	417	0.080	6	0.030	56	0.040	S	1.4E-5

Site-unit	Xe-133		I-131		Cs-137		Te-132		Sr-90		Ru-106		Type	Rel. freq. (a^{-1})
	PBq	fraction	PBq	fraction	PBq	fraction	PBq	fraction	PBq	fraction	PBq	fraction		
Khmelnitskiy-3	7517	1.000	1641	0.449	74	0.272	85	0.016	7	0.036	63	0.045	Q	3.0E-8
Khmelnitskiy-4	7517	1.000	1641	0.449	74	0.272	85	0.016	7	0.036	63	0.045	Q	3.0E-8
Kola-1	3040	1.000	962	0.650	81	0.650	633	0.300	11	0.120	3	0.005	P	2.3E-5
Kola-2	3040	1.000	962	0.650	81	0.650	633	0.300	11	0.120	3	0.005	P	2.3E-5
Kola-3	3230	1.000	1021	0.650	76	0.650	672	0.300	10	0.120	3	0.005	P	1.1E-5
Kola-4	3230	1.000	1021	0.650	76	0.650	672	0.300	10	0.120	3	0.005	P	1.1E-5
Kozloduy-5	6014	0.800	731	0.200	54	0.200	417	0.080	6	0.030	56	0.040	S	1.4E-5
Kozloduy-6	6014	0.800	731	0.200	54	0.200	417	0.080	6	0.030	56	0.040	S	1.4E-5
Krsko-1	3675	1.000	539	0.300	69	0.300	306	0.120	10	0.060	78	0.080	U	3.8E-7
Kruemmel-1	7652	1.000	2405	0.610	522	0.610	1712	0.310	64	0.120	36	0.010	J	1.1E-6
Kursk-1	6636	1.000	2051	0.600	297	0.400	2873	0.600	23	0.050	111	0.035	I	7.4E-6
Kursk-2	6636	1.000	2051	0.600	297	0.400	2873	0.600	23	0.050	111	0.035	I	7.4E-6
Kursk-3	6636	1.000	2051	0.600	297	0.400	2873	0.600	23	0.050	111	0.035	I	7.4E-6
Kursk-4	6636	1.000	2051	0.600	297	0.400	2873	0.600	23	0.050	111	0.035	I	7.4E-6
Leibstadt-1	7465	1.000	538	0.140	117	0.140	754	0.140	0	0.000	0	0.000	G	3.0E-7
Leningrad-1	6636	1.000	2051	0.600	297	0.400	2873	0.600	23	0.050	111	0.035	I	7.4E-6
Leningrad-2	6636	1.000	2051	0.600	297	0.400	2873	0.600	23	0.050	111	0.035	I	7.4E-6
Leningrad-3	6636	1.000	2051	0.600	297	0.400	2873	0.600	23	0.050	111	0.035	I	7.4E-6
Leningrad-4	6636	1.000	2051	0.600	297	0.400	2873	0.600	23	0.050	111	0.035	I	7.4E-6
Leningrad-II-1	6014	0.800	731	0.200	54	0.200	417	0.080	6	0.030	56	0.040	T	1.0E-7
Leningrad-II-2	6014	0.800	731	0.200	54	0.200	417	0.080	6	0.030	56	0.040	T	1.0E-7
Leningrad-II-3	6014	0.800	731	0.200	54	0.200	417	0.080	6	0.030	56	0.040	T	1.0E-7
Leningrad-II-4	6014	0.800	731	0.200	54	0.200	417	0.080	6	0.030	56	0.040	T	1.0E-7
Loviisa-1	2790	1.000	405	0.300	32	0.300	232	0.120	5	0.060	43	0.080	O	2.8E-7
Loviisa-2	2790	1.000	405	0.300	32	0.300	232	0.120	5	0.060	43	0.080	O	2.8E-7
Medzamor-2	3040	1.000	962	0.650	81	0.650	633	0.300	11	0.120	3	0.005	P	2.3E-5
Mochovce-1	3230	1.000	1021	0.650	76	0.650	672	0.300	10	0.120	3	0.005	P	1.1E-5
Mochovce-2	3230	1.000	1021	0.650	76	0.650	672	0.300	10	0.120	3	0.005	P	1.1E-5
Mochovce-3	3230	1.000	1021	0.650	76	0.650	672	0.300	10	0.120	3	0.005	P	1.1E-5
Mochovce-4	3230	1.000	1021	0.650	76	0.650	672	0.300	10	0.120	3	0.005	P	1.1E-5

Site-unit	Xe-133		I-131		Cs-137		Te-132		Sr-90		Ru-106		Type	Rel. freq.
	PBq	fraction	PBq	fraction	PBq	fraction	PBq	fraction	PBq	fraction	PBq	fraction		(a^{-1})
Muehleberg-1	2275	1.000	398	0.340	87	0.340	279	0.170	2	0.010	24	0.023	F	4.0E-8
Neckarwestheim-1	3894	0.800	405	0.200	64	0.200	278	0.080	5	0.030	76	0.040	M	1.9E-7
Neckarwestheim-2	6004	0.800	624	0.200	99	0.200	429	0.080	8	0.030	117	0.040	N	1.0E-9
Nogent-1	7034	1.000	1032	0.300	132	0.300	585	0.120	19	0.060	150	0.080	D	5.0E-8
Nogent-2	7034	1.000	1032	0.300	132	0.300	585	0.120	19	0.060	150	0.080	D	5.0E-8
Novovoronezh-3	3040	1.000	962	0.650	81	0.650	633	0.300	11	0.120	3	0.005	P	2.4E-5
Novovoronezh-4	3040	1.000	962	0.650	81	0.650	633	0.300	11	0.120	3	0.005	P	2.4E-5
Novovoronezh-5	7442	0.990	2996	0.820	218	0.800	2450	0.470	113	0.570	169	0.120	R	2.9E-6
Novovoronezh-II-1	6014	0.800	731	0.200	54	0.200	417	0.080	6	0.030	56	0.040	T	1.0E-7
Novovoronezh-II-2	6014	0.800	731	0.200	54	0.200	417	0.080	6	0.030	56	0.040	T	1.0E-7
Oldbury-A1	1480	1.000	426	0.600	23	0.400	102	0.100	0	0.010	2	0.007	B	1.0E-6
Oldbury-A2	1338	1.000	385	0.600	21	0.400	93	0.100	0	0.010	2	0.007	B	1.0E-6
Olkiluoto-1	2491	0.570	202	0.094	25	0.089	119	0.039	1	0.004	3	0.003	A	1.5E-6
Olkiluoto-2	2491	0.570	202	0.094	25	0.089	119	0.039	1	0.004	3	0.003	A	1.5E-6
Olkiluoto-3	7924	1.000	852	0.220	174	0.350	1647	0.300	47	0.130	6	0.003	C	3.9E-8
Oskarshamn-1	1442	0.570	116	0.094	26	0.089	68	0.039	1	0.004	2	0.003	A	1.5E-6
Oskarshamn-2	1887	0.570	152	0.094	34	0.089	89	0.039	1	0.004	3	0.003	A	1.5E-6
Oskarshamn-3	3901	0.570	332	0.094	68	0.089	192	0.039	2	0.004	9	0.003	A	1.5E-6
Ostrovets-1	6014	0.800	731	0.200	54	0.200	417	0.080	6	0.030	56	0.040	T	1.0E-7
Paks-1	3488	1.000	1102	0.650	82	0.650	726	0.300	11	0.120	3	0.005	P	1.1E-5
Paks-2	3230	1.000	1021	0.650	76	0.650	672	0.300	10	0.120	3	0.005	P	1.1E-5
Paks-3	3230	1.000	1021	0.650	76	0.650	672	0.300	10	0.120	3	0.005	P	1.1E-5
Paks-4	3230	1.000	1021	0.650	76	0.650	672	0.300	10	0.120	3	0.005	P	1.1E-5
Paluel-1	7034	1.000	1032	0.300	132	0.300	585	0.120	19	0.060	150	0.080	D	5.0E-8
Paluel-2	7034	1.000	1032	0.300	132	0.300	585	0.120	19	0.060	150	0.080	D	5.0E-8
Paluel-3	7034	1.000	1032	0.300	132	0.300	585	0.120	19	0.060	150	0.080	D	5.0E-8
Paluel-4	7034	1.000	1032	0.300	132	0.300	585	0.120	19	0.060	150	0.080	D	5.0E-8
Penly-1	7034	1.000	1032	0.300	132	0.300	585	0.120	19	0.060	150	0.080	D	5.0E-8
Penly-2	7034	1.000	1032	0.300	132	0.300	585	0.120	19	0.060	150	0.080	D	5.0E-8
Philippsburg-1	5340	1.000	1678	0.610	364	0.610	1194	0.310	44	0.120	25	0.010	J	8.2E-7

Site-unit	Xe-133		I-131		Cs-137		Te-132		Sr-90		Ru-106		Type	Rel. freq. (a^{-1})
	PBq	fraction	PBq	fraction	PBq	fraction	PBq	fraction	PBq	fraction	PBq	fraction		
Philippsburg-2	6160	0.800	640	0.200	102	0.200	440	0.080	9	0.030	120	0.040	N	1.0E-9
Ringhals-1	3002	0.570	255	0.094	53	0.089	148	0.039	1	0.004	7	0.003	A	1.5E-6
Ringhals-2	4902	1.000	719	0.300	92	0.300	408	0.120	13	0.060	105	0.080	V	2.0E-7
Ringhals-3	5824	1.000	854	0.300	109	0.300	484	0.120	16	0.060	124	0.080	V	2.0E-7
Ringhals-4	5114	1.000	750	0.300	96	0.300	425	0.120	14	0.060	109	0.080	V	2.0E-7
Rowno-1	3230	1.000	1021	0.650	76	0.650	672	0.300	10	0.120	3	0.005	P	1.1E-5
Rowno-2	3230	1.000	1021	0.650	76	0.650	672	0.300	10	0.120	3	0.005	P	1.1E-5
Rowno-3	5638	0.800	685	0.200	51	0.200	391	0.080	6	0.030	53	0.040	S	1.4E-5
Rowno-4	5638	0.800	685	0.200	51	0.200	391	0.080	6	0.030	53	0.040	S	1.4E-5
Sizewell-B	6312	1.000	926	0.300	119	0.300	525	0.120	17	0.060	135	0.080	W	1.6E-7
S. Maria de Garona-1	2469	0.972	500	0.403	111	0.377	121	0.069	2	0.010	19	0.023	E	2.4E-8
Smolensk-1	6636	1.000	2051	0.600	297	0.400	2873	0.600	23	0.050	111	0.035	I	7.4E-6
Smolensk-2	6636	1.000	2051	0.600	297	0.400	2873	0.600	23	0.050	111	0.035	I	7.4E-6
Smolensk-3	6636	1.000	2051	0.600	297	0.400	2873	0.600	23	0.050	111	0.035	I	7.4E-6
South Ukraine-1	6977	0.990	2809	0.820	204	0.800	2297	0.470	106	0.570	159	0.120	R	2.9E-6
South Ukraine-2	6977	0.990	2809	0.820	204	0.800	2297	0.470	106	0.570	159	0.120	R	2.9E-6
South Ukraine-3	5638	0.800	685	0.200	51	0.200	391	0.080	6	0.030	53	0.040	S	1.4E-5
St. Alban-1	7034	1.000	1032	0.300	132	0.300	585	0.120	19	0.060	150	0.080	D	5.0E-8
St. Alban-2	7034	1.000	1032	0.300	132	0.300	585	0.120	19	0.060	150	0.080	D	5.0E-8
St. Laurent-B1	5429	1.000	677	0.300	108	0.300	465	0.120	12	0.060	169	0.080	D	1.6E-6
St. Laurent-B2	5429	1.000	677	0.300	108	0.300	465	0.120	12	0.060	169	0.080	D	1.6E-6
Temelin-1	5638	0.800	685	0.200	51	0.200	391	0.080	6	0.030	53	0.040	S	1.4E-5
Temelin-2	5638	0.800	685	0.200	51	0.200	391	0.080	6	0.030	53	0.040	S	1.4E-5
Tihange-1	5295	1.000	777	0.300	99	0.300	440	0.120	14	0.060	113	0.080	D	1.6E-6
Tihange-2	5973	1.000	745	0.300	119	0.300	512	0.120	13	0.060	186	0.080	V	2.0E-7
Tihange-3	5529	1.000	811	0.300	104	0.300	460	0.120	15	0.060	118	0.080	V	2.0E-7
Torness Point-1	3291	1.000	947	0.600	52	0.400	228	0.100	1	0.010	4	0.007	B	1.0E-6
Torness Point-2	3291	1.000	947	0.600	52	0.400	228	0.100	1	0.010	4	0.007	B	1.0E-6
Tricastin-1	5429	1.000	677	0.300	108	0.300	465	0.120	12	0.060	169	0.080	D	1.6E-6
Tricastin-2	5429	1.000	677	0.300	108	0.300	465	0.120	12	0.060	169	0.080	D	1.6E-6

Site-unit	Xe-133		I-131		Cs-137		Te-132		Sr-90		Ru-106		Type	Rel. freq. (a^{-1})
	PBq	fraction	PBq	fraction	PBq	fraction	PBq	fraction	PBq	fraction	PBq	fraction		
Tricastin-3	5429	1.000	677	0.300	108	0.300	465	0.120	12	0.060	169	0.080	D	1.6E-6
Tricastin-4	5429	1.000	677	0.300	108	0.300	465	0.120	12	0.060	169	0.080	D	1.6E-6
Trillo-1	5657	0.800	687	0.200	51	0.200	392	0.080	6	0.030	53	0.040	M	1.9E-7
Tsentral-1	6014	0.800	731	0.200	54	0.200	417	0.080	6	0.030	56	0.040	T	1.0E-7
Tsentral-2	6014	0.800	731	0.200	54	0.200	417	0.080	6	0.030	56	0.040	T	1.0E-7
Tsentral-3	6014	0.800	731	0.200	54	0.200	417	0.080	6	0.030	56	0.040	T	1.0E-7
Tsentral-4	6014	0.800	731	0.200	54	0.200	417	0.080	6	0.030	56	0.040	T	1.0E-7
Unterweser-1	6082	0.800	632	0.200	101	0.200	434	0.080	9	0.030	118	0.040	N	1.0E-9
Vandellos-2	5420	1.000	795	0.300	102	0.300	451	0.120	15	0.060	116	0.080	V	2.0E-7
Visaginas-1	7924	1.000	852	0.220	174	0.350	1647	0.300	47	0.130	6	0.003	C	3.9E-8
Volgodonsk-1	5638	0.800	685	0.200	51	0.200	391	0.080	6	0.030	53	0.040	S	1.4E-5
Volgodonsk-2	5638	0.800	685	0.200	51	0.200	391	0.080	6	0.030	53	0.040	S	1.4E-5
Volgodonsk-3	5638	0.800	685	0.200	51	0.200	391	0.080	6	0.030	53	0.040	S	1.4E-5
Volgodonsk-4	5638	0.800	685	0.200	51	0.200	391	0.080	6	0.030	53	0.040	S	1.4E-5
Wylfa-1	3893	1.000	1120	0.600	62	0.400	270	0.100	1	0.010	5	0.007	B	1.0E-6
Wylfa-2	3893	1.000	1120	0.600	62	0.400	270	0.100	1	0.010	5	0.007	B	1.0E-6
Zaporoshje-1	5638	0.800	685	0.200	51	0.200	391	0.080	6	0.030	53	0.040	S	1.4E-5
Zaporoshje-2	5638	0.800	685	0.200	51	0.200	391	0.080	6	0.030	53	0.040	S	1.4E-5
Zaporoshje-3	5638	0.800	685	0.200	51	0.200	391	0.080	6	0.030	53	0.040	S	1.4E-5
Zaporoshje-4	5638	0.800	685	0.200	51	0.200	391	0.080	6	0.030	53	0.040	S	1.4E-5
Zaporoshje-5	5638	0.800	685	0.200	51	0.200	391	0.080	6	0.030	53	0.040	S	1.4E-5
Zaporoshje-6	5638	0.800	685	0.200	51	0.200	391	0.080	6	0.030	53	0.040	S	1.4E-5
Chernobyl-4	6500	1.000	1920	0.600	112	0.400	1620	0.600	10	0.050	74	0.035	I	7.4E-6

Appendix C: Accident sequences

release type	release shape[2]	reactor type(s)	Accident	Frequency[1]	Source
A	IV	ABB-Atom BWR	Early containment failure due to aggressive phenomena (such as RPV failure at high pressure, resulting in high pressure melt ejection and direct containment heating).	1.5E-06	STUK (2010); Himanen and Sjövall (2004)
B	VIII	AGR / MAGNOX	Generic severe accident source term.	1.0E-06	Slaper et al. (1994)
C	II	AREVA EPR	Core damage with potential early containment failure.	3.9E-08	Large (2007); AREVA (2009)
D	II	Framatome CP / N4,P4	Interfacing system LOCA (ISLOCA), containment bypass.	1.6E-06	Brisbois et al. (1991); IRSN and CEA (2007); Khatib-Rahbar (2001)
E	V	General Electric BWR/3 Mark I	Interfacing LOCA, with coolant loss outside containment, and core concrete interactions occur after vessel breach due to lack of water (CAPB 19).	2.4E-08	Entergy (2006)
F	IV	General Electric BWR/4 Mark I	Containment and filtered venting system bypass.	4.0E-08	HSK (2007)
G	IV	General Electric BWR/6 Mark III	Severe accident with early failure of containment airlock, core debris uncooled.	3.0E-07	ENSI (2009)
H	VI	AECL CANDU-6	Early core disassembly due to failure to shutdown, hydrogen combustion leading to early containment failure.	8.2E-07	KEMA (1987)
I	VII	RBMK-1000	Core power excursion with reactivity-initiated steam explosion resulting in upper head failure and a large early release.	7.4E-06	Usburus et al. (2007); OECD/NEA (2002)

[1] This is the generic frequency which was used if no specific frequency could be identified for a unit
[2] see Table 16, p. 58.

J	IV	Siemens BWR/69	Containment bypass due to failure of main steam lines outside containment with failure to isolate the main steam lines.	4.4E-07	Löffler and Sonnenkalb (2006)
K	IV	Siemens BWR/72	Severe accident with large early release.	1.0E-06	SSK (2003)
L	I	KWU 2-loop	Steam generator tube rupture.	3.7E-08	Khatib-Rahbar (2001); OECD/NEA (2007b)
M	I	KWU 3-loop	Steam generator tube rupture with containment and filtered venting system bypass.	1.9E-07	Khatib-Rahbar (2001); HSK (1999)
N	II	KWU 4-loop	Interfacing System LOCA with containment and filtered venting system bypass.	1.0E-09	Khatib-Rahbar (2001); SSK (2003)
O	III	Gidropress 6-loop VVER 440/311	Steam generator collector or rupture, in-vessel portion of sequence only.	2.8E-07	OECD/NEA (2007b); Siltanen et al. (2005)
P	III	Gidropress 6-loop VVER 440	Generic severe accident with core melt and late containment failure due to core debris interaction with reactor cavity door and/or hydrogen combustion.	1.1E-05	USNRC (1995); Lajtha et al. (2005)
Q	I	Gidropress 4-loop VVER 1000/446	Steam generator tube rupture, containment and filtration system bypass.	3.0E-08	NEK (2007); USNRC (2004)
R	II	Gidropress 4-loop VVER 1000/187, 302 or 338	Early containment failure and no spray (due to hydrogen combustion), or containment bypass, or core melt with containment isolation failure.	2.9E-06	USNRC (2005)
S	I	Gidropress 4-loop VVER 1000/320	Steam generator tube rupture, containment bypass.	1.4E-05	Khatib-Rahbar (2001); Russian Federation (2007)
T	I	Gidropress 4-loop VVER 1200	Steam generator tube rupture, containment bypass.	1.0E-07	Khatib-Rahbar (2001); Ivkov (2010)
U	I	Westinghouse 2-loop	Containment bypass accident.	3.8E-07	Khatib-Rahbar (2001); OECD/NEA (2007b); UBA (2002)
V	II	Westinghouse 3-loop	Interfacing systems loss of coolant accident (ISLOCA), loss of coolant outside containment.	2.0E-07	Khatib-Rahbar (2001); Entergy (2007)
W	II	Westinghouse 4-loop	Interfacing system LOCA (ISLOCA), containment bypass.	1.6E-07	Khatib-Rahbar (2001); Meyer and Stokke (1997)